PERIODIC CRACK PROBLEM FOR AN FGM COATED HALF PLANE

A THESIS SUBMITTED TO
THE GRADUATE SCHOOL OF NATURAL AND APPLIED SCIENCES
OF
MIDDLE EAST TECHNICAL UNIVERSITY

BY

İSMET İNCE

IN PARTIAL FULFILLMENT OF THE REQUIREMENTS
FOR
THE DEGREE OF MASTER OF SCIENCE
IN
MECHANICAL ENGINEERING

MAY 2012

Approval of the thesis:

PERIODIC CRACK PROBLEM FOR AN FGM COATED HALF PLANE

submitted by **İSMET İNCE** in partial fulfillment of the requirements for the degree of **Master of Science in Mechanical Engineering Department, Middle East Technical University** by,

Prof. Dr. Canan ÖZGEN
Dean, Graduate School of **Natural and Applied Sciences** _____

Prof. Dr. Süha ORAL
Head of Department, **Mechanical Engineering** _____

Prof. Dr. Suat KADIOĞLU
Supervisor, **Mechanical Engineering Dept., METU** _____

Examining Committee Members:

Prof. Dr. Bülent DOYUM
Mechanical Engineering Dept., METU _____

Prof. Dr. Suat KADIOĞLU
Mechanical Engineering Dept., METU _____

Prof. Dr. Levend PARNAS
Mechanical Engineering Dept., METU _____

Assoc. Prof. Dr. Serkan DAĞ
Mechanical Engineering Dept., METU _____

Assoc. Prof. Dr. Bora YILDIRIM
Mechanical Engineering Dept., Hacettepe University _____

Date: May 30, 2012

I hereby declare that all information in this document has been obtained and presented in accordance with academic rules and ethical conduct. I also declare that, as required by these rules and conduct, I have fully cited and referenced all material and results that are not original to this work.

Name, Surname:

Signature :

ABSTRACT

PERIODIC CRACK PROBLEM FOR AN FGM COATED HALF PLANE

İnce, İsmet
M.S., Department of Mechanical Engineering
Supervisor: Prof. Dr. Suat Kadıoğlu

May 2012, 123 pages

An elastic FGM layer bonded to a semi-infinite linear elastic, isotropic, homogeneous half plane is considered. The half plane contains periodic cracks perpendicular to the interface. Mechanical loading is applied through crack surface pressure, resulting in a mode I crack problem. The plane elasticity problem described above is formulated by using Fourier transforms and Fourier series. A singular integral equation is obtained for the auxiliary variable, namely derivative of the crack surface displacement. Solution is obtained, and stress intensity factors are calculated for various values of crack period, crack length, crack location, layer thickness and material gradation.

Keywords: Functionally Graded Material (FGM), Stress Intensity Factors, Periodic Cracks, Plane Elasticity Problem

ÖZ

YARIM DÜZLEM ÜZERİNE KAPLANAN FONKSİYONEL OLARAK DERECELENMİŞ MALZEME İÇİN PERİYODİK ÇATLAK PROBLEMİ

İnce, İsmet
Yüksek Lisans, Makine Mühendisliği Bölümü
Tez Yöneticisi : Prof. Dr. Suat Kadıoğlu

Mayıs 2012, 123 sayfa

Bu çalışmada, elastik, eşyönlü, homojen, yarı-sonsuz düzlem üzerine bağlanan fonksiyonel olarak derecelenmiş elastik bir malzeme katmanı modellenmiştir. Yarı-sonsuz düzlem, arayüze dik periyodik çatlaklar içermektedir. 1. mod çatlak problemine neden olan çatlak yüzey basıncı yoluyla mekanik yükleme uygulanmaktadır. Yukarıda ifade edilen düzlem elastisite problemi, Fourier dönüşümleri ve serileri kullanılarak formüle edilmektedir. Yardımcı değişken, yani çatlak yüzey yer değiştirmesinin türevi için bir tekil integral denklemi elde edilmektedir. Çözüm bulunduktan sonra gerilme şiddeti faktörü, çeşitli çatlak aralığı, çatlak uzunluğu, çatlak konumu, katman kalınlığı ve malzeme dereceleme değerleri için hesaplanmaktadır.

Anahtar Kelimeler: Fonksiyonel Olarak Derecelenmiş Malzeme, Gerilme Şiddeti Çarpanı, Periyodik Çatlaklar, Düzlem Elastisite Problemi

ACKNOWLEDGEMENTS

First of all, I would like to thank my supervisor Prof. Dr. Suat KADIOĞLU for his continuous help, guidance, valuable suggestions and encouragements throughout the study.

Also, I would like to give special thanks to Assoc. Prof. Dr. Bora YILDIRIM who helped me provide the results based on finite element method using Ansys computer program for numerical validation of this study.

Moreover, I want to thank my sister Asiye GÜNEŞ for giving her endless support in every moment of my life.

TABLE OF CONTENTS

ABSTRACT iv

ÖZ v

ACKNOWLEDGEMENTS vi

TABLE OF CONTENTS vii

LIST OF TABLES ix

LIST OF FIGURES xii

NOMENCLATURE xv

CHAPTERS

1. INTRODUCTION 1

1.1 Literature survey 2

1.2 Scope of the study 5

2. ANALYSIS OF THE PROBLEM 8

2.1 Formulation of the crack problem 8

2.2 Formulation of homogeneous halfplane containing periodic cracks 10

2.3 Application of boundary conditions for the homogeneous domain 18

2.4 Formulation of FGM strip 22

2.5 Application of remaining boundary conditions 27

2.5.1 Continuity conditions 28

2.5.2 Free surface conditions 36

2.5.3 Final form of boundary conditions 38

2.6 Derivation of singular integral equation 39

2.7 Numerical solution of singular integral equation 43
3. NUMERICAL RESULTS 47
4. DISCUSSION 100
5. CONCLUSION 103
REFERENCES 106
APPENDICES
A. REQUIRED INTEGRALS 109
B. SOLUTION OF THE RESULTING MATRIX ..... .112
C. DERIVATION OF SINGULAR INTEGRAL EQUATION 119
D. MANIPULATIONS ON RIZK'S SINGULAR INTEGRAL EQUATION ... 122

LIST OF TABLES

TABLES

Table 3.1: Comparison of *k*(a)* and *k*(b)* for a thick FGM layer under uniform loading for different *NP* and *NS* numbers and for *l/(l+2c)=0,5* and $h\beta=10^{-3}$. 49

Table 3.2: Comparison of *k*(a)* and *k*(b)* for a thick FGM layer under uniform loading for different *NP* and *NS* numbers and for *l/(l+2c)=0,5* and *hβ*=1. 50

Table 3.3: Comparison of k*(a)s provided by Ansys and current study for different nonhomogeneity parameters hβ and for a thick FGM layer under uniform loading . 51

Table 3.4: Comparison of *k*(a)*s provided by Ansys and current study for different nonhomogeneity parameters *hβ* and for a thick FGM layer under parabolic loading 52

Table 3.5: Comparison of $k^*(a)$ for imbedded periodic cracks with Rizk (2003) and Murakami (1987), $\beta h = 10^{-3}$ and $\frac{h}{a} = 0,5$ 53

Table 3.6: Comparison of $k^*(b)$ for imbedded periodic cracks with Rizk (2003), $\beta h = 10^{-3}$ and $\frac{h}{a} = 0,5$ 54

Table 3.7: Comparison of $k^*(a)$ and $k^*(b)$ for $\frac{h}{a} = 0,5$ 55

Table 3.8: Comparison of $k^*(a)$ and $k^*(b)$ for $\frac{h}{a} = 0,5$ 58

Table 3.9: Comparison of $k^*(a)$ and $k^*(b)$ for $\frac{h}{a} = 0,5$ 60

Table 3.10: Comparison of *k*(a)* and *k*(b)* for a thick FGM layer under uniform loading for different nonhomogeneity parameters, $h\beta$ and for *l/(l+2c)=0,5*. 62

Table 3.11: Comparison of *k*(a)* and *k*(b)* for a thick FGM layer under uniform loading for different nonhomogeneity parameters, $h\beta$ and for *l/(l+2c)=0,8*. 64

Table 3.12: Comparison of *k*(a)* and *k*(b)* for a thin FGM layer under uniform loading for different nonhomogeneity parameters, $h\beta$ and for *l/(l+2c)=0,5*. 66

Table 3.13: Comparison of *k*(a)* and *k*(b)* for a thin FGM layer under uniform loading for different nonhomogeneity parameters, $h\beta$ and for *l/(l+2c)*=0,8. 68

Table 3.14: Comparison of *k*(a)* and *k*(b)* for different nonhomogeneity parameters $h\beta$ and for a thick FGM layer under uniform loading. 70

Table 3.15: Comparison of *k*(a)* and *k*(b)* for different nonhomogeneity parameters $h\beta$ and for a very thin FGM layer. 77

Table 3.16: Comparison of *k*(a)* and *k*(b)* for different nonhomogeneity parameters $h\beta$ and for a very thin FGM layer. 78

Table 3.17: Comparison of $k^*(a)$ and $k^*(b)$ for different nonhomogeneity parameters $h\beta$ and for a thin FGM layer. 81

Table 3.18: Comparison of *k*(a)* and *k*(b)* for different nonhomogeneity parameters $h\beta$ and for a thin FGM layer. 82

Table 3.19: Comparison of $k^*(a)$ and $k^*(b)$ for different nonhomogeneity parameters $h\beta$ and for a thick FGM layer. 86

Table 3.20: Comparison of *k*(a)* and *k*(b)* for different nonhomogeneity parameters $h\beta$ and for a thick FGM layer 87

Table 3.21: Comparison of $k^*(a)$ and $k^*(b)$ under uniform crack surface traction σ_0 for $h\beta = 0,5$ 92

Table 3.22: Comparison of $k^*(a)$ and $k^*(b)$ under linear crack surface traction $\sigma_0(\frac{x-a}{l})$ for $h\beta = 0,5$ 93

Table 3.23: Comparison of $k^*(a)$ and $k^*(b)$ under parabolic crack surface traction $\sigma_0(\frac{x-a}{l})^2$ for $h\beta = 0,5$ 94

Table 3.24: Comparison of $k^*(a)$ and $k^*(b)$ under cubic crack surface traction $\sigma_0(\frac{x-a}{l})^3$ for $h\beta = 0,5$ 95

Table 3.25: Comparison of $k^*(a)$ and $k^*(b)$ under uniform crack surface traction σ_0 for $h\beta = -0,5$ 96

Table 3.26: Comparison of $k^*(a)$ and $k^*(b)$ under linear crack surface traction $\sigma_0(\frac{x-a}{l})$ for $h\beta = -0,5$. 97

Table 3.27: Comparison of $k^*(a)$ and $k^*(b)$ under parabolic crack surface traction $\sigma_0(\frac{x-a}{l})^2$ for $h\beta = -0,5$ 98

Table 3.28: Comparison of $k^*(a)$ and $k^*(b)$ under cubic crack surface traction $\sigma_0(\frac{x-a}{l})^3$ for $h\beta = -0,5$ 99

LIST OF FIGURES

FIGURES

Figure 1.1: Different microstructures of an FGM (Aboudi *et al.*, 2001) 1

Figure 1.2: Cooling and heating thermal shocks..... 7

Figure 2.1: Geometry of the problem..... 9

Figure 2.2: Superposition procedure 10

Figure 2.3: Geometry of FGM strip 22

Figure 3.1: $k^*(a)$ under uniform applied stress for $\frac{h}{a}=0,5$ and $\beta h=10^{-3}$ 56

Figure 3.2: $k^*(b)$ under uniform applied stress for $\frac{h}{a}=0,5$ and $\beta h=10^{-3}$ 56

Figure 3.3: $k^*(a)$ under uniform applied stress for $\frac{h}{a}=0,5$ and $\beta h=0,5$ 59

Figure 3.4: $k^*(b)$ under uniform applied stress for $\frac{h}{a}=0,5$ and $\beta h=0,5$ 59

Figure 3.5: $k^*(a)$ under uniform applied stress for $\frac{h}{a}=0,5$ and $\beta h=-0,5$ 61

Figure 3.6: $k^*(b)$ under uniform applied stress for $\frac{h}{a}=0,5$ and $\beta h=-0,5$ 61

Figure 3.7: $k^*(a)$ under uniform applied stress for $\frac{h}{a}=0,9$ and *l/(l+2c)*=0,5 63

Figure 3.8: $k^*(b)$ under uniform applied stress for $\frac{h}{a}=0,9$ and *l/(l+2c)*=0,5..... 63

Figure 3.9: $k^*(a)$ under uniform applied stress for $\frac{h}{a}=0,9$ and *l/(l+2c)*=0,8 65

Figure 3.10: $k^*(b)$ under uniform applied stress for $\frac{h}{a}=0,9$ and *l/(l+2c)*=0,8..... 65

Figure 3.11: $k^*(a)$ under uniform applied stress for $\frac{h}{a}=0,5$ and *l/(l+2c)*=0,5….67

Figure 3.12: $k^*(b)$ under uniform applied stress for $\frac{h}{a}=0,5$ and *l/(l+2c)*=0,5..... 67

Figure 3.13: $k^*(a)$ under uniform applied stress for $\frac{h}{a}=0,5$ and *l/(l+2c)*=0,8…69

Figure 3.14: $k^*(b)$ under uniform applied stress for $\frac{h}{a}=0,5$ and *l/(l+2c)*=0,8..... 69

Figure 3.15: $k^*(a)$ under uniform applied stress for $\frac{h}{a}=0,9$ 75

Figure 3.16: $k^*(b)$ under uniform applied stress for $\frac{h}{a}=0,9$ 75

Figure 3.17: $k^*(a)$ for $h/a=0,1$ and $l/a=1$..... 79

Figure 3.18: $k^*(b)$ for $h/a=0,1$ and $l/a=1$..... 79

Figure 3.19: $k^*(a)$ for $h/a=0,1$ and $l/a=1$..... 80

Figure 3.20: $k^*(b)$ for $h/a = 0,1$ and $l/a = 1$ 80

Figure 3.21: $k^*(a)$ for $h/a = 0,5$ and $l/a = 1$ 83

Figure 3.22: $k^*(b)$ for $h/a = 0,5$ and $l/a = 1$ 83

Figure 3.23: $k^*(a)$ for $h/a = 0,5$ and $l/a = 1$ 84

Figure 3.24: $k^*(b)$ for $h/a = 0,5$ and $l/a = 1$ 84

Figure 3.25: $k^*(a)$ for $h/a = 0,9$ and $l/a = 1$ 88

Figure 3.26: $k^*(b)$ for $h/a = 0,9$ and $l/a = 1$ 88

Figure 3.27: $k^*(a)$ for $h/a = 0,9$ and $l/a = 1$ 89

Figure 3.28: $k^*(b)$ for $h/a = 0,9$ and $l/a = 1$ 89

Figure 3.29: The geometry of plane when linear crack surface traction applied 91

Figure 5.1: Geometry of periodic crack problem when homogeneous half plane with free surface (left) and with fixed surface (right) 105

NOMENCLATURE

$a,\ b$	: Start and end point coordinates of the crack
l	: Crack length $(l = b - a)$
$2c$	: Crack period
h	: Thickness of nonhomogeneous FGM strip
FGM	: Functionally graded material
$\mu(x)$	: Shear modulus for FGM
β	: Nonhomogenity constant for elastic modulus
ν	: Poisson's ratio
κ	: Kolosov constant $\begin{cases}(3-4\nu) & \text{for plane strain}\\ (3-\nu)/(1+\nu) & \text{for plane stress}\end{cases}$
$u,\ v$	: Displacement components of homogeneous material in x- and y- directions
$u_f,\ v_f$	: Displacement components of FGM in x- and y-directions
σ_{ij}	: Stress components of homogeneous material $(i,\ j = x,\ y)$
σ_{ij_f}	: Stress components of FGM $(i,\ j = x,\ y)$
$g(t)$	: Unknown auxiliary function
ρ	: Fourier transform variable

$\alpha_n,\ \alpha_m$	: Fourier series variables, $\alpha_n = \frac{n\pi}{c}$ and $\alpha_m = \frac{m\pi}{c}$ where $(n,\ m = 0,\ 1,\ 2..)$
$\Delta_1,\ \Delta_2,\ \Delta_f$	: Determinants of the coefficient matrices for displacement equations
n_i	: Roots of characteristic equation where $(i = 1,\ 2)$
p_j	: Roots of characteristic equation where $(j = 1,\ 2,\ 3,\ 4)$
$A_i,\ B_i,\ C_i,\ D_i,\ E_i,\ F_i$	: Unknown functions in displacement expressions
m_i	: Coefficients of displacement function of B_i where $(i = 1,\ 2,\ 3,\ 4)$
q_i	: Coefficients of displacement function of F_i where $(i = 1,\ 2,\ 3,\ 4)$
k_n	: Terms defined in orthogonality condition where $(n = 0,\ 1,\ 2..)$
$G_{in},\ H_{in}, J_{in}, L_{in},\ M_{in},\ R_{in}$	: Coefficients obtained in boundary conditions where $(i = 1,\ 2,\ 3,\ 4)$ and $(n = 0,\ 1,\ 2..)$
Z_i	: Coefficient of unknown auxiliary function defined in matrix system of boundary conditions where $(i = 1,\ 2,\ 3,\ 4)$
$K_1,\ K_2$	: Kernels of singular integral equation
$P(x)$	: Crack surface pressure
NP	: Node number of Gauss-Jacobi numerical integration
NS	: Term number in series solution
SIFs	: Stress intensity factors

$k(a),\ k(b)$	: Stress intensity factors at $x=a$ and $x=b$, respectively
$k^*(a),\ k^*(b)$	: Normalized stress intensity factors at $x=a$ and $x=b$, respectively

CHAPTER 1

INTRODUCTION

FGMs are multifunctional materials exhibiting spatial variations in composition and microstructure. They are produced for their superior thermal, structural or functional properties. Generally, they are a combination of ceramic and metallic materials as seen in Figure 1.1.

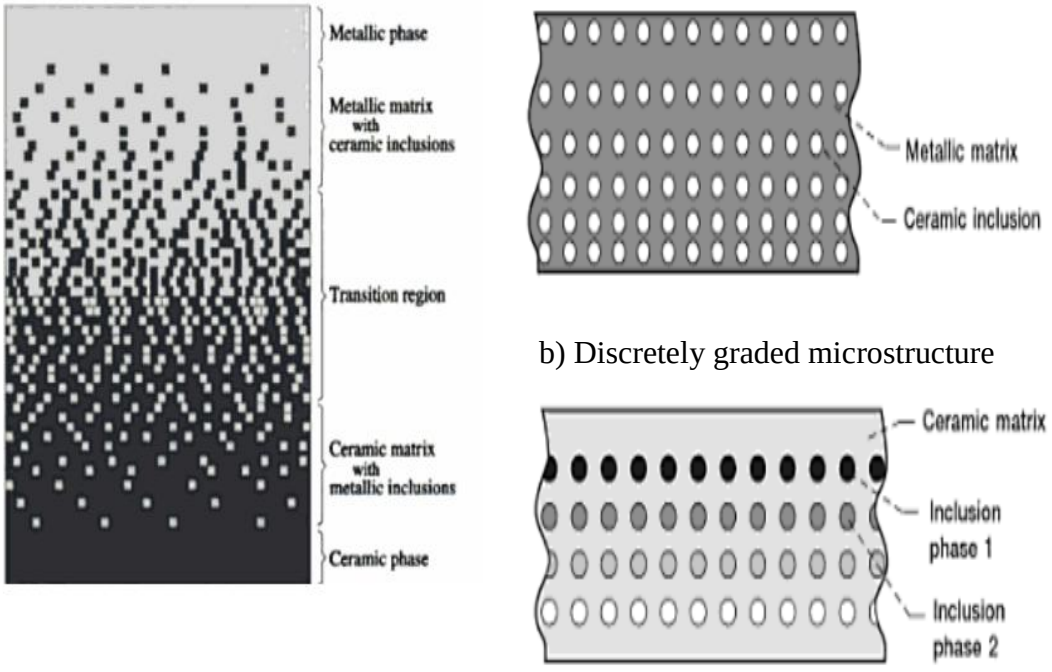

a) Continuously graded microstructure

b) Discretely graded microstructure

c) Multi-phase graded microstructure

Figure 1.1: Different microstructures of an FGM (Aboudi *et al.*, 2001)

Metal ceramic FGMs are first proposed as thermal barrier coatings. On one hand, metals have high toughness but a relatively low melting point and the strength of metal is reduced when it is in a high temperature environment. On the other hand, ceramic materials have excellent characteristics in strength and heat resistance but they have low toughness. To solve this problem, FGM coating was proposed in Japan around 1984-1985 during a space plane project. Thus, FGMs are created because of many advantages like high resistance to temperature gradients, high wear resistance and so on. There are a number of manufacturing processes to produce such materials such as physical and chemical vapor deposition methods. In today's world, there are many applications of FGMs. For instance, rocket engine components, microelectronic applications, heat exchanger tubes, complex shaped automotive parts, nuclear reactor components etc. are produced from FGMs to withstand severe operating conditions (Ruys and Sun, 2006).

1.1 Literature survey

There have been many research studies on cracking of FGMs since the late 80's until very recently. Here, mostly periodic cracking problems and some single crack problems relevant to the problem considered in this thesis will be briefly reviewed.

In the following, studies about periodic crack problems for homogeneous and nonhomogeneous media are given first. In these studies both analytical and numerical methods have been employed. Periodic array of cracks in a homogeneous half plane subjected to arbitrary normal crack surface tractions was studied by using a hypersingular integral equation in Nied (1987a). In Bao and Wang (1995), multiple cracking of FGMs was analyzed under mechanical and thermal loading by finite element method. In Erdoğan and Öztürk (1995), a hypersingular integral equation was used for the antiplane problem of a homogeneous half space with an FGM

coating having periodic cracks perpendicular to the surface. In Choi (1997), considering mode I and mode II loading conditions, the periodic array of parallel cracks in an infinite FG medium was analyzed. A hypersingular integral equation was derived for each loading mode and SIFs were found as functions of crack surface displacements for different values of the material nonhomogeneity. In Schulze and Erdogan (1998), using Fourier series and Fourier transforms, periodic cracking of an elastic homogeneous coating bonded to a homogeneous substrate was considered. Apart from the findings on influence of length parameters on SIFs at the crack tips, strain energy released during periodic cracking was studied. Afsar and Sekine (2000) discussed the effect of crack spacing for a semi-infinite FGM plane having periodic edge cracks where material gradation is implemented by introducing an incompatible eigenstrain. Ueda (2002) studied graded layer bonded between a homogeneous substrate and a homogeneous coating. The graded layer contained parallel array of cracks perpendicular to the boundaries and the problem was examined by finite element method considering temperature and position dependent thermal and elastic properties for the materials. On the other hand, Rizk (2003) considered a transient thermal stres problem for a homogeneous half plane having periodic cracks and the problem was solved by using Cauchy type singular integral equation. Rizk (2005) also studied an infinitely long plate with periodic edge cracks under thermal loading. Using superposition technique, a hypersingular integral equation whose unkown is the crack surface displacement was obtained and solved. In Yıldırım *et al.* (2005), FGM having cracks bonded to a homogeneous substrate was examined. Surface cracks were assumed to be semi-elliptical and 3-D finite element method was used to solve thermal and structural problems. Wang and Mai (2005) investigated an infinite FGM plane containing periodic array of cracks under mechanical and/or thermal loading. Crack closure problem was considered. Singular integral equation was expressed with crack contact length as an unknown variable. Numerical results were obtained for SIFs and crack contact length as functions of crack spacing. It was shown in this study that SIFs have a strong dependence on the non-homogeneity parameters in addition to loading conditions. Furthermore, the

same crack geometry was considered under transient loading in Wang and Mai (2006b). In this case, singular integral equation was derived by taking mode I and mode II loading conditions into account. Numerical results for mode I and mode II SIFs are presented and it is observed that in the case of multiple cracking, different loading modes exhibited different characteristics. Mode I SIF was decreased by multiple cracking but mode II SIF was increased. Wang and Mai (2006a) also considered periodic antiplane cracks in graded coatings under static or transient loadings. The results showed that stress and SIF can be decreased by increasing crack density. Chen (2006) studied FG coating on a substrate containing periodic array of parallel cracks. Hypersingular integral equations were obtained to solve the static and dynamic anti-plane problem by using Fourier transforms and series. In Dağ *et al.* (2008), a three dimensional finite element method was proposed to solve periodic surface cracking problem in a FG coating under thermal stresses. Temperature and displacement fields were calculated from finite element analysis and mode I SIFs were found by means of the displacement correlation technique. Ding and Li (2008) analysed an FGM coating on an elastic substrate, the coating containing either a single crack or an array of periodic interface cracks under antiplane shear loads. Cauchy type and Hilbert type singular kernels were used for the single and the periodic crack problems, respectively. Finally, SIFs were compared between single and periodic crack cases and results showed that the magnitude of the SIF decreased with an increase of material gradient, thickness of homogeneous substrate and coating. Jin and Feng (2008) develeoped a thermo-fracture mechanics model for FG ceramics having multiple surface cracking to find the effect of cracking under thermal shock. In Jin and Feng (2009), parallel edge cracks with alternating lengths in an elastic plate under thermal shock are considered. Integral equations were derived by using Fourier transform method and numerical solution was carried out for thermal stress intensity factors. In these last two studies, materials are assumed to have variable thermal but uniform elastic properties. Two recent studies where a single crack in an FGM layer has been considered are as follows: El-Borgi *et al.* (2008) considered a surface crack of an FGM bonded to a

homogeneous material under thermal loading by using orthogonal Jacobi polynomials to calculate SIFs. In Noda and Guo (2008), by using perturbation method, fracture behavior of FGM containing a surface crack is studied.

From this literature survey, it is seen that,

- periodic cracking problems are encountered in a number of important technological applications, especially those involving thermal shocks,
- such problems can be dealt with analytical singular integral equation or numerical (finite element) methods,
- to help predicting the fracture behavior, SIFs can be found as functions of geometric and material parameters,
- and knowing the general trends for SIFs, coatings can be tailored to resist fracture better.

1.2 Scope of the study

As one can observe from the literature survey, existing studies mostly addressed the cracking of FGM coatings which is likely to occur during a cooling thermal shock. Such a situation arises during the manufacturing of FGM coatings while their temperature drops to room temperature from processing temperature. On the other hand, during a heating thermal shock the stress state in the coating becomes compressive and the stress state in the substrate becomes tensile as shown in Figure 1.2. This might cause cracking of the substrate. Furthermore, crack closure might also occur at later stages of the surface heating. This type of problems involving sub-surface cracking have received relatively less attention. There are a few examples such as Nied (1984) and Nied (1987b) for homogeneous materials, but to the best of

author's knowledge, the problem of periodic cracking underneath an FGM coating has not been addressed so far.

In the current study, there is an FGM layer coated to homogeneous semi-infinite half plane having imbedded periodic cracks. Crack surface pressure is considered to be the only loading. This is opening mode so only mode-I problem is considered. For solving the problem, Fourier transform integral equation method is used. A cauchy type singular integral equation is formulated in terms of an auxiliary function (derivative of crack surface displacement) by using homogeneous and mixed boundary conditions. The main objective of the study is to examine the effect of crack period, crack length, crack location, layer thickness and material gradation on SIFs. Uniform, linear, quadratic and cubic variations of surface pressure is considered. By appropriately combining SIFs for these cases, one can obtain SIFs for different loading conditions such as thermal shock. This requires solution of conduction and thermal stress problems for the crack free medium which is beyond the scope of this thesis study.

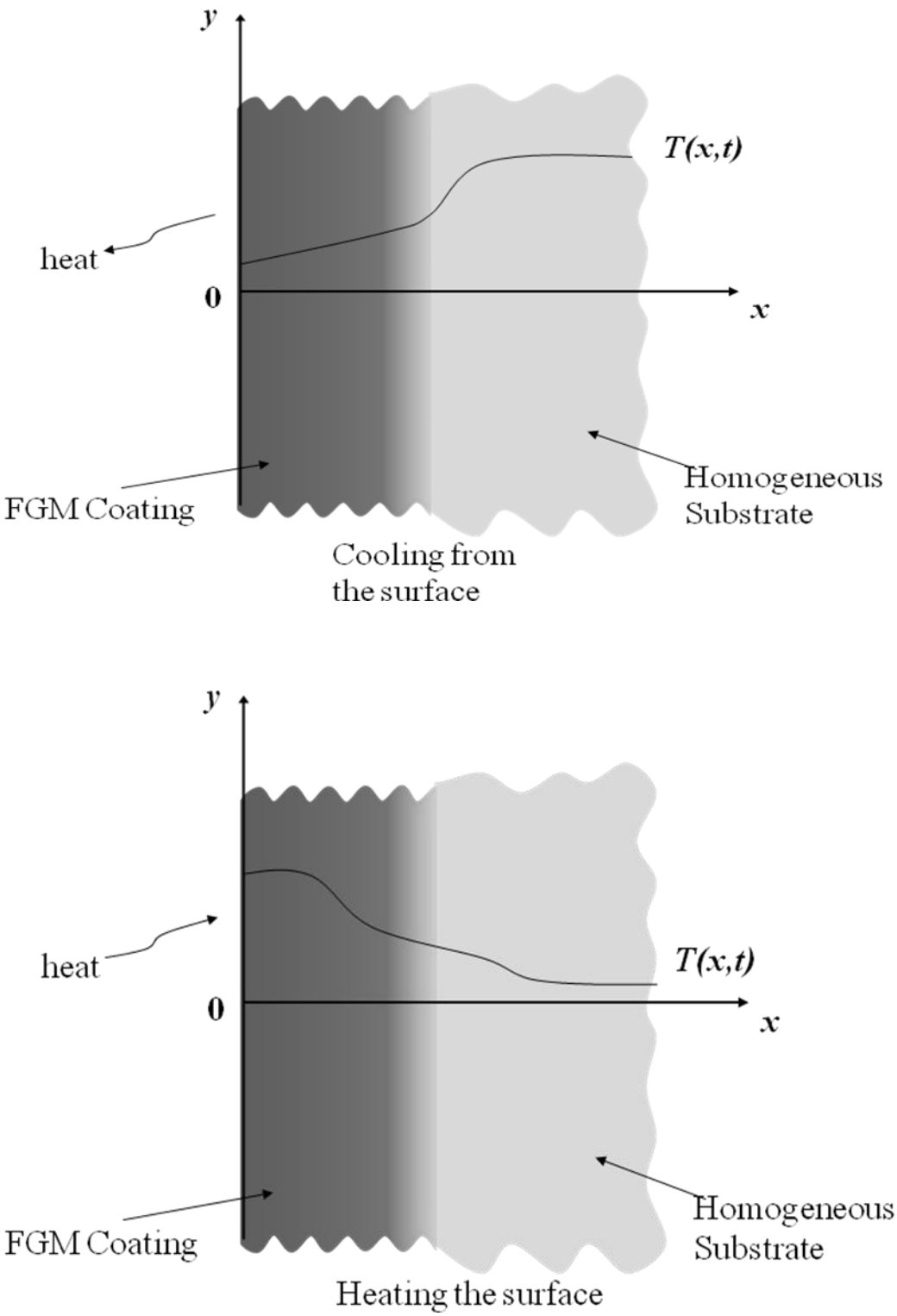

Figure 1.2: Cooling and heating thermal shocks

CHAPTER 2

ANALYSIS OF THE PROBLEM

2.1 Formulation of the crack problem

The geometry of the elasticity problem is shown in figure 1. Homogeneous subtrate containing periodic cracks is bonded to a FGM coating. It is assumed that a crack surface pressure is applied resulting in a mode-I crack problem. To solve the problem, the semi-infinite medium is separated into two parts. The first part is the homogeneous substrate containing the periodic cracks and the second part is the FGM coating. The shear modulus is assumed to be continuous at the interface.

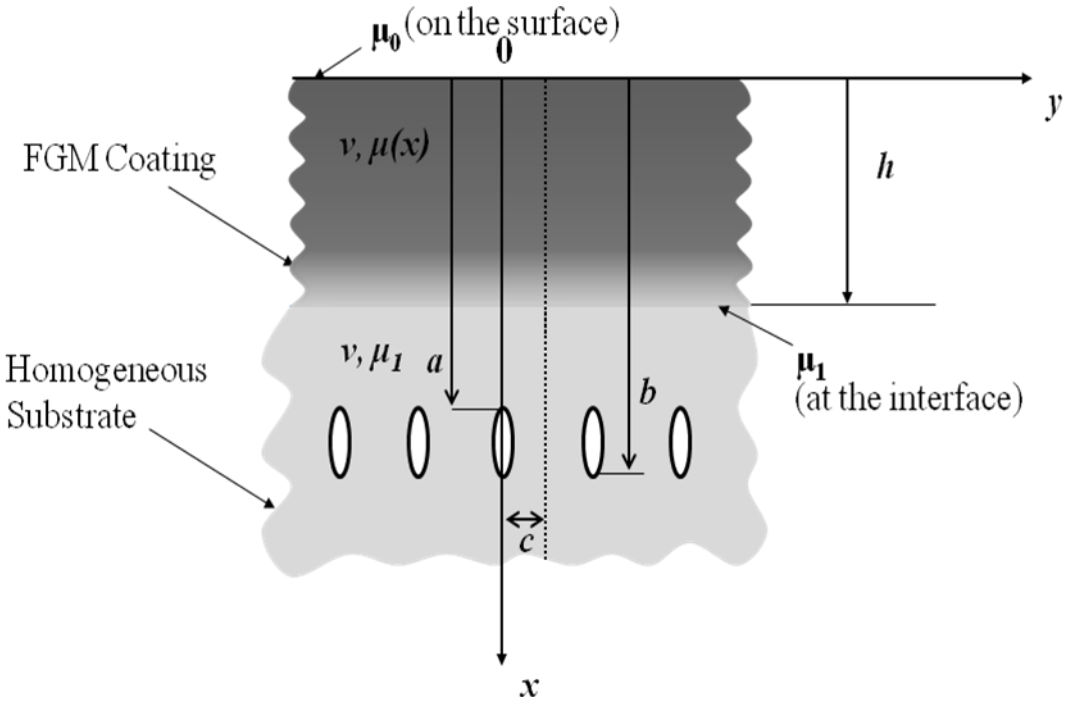

Figure 2.1: Geometry of the problem

For the first part as seen below, by using superposition technique, homogeneous substrate is examined in two parts. In the upper part, strip solution with symmetry boundary conditions containing a crack on the boundary and in the lower part, periodic half plane without any cracks are described. The elasticity solutions (i.e. stresses and displacements) for these domains which contain arbitrary functions can be found separately. After finding these distinct solutions, homogeneous substrate solution with periodic cracks can be obtained by superposing them. In this process, the arbitrary functions are determined such that the overall solution satisfies the required overall boundary conditions.

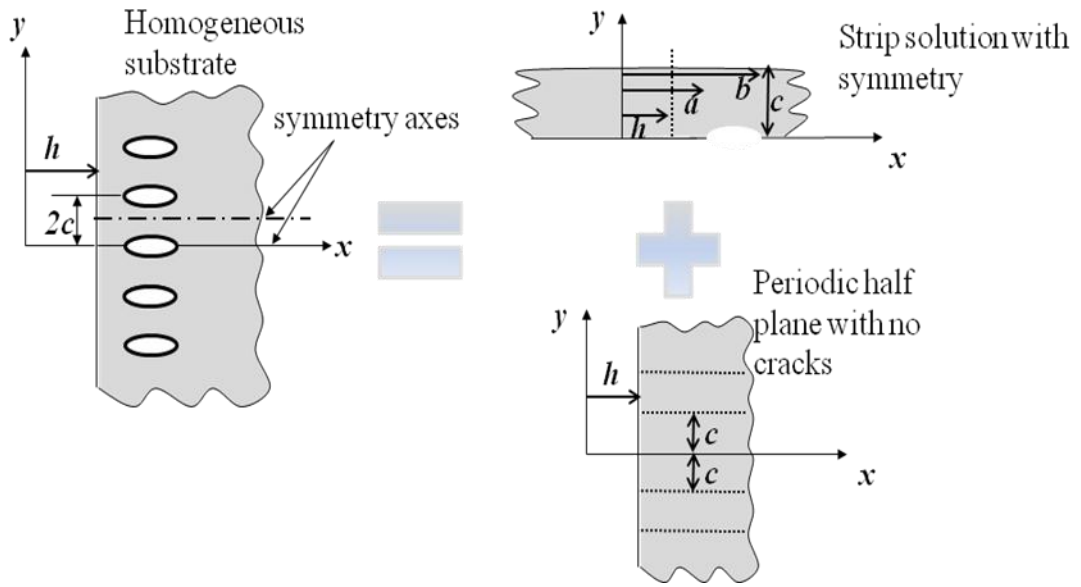

Figure 2.2: Superposition procedure

Material properties are actually constant throughout the homogeneous part but in the FGM coating shear modulus is given as

$$\mu(x) = \mu_0 e^{\beta x} \quad \text{for } 0 \le x \le h, \tag{1}$$

$$\mu_1 = \mu(h) = \mu_0 e^{\beta h} \quad \text{for } h \le x, \tag{2}$$

where β is non-homogeneity constant.

Kolosov constant is defined as $\kappa = 3 - 4\nu$ for plane strain and $\kappa = \frac{3-\nu}{1+\nu}$ for plane stress. Here ν is the Poisson ratio and it is taken as constant.

2.2 Formulation of homogeneous halfplane containing periodic cracks

According to Hooke's law, stresses may be expressed in terms of the displacements as follows:

$$\sigma_{xx}(x,y)=\frac{\mu_1}{(\kappa-1)}((\kappa+1)\frac{\partial u}{\partial x}+(3-\kappa)\frac{\partial v}{\partial y}), \tag{3}$$

$$\sigma_{yy}(x,y)=\frac{\mu_1}{(\kappa-1)}((\kappa+1)\frac{\partial v}{\partial y}+(3-\kappa)\frac{\partial u}{\partial x}), \tag{4}$$

$$\sigma_{xy}(x,y)=\mu_1(\frac{\partial u}{\partial y}+\frac{\partial v}{\partial x}). \tag{5}$$

Stresses given in equations ((3)-(5)) must satisfy equilibrium equations which are written below in the absence of body forces:

$$\frac{\partial \sigma_{xx}}{\partial x}+\frac{\partial \sigma_{xy}}{\partial y}=0, \tag{6}$$

$$\frac{\partial \sigma_{xy}}{\partial x}+\frac{\partial \sigma_{yy}}{\partial y}=0. \tag{7}$$

Substituting (3), (4) and (5) into (6) and (7), one can obtain:

$$(\kappa+1)\frac{\partial^2 u}{\partial x^2}+(\kappa-1)\frac{\partial^2 u}{\partial y^2}+2\frac{\partial^2 v}{\partial x\partial y}=0, \tag{8}$$

$$(\kappa-1)\frac{\partial^2 v}{\partial x^2}+(\kappa+1)\frac{\partial^2 v}{\partial y^2}+2\frac{\partial^2 u}{\partial x\partial y}=0. \tag{9}$$

A solution which has the capacity to satisfy equations (8) and (9) as well as the boundary conditions can be assumed in the following form (Schulze and Erdoğan, 1998).

$$u(x,y)=\frac{1}{2\pi}\int_{-\infty}^{\infty}U_1(y,\rho)e^{-ix\rho}d\rho+\sum_{n=0}^{\infty}U_2(x,\alpha_n)\cos(y\alpha_n), \tag{10}$$

$$v(x,y)=\frac{1}{2\pi}\int_{-\infty}^{\infty}V_1(y,\rho)e^{-ix\rho}d\rho+\sum_{n=0}^{\infty}V_2(x,\alpha_n)\sin(y\alpha_n), \tag{11}$$

where $\alpha_n = \frac{n\pi}{c}$ for n=0, 1, 2,... (12)

In (10) and (11), the Fourier integrals represent the strip solution and Fourier series represent the crack-free periodic half plane solution, which are shown in Figure 2.2.

Substituting equations (10) and (11) into (8) and (9), one can obtain:

$$\frac{1}{2\pi}\int_{-\infty}^{\infty} e^{-ix\rho}\{(\kappa+1)(-\rho^2)U_1+(\kappa-1)\frac{\partial^2 U_1}{\partial y^2}-2i\rho\frac{\partial V_1}{\partial y}\}d\rho+$$
$$\sum_{n=0}^{\infty}\{(\kappa+1)\frac{\partial^2 U_2}{\partial x^2}-(\kappa-1)\alpha_n{}^2U_2+2\alpha_n\frac{\partial V_2}{\partial x}\}\cos(y\alpha_n)=0, \quad (13)$$

$$\frac{1}{2\pi}\int_{-\infty}^{\infty} e^{-ix\rho}\{(\kappa-1)(-\rho^2)V_1+(\kappa+1)\frac{\partial^2 V_1}{\partial y^2}-2i\rho\frac{\partial U_1}{\partial y}\}d\rho+$$
$$\sum_{n=0}^{\infty}\{(\kappa-1)\frac{\partial^2 V_2}{\partial x^2}-(\kappa+1)\alpha_n{}^2V_2-2\alpha_n\frac{\partial U_2}{\partial x}\}\sin(y\alpha_n)=0. \quad (14)$$

From equations (13) and (14), one can obtain four differential equations:

$$(\kappa-1)\frac{\partial^2 U_1}{\partial y^2}-(\kappa+1)\rho^2U_1-2i\rho\frac{\partial V_1}{\partial y}=0, \quad (15)$$

$$(\kappa+1)\frac{\partial^2 U_2}{\partial x^2}-(\kappa-1)\alpha_n{}^2U_2+2\alpha_n\frac{\partial V_2}{\partial x}=0, \quad (16)$$

$$-2i\rho\frac{\partial U_1}{\partial y}+(\kappa+1)\frac{\partial^2 V_1}{\partial y^2}-(\kappa-1)\rho^2V_1=0, \quad (17)$$

$$-2\alpha_n\frac{\partial U_2}{\partial x}+(\kappa-1)\frac{\partial^2 V_2}{\partial x^2}-(\kappa+1)\alpha_n{}^2V_2=0. \quad (18)$$

These ordinary differential equations are simplified by introducing operator, $D = \frac{d}{dy}$ and $D^2 = \frac{d^2}{dy^2}$. Equations (15), (17) and (16), (18) or two sets of ordinary differential equations and hence they are separately studied. For equations (15) and (17),

$$\begin{bmatrix} (\kappa-1)D^2-(\kappa+1)\rho^2 & -2i\rho D \\ -2i\rho D & (\kappa+1)D^2-(\kappa-1)\rho^2 \end{bmatrix} \begin{bmatrix} U_1 \\ V_1 \end{bmatrix} = \begin{bmatrix} 0 \\ 0 \end{bmatrix}. \tag{19}$$

Determining the determinant of the coefficient matrix, Δ_1

$$\Delta_1 = (\kappa^2-1)(D^2-\rho^2)^2, \tag{20}$$

The equations for U_1 and V_1 can be uncoupled. Then,

$$\Delta_1 U_1(y,\rho) = 0, \tag{21}$$

$$\Delta_1 V_1(y,\rho) = 0. \tag{22}$$

Assuming a solution of the form e^{ny}, one obtains:

$$n_1 = |\rho|, \tag{23}$$

$$n_2 = -|\rho|. \tag{24}$$

There are double roots, therefore the solutions are as follows:

$$V_1(y,\rho) = A_1(\rho)e^{-|\rho|y} + A_2(\rho)ye^{-|\rho|y} + A_3(\rho)e^{|\rho|y} + A_4(\rho)ye^{|\rho|y}, \tag{25}$$

$$U_1(y,\rho) = B_1(\rho)e^{-|\rho|y} + B_2(\rho)ye^{-|\rho|y} + B_3(\rho)e^{|\rho|y} + B_4(\rho)ye^{|\rho|y}. \tag{26}$$

Alternatively, one can express $U_1(\rho, y)$ as

$$U_1(y,\rho) = m_1A_1(\rho)e^{-|\rho|y} + m_2A_2(\rho)ye^{-|\rho|y} + m_3A_3(\rho)e^{|\rho|y} + m_4A_4(\rho)ye^{|\rho|y}. \tag{27}$$

$A_n(\rho)$ and $B_n(\rho)$ are unknown functions and they will be determined after boundary conditions are prescribed. On the other hand, m_1, m_2, m_3 and m_4 can be determined by putting (25) and (27) into (15) or (17). And thus,

$$m_1 = -i\frac{\kappa A_2}{\rho A_1} + i\frac{|\rho|}{\rho}, \tag{28}$$

$$m_2 = i\,\mathrm{sgn}(\rho), \tag{29}$$

$$m_3 = -i\frac{\kappa A_4}{\rho A_3} - i\frac{|\rho|}{\rho}, \tag{30}$$

$$m_4 = -i\,\mathrm{sgn}(\rho). \tag{31}$$

Then, expressing $A_n(\rho)$ and $B_n(\rho)$ in terms of each other:

$$B_1 = -i\kappa\frac{A_2}{\rho} + i\,\mathrm{sgn}(\rho)A_1, \tag{32}$$

$$B_2 = i\,\mathrm{sgn}(\rho)A_2, \tag{33}$$

$$B_3 = -i\kappa\frac{A_4}{\rho} - i\,\mathrm{sgn}(\rho)A_3, \tag{34}$$

$$B_4 = -i\,\mathrm{sgn}(\rho)A_4. \tag{35}$$

or,

$$A_1 = -i\,\mathrm{sgn}(\rho)B_1 - i\kappa\frac{B_2}{\rho}, \tag{36}$$

$$A_2 = -i\,\mathrm{sgn}(\rho)B_2, \tag{37}$$

$$A_3 = i\,\mathrm{sgn}(\rho)B_3 - i\kappa\frac{B_4}{\rho}, \tag{38}$$

$$A_4 = i\,\mathrm{sgn}(\rho) B_4. \tag{39}$$

can be obtained. Now, expressing $U_1(\rho, y)$ and $V_1(\rho, y)$ in terms of $B_n(\rho)$ one obtains

$$U_1(y,\rho) = B_1 e^{-|\rho|y} + B_2 y e^{-|\rho|y} + B_3 e^{|\rho|y} + B_4 y e^{|\rho|y}, \tag{40}$$

$$\begin{aligned} V_1(y,\rho) &= (i\frac{|\rho|}{\rho} B_1 + i\frac{\kappa}{\rho} B_2) e^{-|\rho|y} + i\frac{|\rho|}{\rho} B_2 y e^{-|\rho|y} \\ &+ (-i\frac{|\rho|}{\rho} B_3 + i\frac{\kappa}{\rho} B_4) e^{|\rho|y} + (-i\frac{|\rho|}{\rho} B_4) y e^{|\rho|y}. \end{aligned} \tag{41}$$

Similar procedure is employed for equations (16) and (18),

$$\begin{bmatrix} (\kappa+1)D^2 - (\kappa-1)\alpha_n{}^2 & 2\alpha_n D \\ 2\alpha_n D & -(\kappa-1)D^2 + (\kappa+1)\alpha_n{}^2 \end{bmatrix} \begin{bmatrix} U_2 \\ V_2 \end{bmatrix} = \begin{bmatrix} 0 \\ 0 \end{bmatrix}. \tag{42}$$

by determining the determinant of the coefficient matrix, Δ_2

$$\Delta_2 = (\kappa^2 - 1)(D^2 - \alpha_n{}^2)^2, \tag{43}$$

One can uncouple the equations. Then,

$$\Delta_2 U_2(x, \alpha_n) = 0, \tag{44}$$

$$\Delta_2 V_2(x, \alpha_n) = 0. \tag{45}$$

There are again double roots and by definition $\alpha_n \geq 0$:

$$U_2(x,\alpha_n) = C_1 e^{-\alpha_n x} + C_2 x e^{-\alpha_n x} + C_3 e^{\alpha_n x} + C_4 x e^{\alpha_n x}, \tag{46}$$

$$V_2(x,\alpha_n) = D_1 e^{-\alpha_n x} + D_2 x e^{-\alpha_n x} + D_3 e^{\alpha_n x} + D_4 x e^{\alpha_n x}. \tag{47}$$

Expressing $C_n(\alpha_n)$ and $D_n(\alpha_n)$ in terms of each other:

$$D_1 = C_1 - \frac{\kappa}{\alpha_n} C_2, \tag{48}$$

$$D_2 = C_2, \tag{49}$$

$$D_3 = -C_3 - \frac{\kappa}{\alpha_n} C_4, \tag{50}$$

$$D_4 = -C_4. \tag{51}$$

Hence,

$$U_2(x, \alpha_n) = C_1 e^{-\alpha_n x} + C_2 x e^{-\alpha_n x} + C_3 e^{\alpha_n x} + C_4 x e^{\alpha_n x}, \tag{52}$$

$$V_2(x, \alpha_n) = (C_1 - \frac{\kappa}{\alpha_n} C_2) e^{-\alpha_n x} + C_2 x e^{-\alpha_n x} + (-C_3 - \frac{\kappa}{\alpha_n} C_4) e^{\alpha_n x} - C_4 x e^{\alpha_n x}. \tag{53}$$

Since in our problem, as $x \to \infty$ displacements must be bounded, $C_3(\alpha_n) = C_4(\alpha_n) = 0.$

Then, the displacements can be written as:

$$U_2(x, \alpha_n) = C_1 e^{-\alpha_n x} + C_2 x e^{-\alpha_n x}, \tag{54}$$

$$V_2(x, \alpha_n) = (C_1 - \frac{\kappa}{\alpha_n} C_2 + x C_2) e^{-\alpha_n x}. \tag{55}$$

Thus, the final form of displacements for the semi-infinite homogeneous medium are expressed as follows:

$$\begin{aligned} u(x, y) = {} & \frac{1}{2\pi} \int_{-\infty}^{\infty} e^{i\rho x} (e^{-|\rho| y} (B_1 + B_2 y) + e^{|\rho| y} (B_3 + B_4 y)) d\rho \\ & + \sum_{n=0}^{\infty} e^{-\alpha_n x} (C_{1n} + x C_{2n}) \cos(y \alpha_n), \end{aligned} \tag{56}$$

$$v(x,y)=\frac{1}{2\pi}\left\{\int_{-\infty}^{\infty}e^{i\rho x}\frac{i}{\rho}(e^{-|\rho|y}(|\rho|B_1+\kappa B_2+y|\rho|B_2)\right.$$
$$\left.+e^{|\rho|y}(B_3|\rho|-\kappa B_4+y|\rho|B_4))d\rho\right\} \tag{57}$$
$$+\sum_{n=0}^{\infty}e^{-\alpha_n x}(C_{1n}-\frac{\kappa}{\alpha_n}C_{2n}+xC_{2n})\sin(y\alpha_n).$$

After defining displacements $u(x,y)$ and $v(x,y)$ in terms of unknowns B_1, B_2, B_3, B_4, C_{1n} and C_{2n} stresses can be obtained by putting (56) and (57) into (3), (4) and (5) as follows:

$$\sigma_{xx}(x,y)=\frac{i\mu_1}{\pi}\left\{\int_{-\infty}^{\infty}e^{i\rho x-y|\rho|}[B_1\rho+B_2(\rho y+\frac{(\kappa-3)}{2}\frac{|\rho|}{\rho})\right.$$
$$\left.+B_3\rho e^{2y|\rho|}+B_4(\rho y-\frac{(\kappa-3)}{2}\frac{|\rho|}{\rho})e^{2y|\rho|}]d\rho\right\}$$
$$+\mu_1\sum_{n=0}^{\infty}e^{-\alpha_n x}[-2\alpha_n C_{1n}+C_{2n}(-1+\kappa-2\alpha_n x)]\cos(\alpha_n y), \tag{58}$$

$$\sigma_{yy}(x,y)=-\frac{i\mu_1}{\pi}\left\{\int_{-\infty}^{\infty}e^{i\rho x-y|\rho|}[B_1\rho+B_2(\rho y+\frac{(\kappa+1)}{2}\frac{|\rho|}{\rho})\right.$$
$$\left.+B_3\rho e^{2y|\rho|}+B_4(\rho y-\frac{(\kappa+1)}{2}\frac{|\rho|}{\rho})e^{2y|\rho|}]d\rho\right\}$$
$$+\mu_1\sum_{n=0}^{\infty}e^{-\alpha_n x}[2\alpha_n C_{1n}+C_{2n}(-3-\kappa+2\alpha_n x)]\cos(\alpha_n y), \tag{59}$$

$$\sigma_{xy}(x,y)=\frac{\mu_1}{\pi}\left\{\int_{-\infty}^{\infty}e^{i\rho x-y|\rho|}[-B_1|\rho|+B_2(\frac{(1-\kappa)}{2}-y|\rho|)\right.$$
$$\left.+B_3|\rho|e^{2y|\rho|}+B_4(\frac{(1-\kappa)}{2}+y|\rho|)e^{2y|\rho|}]d\rho\right\}$$
$$+\mu_1\sum_{n=0}^{\infty}e^{-\alpha_n x}[-2\alpha_n C_{1n}+C_{2n}(1+\kappa-2\alpha_n x)]\sin(\alpha_n y). \tag{60}$$

In the expressions above, B_1, B_2, B_3, B_4, C_{1n} and C_{2n} are arbitrary constants which will be determined from boundary conditions.

2.3 Application of boundary conditions for the homogeneous domain

Since crack is on the symmetry axis, displacements and stresses satisfy the mixed boundary condition.

$$v(x,0) = 0 \text{ for } 0 \le x \le a \text{ and } b \le x < \infty, \tag{61}$$

$$\sigma_{yy}(x,0) = P(x) \text{ for } a < x < b, \tag{62}$$

Due to symmetry, following conditions are prescribed:

$$\sigma_{xy}(x,0) = 0 \text{ for } 0 \le x < \infty, \tag{63}$$

$$v(x,c) = 0 \text{ for } 0 \le x < \infty, \tag{64}$$

$$\sigma_{xy}(x,c) = 0 \text{ for } 0 \le x < \infty. \tag{65}$$

From (56)-(60), one can observe that the unknown constants B_i, $i = 1,..4$ can be expressed in terms of an auxiliary function by using the boundary conditions (61), (63), (64) and (65), without finding C_1 and C_2. This can be done since the series terms in $v(x,y)$ and $\sigma_{xy}(x,y)$ vanish because of the $\sin(\alpha_n y)$ term at $y = 0$ or $y = c$.

Now, the auxiliary function is defined for expressing unknowns as follows:

$$g(x) = \frac{\partial v(x,0)}{\partial x} \text{ for } 0 \le x < \infty. \tag{66}$$

at $y = 0$, $g(x)$ is expressed as follows:

$$g(x) = \frac{\partial}{\partial x}(v(x,0)) = -\frac{1}{2\pi}\int_{-\infty}^{\infty} e^{i\rho x}(|\rho| B_1 + \kappa B_2 - |\rho| B_3 + \kappa B_4)d\rho. \quad (67)$$

taking inverse Fourier transform of (67),

$$-\int_a^b e^{-i\rho x} g(x)dx = |\rho| B_1 + \kappa B_2 - |\rho| B_3 + \kappa B_4. \quad (68)$$

from (63),

$$\frac{\mu}{\pi}\int_{-\infty}^{\infty} e^{i\rho x}(-B_1|\rho| + B_2(\frac{1-\kappa}{2}) + B_3|\rho| + B_4(\frac{1-\kappa}{2}))d\rho = 0. \quad (69)$$

taking inverse Fourier transform of (69),

$$-B_1|\rho| + B_2(\frac{1-\kappa}{2}) + B_3|\rho| + B_4(\frac{1-\kappa}{2}) = 0. \quad (70)$$

from (64),

$$\frac{1}{2\pi}\int_{-\infty}^{\infty} e^{i\rho x}\frac{i}{\rho}(e^{-|\rho|c}(|\rho| B_1 + \kappa B_2 + c|\rho| B_2) - e^{|\rho|c}(|\rho| B_3 - \kappa B_4 + c|\rho| B_4))d\rho = 0. \quad (71)$$

taking inverse Fourier transform of (71),

$$e^{-|\rho|c}|\rho| B_1 + e^{-|\rho|c}(\kappa + c|\rho|)B_2 - e^{|\rho|c}|\rho| B_3 + e^{|\rho|c}(\kappa - c|\rho|)B_4 = 0. \quad (72)$$

from (65),

$$\frac{\mu_1}{\pi}\int_{-\infty}^{\infty} e^{i\rho x}(-B_1|\rho| e^{-c|\rho|} + B_2 e^{-c|\rho|}(\frac{1-\kappa}{2} - c|\rho|) + B_3 e^{c|\rho|}|\rho| + B_4 e^{c|\rho|}(\frac{1-\kappa}{2} + c|\rho|))d\rho = 0. \quad (73)$$

taking inverse Fourier transform of (73),

$$-B_1|\rho|e^{-c|\rho|}+B_2e^{-c|\rho|}(\frac{1-\kappa}{2}-c|\rho|)+B_3e^{c|\rho|}|\rho|+B_4e^{c|\rho|}(\frac{1-\kappa}{2}+c|\rho|)=0. \tag{74}$$

Then, from (68), (70), (72) and (74) B_n's are written in term of auxiliary variable, $g(t)$:

$$B_1=\frac{\int_a^b e^{-i\rho t}g(t)dt((1-\kappa)(e^{-c|\rho|}-e^{c|\rho|})-4c|\rho|e^{-c|\rho|}))e^{c|\rho|}}{(e^{-c|\rho|}-e^{c|\rho|})^2(1+\kappa)|\rho|}, \tag{75}$$

$$B_2=\frac{2e^{c|\rho|}\int_a^b e^{-i\rho t}g(t)dt}{(e^{-c|\rho|}-e^{c|\rho|})(1+\kappa)}, \tag{76}$$

$$B_3=\frac{\int_a^b e^{-i\rho t}g(t)dt((1-\kappa)(e^{-c|\rho|}-e^{c|\rho|})-4c|\rho|e^{c|\rho|}))e^{-c|\rho|}}{(e^{-c|\rho|}-e^{c|\rho|})^2(1+\kappa)|\rho|}, \tag{77}$$

$$B_4=\frac{-2e^{-c|\rho|}\int_a^b e^{-i\rho t}g(t)dt}{(e^{-c|\rho|}-e^{c|\rho|})(1+\kappa)}. \tag{78}$$

Thus, displacements and stresses can now be written in terms of this auxiliary function as follows:

$$\begin{aligned}u(x,y)=\frac{1}{2\pi(1+\kappa)}\Bigg\{&\int_a^b g(t)\int_{-\infty}^{\infty}e^{i\rho(x-t)}[e^{-|\rho|y}(-\frac{2e^{2c|\rho|}y}{(-1+e^{2c|\rho|})}\\&+\frac{e^{2c|\rho|}((-1+e^{2c|\rho|})(-1+\kappa)-4c|\rho|)}{(-1+e^{2c|\rho|})^2|\rho|})+e^{|\rho|y}(\frac{2y}{(-1+e^{2c|\rho|})}\\&-\frac{(-(-1+e^{2c|\rho|})(-1+\kappa)+4ce^{2c|\rho|}|\rho|)}{(-1+e^{2c|\rho|})^2|\rho|})]d\rho dt\Bigg\}\\&+\sum_{n=0}^{\infty}e^{-\alpha_n x}(C_{1n}+xC_{2n})\cos(y\alpha_n),\end{aligned} \tag{79}$$

$$v(x,y)=\frac{i/\rho}{2\pi(1+\kappa)}\int_a^b g(t)\int_{-\infty}^{\infty} e^{i\rho(x-t)}[e^{-|\rho|y}(-\frac{2e^{2c|\rho|}\kappa}{(-1+e^{2c|\rho|})}-\frac{2e^{2c|\rho|}y|\rho|}{(-1+e^{2c|\rho|})}$$
$$+\frac{e^{2c|\rho|}((-1+e^{2c|\rho|})(-1+\kappa)-4c|\rho|)}{(-1+e^{2c|\rho|})^2})$$
$$+e^{|\rho|y}(-\frac{2\kappa}{(-1+e^{2c|\rho|})}+\frac{2y|\rho|}{(-1+e^{2c|\rho|})}$$
$$-\frac{(-(-1+e^{2c|\rho|})(-1+\kappa)+4ce^{2c|\rho|}|\rho|)}{(-1+e^{2c|\rho|})^2})]d\rho dt \qquad (80)$$
$$+\sum_{n=0}^{\infty} e^{-\alpha_n x}(C_{1n}-\frac{\kappa}{\alpha_n}C_{2n}+xC_{2n})\sin(y\alpha_n),$$

$$\sigma_{xx}(x,y)=-\frac{i\mu_1}{\pi(1+\kappa)}\left\{\int_a^b g(t)\int_{-\infty}^{\infty} e^{i\rho(x-t)}[e^{-y|\rho|}\frac{2\mathrm{sgn}(\rho)(e^{-c|\rho|}-e^{c|\rho|})+2\rho((2c-y)e^{-c|\rho|}+ye^{c|\rho|})}{(e^{-c|\rho|}-e^{c|\rho|})^2}e^{c|\rho|}\right.$$
$$\left.+e^{y|\rho|}\frac{2\mathrm{sgn}(\rho)(e^{-c|\rho|}-e^{c|\rho|})+2\rho((2c-y)e^{c|\rho|}+ye^{-c|\rho|})}{(e^{-c|\rho|}-e^{c|\rho|})^2}e^{-c|\rho|}]d\rho dt\right\}$$
$$+\mu_1\sum_{n=0}^{\infty} e^{-\alpha_n x}[-2\alpha_n C_{1n}+C_{2n}(-1+\kappa-2\alpha_n x)]\cos(\alpha_n y), \qquad (81)$$

$$\sigma_{yy}(x,y)=-\frac{2i\mu_1}{\pi(1+\kappa)}\left\{\int_a^b g(t)\int_{-\infty}^{\infty} e^{i\rho(x-t)}(e^{(c-y)|\rho|}\frac{(\mathrm{sgn}(\rho)+\rho y)(e^{-c|\rho|}-e^{c|\rho|})-2c\rho e^{-c|\rho|})}{(e^{-c|\rho|}-e^{c|\rho|})^2}\right.$$
$$\left.+e^{(y-c)|\rho|}\frac{(\mathrm{sgn}(\rho)-\rho y)(e^{-c|\rho|}-e^{c|\rho|})-2c\rho e^{c|\rho|})}{(e^{-c|\rho|}-e^{c|\rho|})^2})d\rho dt\right\} \qquad (82)$$
$$+\mu_1\sum_{n=0}^{\infty} e^{-\alpha_n x}[2\alpha_n C_{1n}+C_{2n}(-3-\kappa+2\alpha_n x)]\cos(\alpha_n y),$$

$$\sigma_{xy}(x,y)=\frac{\mu_1}{\pi(1+\kappa)}\left\{\int_a^b g(t)\int_{-\infty}^{\infty} e^{i\rho(x-t)}[2|\rho|e^{-y|\rho|}\frac{2ce^{-c|\rho|}-y(e^{-c|\rho|}-e^{c|\rho|})}{(e^{-c|\rho|}-e^{c|\rho|})^2}e^{c|\rho|}\right.$$
$$\left.-2|\rho|e^{y|\rho|}\frac{2ce^{c|\rho|}+y(e^{-c|\rho|}-e^{c|\rho|})}{(e^{-c|\rho|}-e^{c|\rho|})^2}e^{-c|\rho|}]d\rho dt\right\}$$
$$+\mu_1\sum_{n=0}^{\infty}e^{-\alpha_n x}[-2\alpha_n C_{1n}+C_{2n}(1+\kappa-2\alpha_n x)]\sin(\alpha_n y). \tag{83}$$

The remaning unknowns C_1 and C_2 should be determined by using the boundary conditions at $x=h$.

2.4 Formulation of FGM strip

Now, formulation of the FGM strip is implemented considering Figure 2.3.

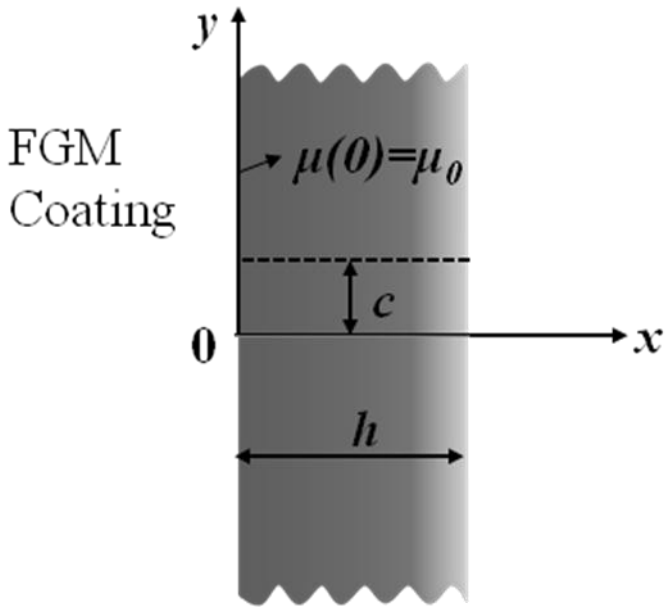

Figure 2.3: Geometry of FGM strip

For the functionally graded material with varying Young's modulus and constant possion ratio, Hooke's law can be written as:

$$\sigma_{xx\_f}(x,y)=\frac{\mu(x)}{(\kappa-1)}((\kappa+1)\frac{\partial u_f}{\partial x}+(3-\kappa)\frac{\partial v_f}{\partial y}), \tag{84}$$

$$\sigma_{yy\_f}(x,y)=\frac{\mu(x)}{(\kappa-1)}((\kappa+1)\frac{\partial v_f}{\partial y}+(3-\kappa)\frac{\partial u_f}{\partial x}), \tag{85}$$

$$\sigma_{xy\_f}(x,y)=\mu(x)(\frac{\partial u_f}{\partial y}+\frac{\partial v_f}{\partial x}), \tag{86}$$

where $\mu(x)=\mu_0 e^{\beta x}$. (87)

Equilibrium equations are as follows:

$$\frac{\partial \sigma_{xx\_f}}{\partial x}+\frac{\partial \sigma_{xy\_f}}{\partial y}=0, \tag{88}$$

$$\frac{\partial \sigma_{xy\_f}}{\partial x}+\frac{\partial \sigma_{yy\_f}}{\partial y}=0. \tag{89}$$

Substituting (84), (85) and (86) into (88) and (89), Navier equations for the displacements are obtained as:

$$(\kappa+1)\frac{\partial^2 u_f}{\partial x^2}+(\kappa-1)\frac{\partial^2 u_f}{\partial y^2}+2\frac{\partial^2 v_f}{\partial x\partial y}+\beta(\kappa+1)\frac{\partial u_f}{\partial x}+\beta(3-\kappa)\frac{\partial v_f}{\partial y}=0, \tag{90}$$

$$(\kappa-1)\frac{\partial^2 v_f}{\partial x^2}+(\kappa+1)\frac{\partial^2 v_f}{\partial y^2}+2\frac{\partial^2 u_f}{\partial x\partial y}+\beta(\kappa-1)\frac{\partial u_f}{\partial y}+\beta(\kappa-1)\frac{\partial v_f}{\partial x}=0. \tag{91}$$

Then, the solution for displacements is assumed to be in the following form:

$$u_f(x,y) = \sum_{n=0}^{\infty} U_f(x,\alpha_n)\cos(y\alpha_n), \tag{92}$$

$$v_f(x,y) = \sum_{n=0}^{\infty} V_f(x,\alpha_n)\sin(y\alpha_n), \tag{93}$$

$$\text{where } \alpha_n = \frac{n\pi}{c}. \tag{94}$$

Substituting (92) and (93) into (90) and (91),

$$\begin{aligned}&\sum_{n=0}^{\infty}\cos(y\alpha_n)((\kappa+1)\frac{\partial^2 U_f}{\partial x^2} - (\kappa-1)\alpha_n{}^2 U_f + 2\alpha_n\frac{\partial V_f}{\partial x}\\ &+\beta(\kappa+1)\frac{\partial U_f}{\partial x} + \beta(3-\kappa)\alpha_n V_f) = 0,\end{aligned} \tag{95}$$

$$\begin{aligned}&\sum_{n=0}^{\infty}\sin(y\alpha_n)((\kappa-1)\frac{\partial^2 V_f}{\partial x^2} - (\kappa+1)\alpha_n{}^2 V_f - 2\alpha_n\frac{\partial U_f}{\partial x}\\ &-\beta(\kappa-1)\alpha_n U_f + \beta(\kappa-1)\frac{\partial V_f}{\partial x}) = 0.\end{aligned} \tag{96}$$

In order to satisfy (95) and (96) for arbitrary values of x and y, each term in the series must be equal to zero.

Then, the governing equations of the problem can be written as follows:

$$(\kappa+1)\frac{\partial^2 U_f}{\partial x^2} - (\kappa-1)\alpha_n{}^2 U_f + 2\alpha_n\frac{\partial V_f}{\partial x} + \beta(\kappa+1)\frac{\partial U_f}{\partial x} + \beta(3-\kappa)\alpha_n V_f = 0 \tag{97}$$

$$(\kappa-1)\frac{\partial^2 V_f}{\partial x^2} - (\kappa+1)\alpha_n{}^2 V_f - 2\alpha_n\frac{\partial U_f}{\partial x} - \beta(\kappa-1)\alpha_n U_f + \beta(\kappa-1)\frac{\partial V_f}{\partial x} = 0 \tag{98}$$

This system of two differential equations are solved by introducing operators, $D = \frac{d}{dy}$ and $D^2 = \frac{d^2}{dy^2}$.

$$\begin{bmatrix} (\kappa+1)D^2 + \beta(\kappa+1)D - (\kappa-1)\alpha_n{}^2 & 2\alpha_n D + \beta(3-\kappa)\alpha_n \\ -2\alpha_n D - \beta(\kappa-1)\alpha_n & (\kappa-1)D^2 + \beta(\kappa-1)D - (\kappa+1)\alpha_n{}^2 \end{bmatrix} \begin{bmatrix} U_f \\ V_f \end{bmatrix} = \begin{bmatrix} 0 \\ 0 \end{bmatrix}, \quad (99)$$

The determinant of the matrix in (99) can be found as

$$\Delta_f = (\kappa^2-1)(D^4 + 2\beta D^3 + (\beta^2 - 2\alpha_n{}^2)D^2 - 2\alpha_n{}^2\beta D + \alpha_n{}^4 + \beta^2\alpha_n{}^2(\frac{3-\kappa}{1+\kappa})). \quad (100)$$

Now, equations can be uncoupled since $\Delta_f U_f = \Delta_f V_f = 0$.

By selecting e^{px} for the solution of U_f or V_f the characteristic equation is obtained.

$$(p^4 + 2\beta p^3 + (\beta^2 - 2\alpha_n{}^2)p^2 - 2\alpha_n{}^2\beta p + \alpha_n{}^4 + \alpha_n{}^2\beta^2\frac{(3-\kappa)}{(1+\kappa)})e^{px} = 0. \quad (101)$$

Since $e^{px} \neq 0$, the multiplicative factor should be equal to zero.

Let this factor be $CE(p)$ and it is written in the following form

$$CE(p) = (p^2 + Cp + D)^2 + F^2 \quad (102)$$

where C, D, F are constants to be determined. The corresponding coefficients in (101) and (102) must be equal to each other. Therefore,

$$C = \beta, \quad (103)$$

$$D = -\alpha_n{}^2, \quad (104)$$

$$F = \pm\alpha_n\beta\sqrt{\frac{3-\kappa}{1+\kappa}}. \quad (105)$$

Then by factorizing (102), the roots of the characteristic equation can be found as follows:

$$p_1 = -\frac{\beta}{2} + \frac{1}{2}\sqrt{\beta^2 + 4{\alpha_n}^2 + 4i\alpha_n\beta\sqrt{\frac{3-\kappa}{1+\kappa}}}, \tag{106}$$

$$p_2 = -\frac{\beta}{2} + \frac{1}{2}\sqrt{\beta^2 + 4{\alpha_n}^2 - 4i\alpha_n\beta\sqrt{\frac{3-\kappa}{1+\kappa}}}, \tag{107}$$

$$p_3 = -\frac{\beta}{2} - \frac{1}{2}\sqrt{\beta^2 + 4{\alpha_n}^2 + 4i\alpha_n\beta\sqrt{\frac{3-\kappa}{1+\kappa}}}, \tag{108}$$

$$p_4 = -\frac{\beta}{2} - \frac{1}{2}\sqrt{\beta^2 + 4{\alpha_n}^2 - 4i\alpha_n\beta\sqrt{\frac{3-\kappa}{1+\kappa}}}. \tag{109}$$

Thus,

$$U_f = E_1(\alpha_n)e^{p_1 x} + E_2(\alpha_n)e^{p_2 x} + E_3(\alpha_n)e^{p_3 x} + E_4(\alpha_n)e^{p_4 x}, \tag{110}$$

$$V_f = F_1(\alpha_n)e^{p_1 x} + F_2(\alpha_n)e^{p_2 x} + F_3(\alpha_n)e^{p_3 x} + F_4(\alpha_n)e^{p_4 x}. \tag{111}$$

Substituting (110) and (111) into (98),

$$\sum_{i=1}^{4} e^{p_i x}[E_i(-2\alpha_n p_i - \beta(\kappa-1)\alpha_n) + F_i((\kappa-1){p_i}^2 + \beta(\kappa-1)p_i - (\kappa+1){\alpha_n}^2)] = 0. \tag{112}$$

Then,

$$E_i = \frac{(\kappa-1)({p_i}^2 + \beta p_i) - (\kappa+1){\alpha_n}^2}{2\alpha_n p_i + \beta(\kappa-1)\alpha_n} F_i, \tag{113}$$

$$q_i = \frac{(\kappa-1)({p_i}^2 + \beta p_i) - (\kappa+1){\alpha_n}^2}{2\alpha_n p_i + \beta(\kappa-1)\alpha_n}. \tag{114}$$

p_i, q_i, E_i and F_i also depend on n through α_n but they are written with sole subscript i rather than with two subscripts in for brevity.

Hence, displacements and stresses for FGM layer are written as follows:

$$u_f(x,y) = \sum_{n=0}^{\infty}\left(\sum_{i=1}^{4} q_i F_i e^{p_i x}\right)\cos(y\alpha_n), \tag{115}$$

$$v_f(x,y) = \sum_{n=0}^{\infty}\left(\sum_{i=1}^{4} F_i e^{p_i x}\right)\sin(y\alpha_n), \tag{116}$$

$$\sigma_{xx\_f} = \frac{\mu_0 e^{\beta x}}{\kappa - 1}\left(\sum_{n=0}^{\infty}\sum_{i=1}^{4} F_i e^{p_i x}(q_i p_i(\kappa+1) + (3-\kappa)\alpha_n)\cos(y\alpha_n)\right), \tag{117}$$

$$\sigma_{yy\_f} = \frac{\mu_0 e^{\beta x}}{\kappa - 1}\left(\sum_{n=0}^{\infty}\sum_{i=1}^{4} F_i e^{p_i x}(\alpha_n(\kappa+1) + (3-\kappa)p_i q_i)\cos(y\alpha_n)\right), \tag{118}$$

$$\sigma_{xy\_f} = \mu_0 e^{\beta x}\left(\sum_{n=0}^{\infty}\sum_{i=1}^{4} F_i e^{p_i x}(-\alpha_n q_i + p_i)\sin(y\alpha_n)\right). \tag{119}$$

Note that this solution readily satisfies $v(x,0) = 0$, $v(x,c)=0$, $\sigma_{xy}(x,0) = 0$, $\sigma_{xy}(x,c) = 0$ $\forall$x. F_i should be determined from the boundary conditions.

2.5 Application of remaining boundary conditions

At this point, homogeneous and FGM solutions which satisfy boundary conditions at $y = 0$ and $y = c$ are obtained.

Referring to Figure 2.1, there are 6 more boundary conditions for FGM coated homogeneous substrate.

Along $x = h$, stresses in both materials, σ_{xx}, σ_{xx_f} and σ_{xy}, σ_{xy_f} are continuous, respectively across the interface between FGM and homogeneous parts. Then, displacements, u and v are also continuous across the interface of FGM and homogeneous parts.

$$\sigma_{xx\_f} = \sigma_{xx} \text{ at } x = h, \tag{120}$$

$$\sigma_{xy\_f} = \sigma_{xy} \text{ at } x = h, \tag{121}$$

$$u_f = u \text{ at } x = h, \tag{122}$$

$$v_f = v \text{ at } x = h. \tag{123}$$

Equations (120), (121), (122) and (123) give the continuity of diplacements and stresses, respectively. Furthermore, stresses, σ_{xx_f} and σ_{xy_f} are zero on the top of FGM strip. This gives the relations of stress free surface of the strip.

$$\sigma_{xx\_f} = 0 \text{ at } x = 0, \tag{124}$$

$$\sigma_{xy\_f} = 0 \text{ at } x = 0. \tag{125}$$

Now, ((120)-(125)) provide six equations for the six unknown functions $F_i (i = 1,..,4)$ and $C_k (k = 1,2)$ so that they can be expressed in terms of auxiliary function $g(x)$. In the forthcoming sections, continuity and free surface conditions are implemented.

2.5.1 Continuity conditions

From (117) at $x = h$,

$$\sigma_{xx\_f} = \frac{\mu_0}{\kappa-1}\sum_{n=0}^{\infty}[F_1 e^{h(\beta+p_1)}(q_1 p_1(\kappa+1)+(3-\kappa)\alpha_n) + F_2 e^{h(\beta+p_2)}(q_2 p_2(\kappa+1)+(3-\kappa)\alpha_n) + F_3 e^{h(\beta+p_3)}(q_3 p_3(\kappa+1)+(3-\kappa)\alpha_n) + F_4 e^{h(\beta+p_4)}(q_4 p_4(\kappa+1)+(3-\kappa)\alpha_n)]\cos(y\alpha_n). \tag{126}$$

For the homogeneous part, $\mu_1 = \mu_0 e^{\beta h}$ since there is no material gradation.

At $x = h$ from (81);

$$\sigma_{xx} = -\frac{i\mu_1}{\pi(1+\kappa)}\int_a^b g(t)\int_{-\infty}^{\infty} e^{-i\rho(t-h)}[e^{-y|\rho|}(\frac{2\,\mathrm{sgn}(\rho)(e^{-c|\rho|}-e^{c|\rho|})+2\rho((2c-y)e^{-c|\rho|}+ye^{c|\rho|})}{(e^{-c|\rho|}-e^{c|\rho|})^2}e^{c|\rho|}) + e^{y|\rho|}(\frac{2\,\mathrm{sgn}(\rho)(e^{-c|\rho|}-e^{c|\rho|})+2\rho((2c-y)e^{c|\rho|}+ye^{-c|\rho|})}{(e^{-c|\rho|}-e^{c|\rho|})^2}e^{-c|\rho|})]d\rho dt + \mu_1\sum_{n=0}^{\infty} e^{-\alpha_n h}(-2\alpha_n C_{1n} + C_{2n}(-1+\kappa-2\alpha_n h))\cos(\alpha_n y). \tag{127}$$

Then applying (120), for $\sigma_{xx\_f} = \sigma_{xx}$

$$\sum_{n=0}^{\infty}(F_{1n}G_{1n}+F_{2n}G_{2n}+F_{3n}G_{3n}+F_{4n}G_{4n}+2\alpha_n e^{-\alpha_n h}C_{1n}-(-1+\kappa-2\alpha_n h)e^{-\alpha_n h}C_{2n})\cos(y\alpha_n) = -\frac{i}{\pi(1+\kappa)}\int_a^b g(t)\int_{-\infty}^{\infty} e^{-i\rho(t-h)}[e^{-y|\rho|}(\frac{2\,\mathrm{sgn}(\rho)(e^{-c|\rho|}-e^{c|\rho|})+2\rho((2c-y)e^{-c|\rho|}+ye^{c|\rho|})}{(e^{-c|\rho|}-e^{c|\rho|})^2}e^{c|\rho|}) + e^{y|\rho|}(\frac{2\,\mathrm{sgn}(\rho)(e^{-c|\rho|}-e^{c|\rho|})+2\rho((2c-y)e^{c|\rho|}+ye^{-c|\rho|})}{(e^{-c|\rho|}-e^{c|\rho|})^2}e^{-c|\rho|})]d\rho dt \tag{128}$$

where

$$G_{1n} = \frac{e^{hp_1}((3-\kappa)\alpha_n+(1+\kappa)p_1 q_1)}{(\kappa-1)}, \tag{129}$$

$$G_{2n} = \frac{e^{hp_2}((3-\kappa)\alpha_n+(1+\kappa)p_2 q_2)}{(\kappa-1)}, \tag{130}$$

$$G_{3n} = \frac{e^{hp_3}((3-\kappa)\alpha_n+(1+\kappa)p_3 q_3)}{(\kappa-1)}, \tag{131}$$

$$G_{4n} = \frac{e^{hp_4}((3-\kappa)\alpha_n + (1+\kappa)p_4 q_4)}{(\kappa - 1)}. \tag{132}$$

Now, recall that $\alpha_n = \frac{n\pi}{c}$ and $\alpha_m = \frac{m\pi}{c}$ for m, n= 0, 1, 2, 3,...

By using orthogonality condition,

$$\int_0^c \cos(\alpha_n y)\cos(\alpha_m y)dy = \begin{cases} c, n = m = 0 \\ c/2, n = m \neq 0, \\ 0, n \neq m \end{cases} \tag{133}$$

multiplying both sides of (128) with $\cos(\alpha_m y)$ and integrating over y from 0 to c, the following equation can be obtained.

$$\begin{aligned} &F_{1n}G_{1n} + F_{2n}G_{2n} + F_{3n}G_{3n} + F_{4n}G_{4n} + 2\alpha_n e^{-\alpha_n h}C_{1n} - (-1+\kappa-2\alpha_n h)e^{-\alpha_n h}C_{2n} = \\ &-\frac{ik_n}{\pi(1+\kappa)}\int_a^b g(t)\int_{-\infty}^{\infty}\int_0^c e^{-i\rho(t-h)}[e^{-y|\rho|}(\frac{2\,\mathrm{sgn}(\rho)(e^{-c|\rho|}-e^{c|\rho|})+2\rho((2c-y)e^{-c|\rho|}+ye^{c|\rho|})}{(e^{-c|\rho|}-e^{c|\rho|})^2})e^{c|\rho|} \\ &\qquad +e^{y|\rho|}(\frac{2\,\mathrm{sgn}(\rho)(e^{-c|\rho|}-e^{c|\rho|})+2\rho((2c-y)e^{c|\rho|}+ye^{-c|\rho|})}{(e^{-c|\rho|}-e^{c|\rho|})^2}e^{-c|\rho|})] \\ &\qquad \cos(\alpha_n y)dy\,d\rho\,dt, \end{aligned} \tag{134}$$

where $k_n = \begin{cases} \frac{1}{c}, n = 0 \\ \frac{2}{c}, n \neq 0 \end{cases}$.

Using the formulae A.9-A15 given in Appendix A, integration over y can be performed leading to

$$\begin{aligned} &F_{1n}G_{1n} + F_{2n}G_{2n} + F_{3n}G_{3n} + F_{4n}G_{4n} + 2\alpha_n e^{-\alpha_n h}C_{1n} - (-1+\kappa-2\alpha_n h)e^{-\alpha_n h}C_{2n} = \\ &\frac{2ik_n}{\pi(1+\kappa)}\int_a^b g(t)\int_{-\infty}^{\infty} e^{-i\rho(t-h)}(\frac{\rho}{\rho^2+\alpha_n{}^2}(1-\frac{\rho^2-\alpha_n{}^2}{\rho^2+\alpha_n{}^2}))d\rho\,dt. \end{aligned} \tag{135}$$

Next, from (119), at $x = h$

$$\sigma_{xy\_f} = \mu_0 \sum_{n=0}^{\infty} [F_1 e^{h(\beta+p_1)}(p_1 - \alpha_n q_1) + F_2 e^{h(\beta+p_2)}(p_2 - \alpha_n q_2) + F_3 e^{h(\beta+p_3)}(p_3 - \alpha_n q_3) + \mathrm{F}_4 e^{h(\beta+p_4)}(p_4 - \alpha_n q_4)]\sin(y\alpha_n). \tag{136}$$

at $x = h$, from (83);

$$\sigma_{xy} = \frac{\mu_1}{\pi(1+\kappa)} \int_a^b g(t) \int_{-\infty}^{\infty} e^{-i\rho(t-h)} [2|\rho| e^{-y|\rho|} (\frac{2ce^{-c|\rho|} - y(e^{-c|\rho|} - e^{c|\rho|})}{(e^{-c|\rho|} - e^{c|\rho|})^2} e^{c|\rho|}) - 2|\rho| e^{y|\rho|} (\frac{2ce^{c|\rho|} + y(e^{-c|\rho|} - e^{c|\rho|})}{(e^{-c|\rho|} - e^{c|\rho|})^2} e^{-c|\rho|})] d\rho dt + \mu_1 \sum_{n=0}^{\infty} e^{-\alpha_n h} (-2\alpha_n C_{1n} + C_{2n}(1+\kappa-2\alpha_n h)) \sin(\alpha_n y). \tag{137}$$

Then, applying (121) for $\sigma_{xy\_f} = \sigma_{xy}$

$$\sum_{n=0}^{\infty} (F_{1n} H_{1n} + F_{2n} H_{2n} + F_{3n} H_{3n} + F_{4n} H_{4n} + 2\alpha_n e^{-\alpha_n h} C_{1n} - (1+\kappa-2\alpha_n h) e^{-\alpha_n h} C_{2n}) \sin(y\alpha_n) = \frac{1}{\pi(1+\kappa)} \int_a^b g(t) \int_{-\infty}^{\infty} e^{-i\rho(t-h)} [2|\rho| e^{-y|\rho|} (\frac{2ce^{-c|\rho|} - y(e^{-c|\rho|} - e^{c|\rho|})}{(e^{-c|\rho|} - e^{c|\rho|})^2} e^{c|\rho|}) - 2|\rho| e^{y|\rho|} (\frac{2ce^{c|\rho|} + y(e^{-c|\rho|} - e^{c|\rho|})}{(e^{-c|\rho|} - e^{c|\rho|})^2} e^{-c|\rho|})] d\rho dt, \tag{138}$$

where

$$H_{1n} = e^{hp_1}(p_1 - \alpha_n q_1), \tag{139}$$

$$H_{2n} = e^{hp_2}(p_2 - \alpha_n q_2), \tag{140}$$

$$H_{3n} = e^{hp_3}(p_3 - \alpha_n q_3), \tag{141}$$

$$H_{4n} = e^{hp_4}(p_4 - \alpha_n q_4). \tag{142}$$

By using orthogonality condition,

$$\int_0^c \sin(\alpha_n y)\sin(\alpha_m y)dy = \begin{cases} 0, n = m = 0 \\ c/2, n = m \neq 0, \\ 0, n \neq m \end{cases} \tag{143}$$

multiplying both sides of (138) with $\sin(\alpha_m y)$ and integrating over y from 0 to c, the following equation can be obtained and one can get;

$$\begin{aligned} &F_{1n}H_{1n} + F_{2n}H_{2n} + F_{3n}H_{3n} + F_{4n}H_{4n} + 2\alpha_n e^{-\alpha_n h}C_{1n} - (1+\kappa-2\alpha_n h)e^{-\alpha_n h}C_{2n} = \\ &\frac{2/c}{\pi(1+\kappa)}\int_a^b g(t)\int_{-\infty}^{\infty}\int_0^c e^{-i\rho(t-h)}[2|\rho|e^{-y|\rho|}(\frac{2ce^{-c|\rho|} - y(e^{-c|\rho|} - e^{c|\rho|})}{(e^{-c|\rho|} - e^{c|\rho|})^2}e^{c|\rho|}) - \\ &\qquad 2|\rho|e^{y|\rho|}(\frac{2ce^{c|\rho|} + y(e^{-c|\rho|} - e^{c|\rho|})}{(e^{-c|\rho|} - e^{c|\rho|})^2}e^{-c|\rho|})]\sin(\alpha_n y)dyd\rho dt \end{aligned} \tag{144}$$

Again, using the formulae A.9-A15 given in appendix A, the integral over y can be taken and it leads to

$$\begin{aligned} &F_{1n}H_{1n} + F_{2n}H_{2n} + F_{3n}H_{3n} + F_{4n}H_{4n} + 2\alpha_n e^{-\alpha_n h}C_{1n} - (1+\kappa-2\alpha_n h)e^{-\alpha_n h}C_{2n} = \\ &\frac{2/c}{\pi(1+\kappa)}\left\{\int_a^b g(t)\int_{-\infty}^{\infty} e^{-i\rho(t-h)}\frac{4\rho^2\alpha_n}{(\rho^2+\alpha_n{}^2)^2}d\rho dt\right\}. \end{aligned} \tag{145}$$

Displacement continuity equations are obtained in a similar way. Applying (122) along with (115) and (79) at $x = h$

$$u_f = \sum_{n=0}^{\infty}(F_1 e^{hp_1}q_1 + F_2 e^{hp_2}q_2 + F_3 e^{hp_3}q_3 + F_4 e^{hp_4}q_4)\cos(y\alpha_n) \tag{146}$$

$$u=\frac{1}{2\pi(1+\kappa)}\int_a^b g(t)\int_{-\infty}^{\infty} e^{-i\rho(t-h)}[e^{-|\rho|y}(-\frac{2e^{2c|\rho|}y}{(-1+e^{2c|\rho|})}+\frac{e^{2c|\rho|}((-1+e^{2c|\rho|})(-1+\kappa)-4c|\rho|)}{(-1+e^{2c|\rho|})^2|\rho|})$$

$$+e^{|\rho|y}(\frac{2y}{(-1+e^{2c|\rho|})}-\frac{(-(-1+e^{2c|\rho|})(-1+\kappa)+4ce^{2c|\rho|}|\rho|)}{(-1+e^{2c|\rho|})^2|\rho|})]d\rho dt$$

$$+\sum_{n=0}^{\infty}e^{-\alpha_n h}(C_{1n}+hC_{2n})\cos(y\alpha_n). \tag{147}$$

Then, for $u_f=u$

$$\sum_{n=0}^{\infty}(F_{1n}J_{1n}+F_{2n}J_{2n}+F_{3n}J_{3n}+F_{4n}J_{4n}-C_{1n}e^{-\alpha_n h}-he^{-\alpha_n h}C_{2n})\cos(y\alpha_n)=$$

$$\frac{1}{2\pi(1+\kappa)}\int_a^b g(t)\int_{-\infty}^{\infty} e^{-i\rho(t-h)}[e^{-|\rho|y}(-\frac{2e^{2c|\rho|}y}{(-1+e^{2c|\rho|})}+\frac{e^{2c|\rho|}((-1+e^{2c|\rho|})(-1+\kappa)-4c|\rho|)}{(-1+e^{2c|\rho|})^2|\rho|})$$

$$+e^{|\rho|y}(\frac{2y}{(-1+e^{2c|\rho|})}-\frac{(-(-1+e^{2c|\rho|})(-1+\kappa)+4ce^{2c|\rho|}|\rho|)}{(-1+e^{2c|\rho|})^2|\rho|})]d\rho dt, \tag{148}$$

where

$$J_{1n}=e^{hp_1}q_1, \tag{149}$$

$$J_{2n}=e^{hp_2}q_2, \tag{150}$$

$$J_{3n}=e^{hp_3}q_3, \tag{151}$$

$$J_{4n}=e^{hp_4}q_4. \tag{152}$$

By using orthogonality relation (133),

$$F_{1n}J_{1n}+F_{2n}J_{2n}+F_{3n}J_{3n}+F_{4n}J_{4n}-C_{1n}e^{-\alpha_n h}-he^{-\alpha_n h}C_{2n}=$$

$$\frac{k_n}{2\pi(1+\kappa)}\int_a^b g(t)\int_{-\infty}^{\infty}\int_0^c e^{-i\rho(t-h)}[e^{-|\rho|y}(-\frac{2e^{2c|\rho|}y}{(-1+e^{2c|\rho|})}+\frac{e^{2c|\rho|}((-1+e^{2c|\rho|})(-1+\kappa)-4c|\rho|)}{(-1+e^{2c|\rho|})^2|\rho|})$$

$$+e^{|\rho|y}(\frac{2y}{(-1+e^{2c|\rho|})}-\frac{(-(-1+e^{2c|\rho|})(-1+\kappa)+4ce^{2c|\rho|}|\rho|)}{(-1+e^{2c|\rho|})^2|\rho|})]\cos(\alpha_n y)dyd\rho dt \tag{153}$$

Using the formulae A.9-A15 given in appendix A and taking the integral over y,

$$F_{1n}J_{1n}+F_{2n}J_{2n}+F_{3n}J_{3n}+F_{4n}J_{4n}-C_{1n}e^{-\alpha_n h}-he^{-\alpha_n h}C_{2n}=$$
$$\frac{k_n}{2\pi(1+\kappa)}\int_a^b g(t)\int_{-\infty}^{\infty}e^{-i\rho(t-h)}[-\frac{2(\rho^2-{\alpha_n}^2)}{(\rho^2+{\alpha_n}^2)^2}+\frac{(-1+\kappa)}{\rho^2+{\alpha_n}^2}]d\rho dt. \tag{154}$$

Finally, applying (123) along with (80) and (116), at $x=h$ one obtains

$$v_f=\sum_{n=0}^{\infty}(F_1e^{hp_1}+F_2e^{hp_2}+F_3e^{hp_3}+F_4e^{hp_4})\sin(y\alpha_n). \tag{155}$$

for the FGM and

$$v=\frac{i/\rho}{2\pi(1+\kappa)}\int_a^b g(t)\int_{-\infty}^{\infty}e^{-i\rho(t-h)}[e^{-|\rho|y}(-\frac{2e^{2c|\rho|}\kappa}{(-1+e^{2c|\rho|})}-\frac{2e^{2c|\rho|}y|\rho|}{(-1+e^{2c|\rho|})}$$
$$+\frac{e^{2c|\rho|}((-1+e^{2c|\rho|})(-1+\kappa)-4c|\rho|)}{(-1+e^{2c|\rho|})^2})+e^{|\rho|y}(-\frac{2\kappa}{(-1+e^{2c|\rho|})}+\frac{2y|\rho|}{(-1+e^{2c|\rho|})}$$
$$-\frac{(-(-1+e^{2c|\rho|})(-1+\kappa)+4ce^{2c|\rho|}|\rho|)}{(-1+e^{2c|\rho|})^2})]d\rho dt$$
$$+\sum_{n=0}^{\infty}e^{-\alpha_n h}(C_{1n}+(-\frac{\kappa}{\alpha_n}+h)C_{2n})\sin(y\alpha_n). \tag{156}$$

for the homogeneous half plane. Then, for $v_f=v$

$$\sum_{n=0}^{\infty}(F_{1n}L_{1n}+F_{2n}L_{2n}+F_{3n}L_{3n}+F_{4n}L_{4n}-C_{1n}e^{-\alpha_n h}+(\frac{\kappa}{\alpha_n}-h)e^{-\alpha_n h}C_{2n})\sin(y\alpha_n)=$$
$$\frac{i/\rho}{2\pi(1+\kappa)}\int_a^b g(t)\int_{-\infty}^{\infty}e^{-i\rho(t-h)}[e^{-|\rho|y}(-\frac{2e^{2c|\rho|}\kappa}{(-1+e^{2c|\rho|})}-\frac{2e^{2c|\rho|}y|\rho|}{(-1+e^{2c|\rho|})}$$
$$+\frac{e^{2c|\rho|}((-1+e^{2c|\rho|})(-1+\kappa)-4c|\rho|)}{(-1+e^{2c|\rho|})^2})$$
$$+e^{|\rho|y}(-\frac{2\kappa}{(-1+e^{2c|\rho|})}+\frac{2y|\rho|}{(-1+e^{2c|\rho|})}$$
$$-\frac{(-(-1+e^{2c|\rho|})(-1+\kappa)+4ce^{2c|\rho|}|\rho|)}{(-1+e^{2c|\rho|})^2})]d\rho dt, \tag{157}$$

where

$$L_{1n}=e^{hp_1}, \tag{158}$$

$$L_{2n}=e^{hp_2}, \tag{159}$$

$$L_{3n}=e^{hp_3}, \tag{160}$$

$$L_{4n}=e^{hp_4}. \tag{161}$$

Applying orthogonality condition (143), after integrating from 0 to *c* with respect to *y*, one obtains;

$$F_{1n}L_{1n}+F_{2n}L_{2n}+F_{3n}L_{3n}+F_{4n}L_{4n}-C_{1n}e^{-\alpha_n h}+(\frac{\kappa}{\alpha_n}-h)e^{-\alpha_n h}C_{2n}=$$
$$\frac{(i/\rho)(2/c)}{2\pi(1+\kappa)}\int_a^b g(t)\int_{-\infty}^{\infty}\int_0^c e^{-i\rho(t-h)}[e^{-|\rho|y}(-\frac{2e^{2c|\rho|}\kappa}{(-1+e^{2c|\rho|})}-\frac{2e^{2c|\rho|}y|\rho|}{(-1+e^{2c|\rho|})}+)$$
$$\frac{e^{2c|\rho|}((-1+e^{2c|\rho|})(-1+\kappa)-4c|\rho|)}{(-1+e^{2c|\rho|})^2}+e^{|\rho|y}(-\frac{2\kappa}{(-1+e^{2c|\rho|})}+\frac{2y|\rho|}{(-1+e^{2c|\rho|})}$$
$$-\frac{(-(-1+e^{2c|\rho|})(-1+\kappa)+4ce^{2c|\rho|}|\rho|)}{(-1+e^{2c|\rho|})^2})]\sin(\alpha_n y)dyd\rho dt. \tag{162}$$

Using the formulae A.9-A15 given in appendix A to take the integral over y, one obtains;

$$F_{1n}L_{1n}+F_{2n}L_{2n}+F_{3n}L_{3n}+F_{4n}L_{4n}-C_{1n}e^{-\alpha_n h}+(\frac{\kappa}{\alpha_n}-h)e^{-\alpha_n h}C_{2n}=$$
$$\frac{-(2/c)}{2\pi(1+\kappa)}\int_a^b g(t)\int_{-\infty}^{\infty}e^{-i\rho(t-h)}\frac{i}{\rho}(\frac{\alpha_n}{\rho^2+\alpha_n{}^2})((1+\kappa)+\frac{4\rho^2}{\rho^2+\alpha_n{}^2})d\rho dt. \quad (163)$$

At this point, the continuity conditions across the interface have been taken care of, so attention could be turned onto free surface conditions.

2.5.2 Free surface conditions

Applying (124) along with (117),

at $x=0$,

$$\sigma_{xx\_f}=\frac{\mu_0}{\kappa-1}\sum_{n=0}^{\infty}(F_1((3-\kappa)\alpha_n+(1+\kappa)p_1q_1)+F_2((3-\kappa)\alpha_n+(1+\kappa)p_2q_2)+$$
$$F_3((3-\kappa)\alpha_n+(1+\kappa)p_3q_3)+F_4((3-\kappa)\alpha_n+(1+\kappa)p_4q_4))\cos(y\alpha_n). \quad (164)$$

Then, for $\sigma_{xx\_f}=0$

$$\sum_{n=0}^{\infty}(F_{1n}M_{1n}+F_{2n}M_{2n}+F_{3n}M_{3n}+F_{4n}M_{4n})\cos(y\alpha_n)=0, \quad (165)$$

where

$$M_{1n}=\frac{((3-\kappa)\alpha_n+(1+\kappa)p_1q_1)}{\kappa-1}, \quad (166)$$

$$M_{2n}=\frac{((3-\kappa)\alpha_n+(1+\kappa)p_2q_2)}{\kappa-1}, \quad (167)$$

$$M_{3n} = \frac{((3-\kappa)\alpha_n + (1+\kappa)p_3 q_3)}{\kappa - 1}, \tag{168}$$

$$M_{4n} = \frac{((3-\kappa)\alpha_n + (1+\kappa)p_4 q_4)}{\kappa - 1}. \tag{169}$$

Multiplying by $\cos(y\alpha_m)dy$ and integrating with respect to y from 0 to c,

$$F_{1n}M_{1n} + F_{2n}M_{2n} + F_{3n}M_{3n} + F_{4n}M_{4n} = 0. \tag{170}$$

Applying (125) along with (119) at $x = 0$,

$$\sigma_{xy\_f} = \mu_0 \sum_{n=0}^{\infty} [F_1(p_1 - \alpha_n q_1) + F_2(p_2 - \alpha_n q_2) + F_3(p_3 - \alpha_n q_3) + F_4(p_4 - \alpha_n q_4)]\sin(y\alpha_n). \tag{171}$$

Then, for $\sigma_{xy\_f} = 0$

$$\mu_0 \sum_{n=0}^{\infty} (F_1 R_1 + F_2 R_2 + F_3 R_3 + F_4 R_4)\sin(y\alpha_n) = 0, \tag{172}$$

where

$$R_{1n} = (p_1 - \alpha_n q_1), \tag{173}$$

$$R_{2n} = (p_2 - \alpha_n q_2), \tag{174}$$

$$R_{3n} = (p_3 - \alpha_n q_3), \tag{175}$$

$$R_{4n} = (p_4 - \alpha_n q_4). \tag{176}$$

Multiplying by $\sin(y\alpha_m)dy$ and integrating with respect to y from 0 to c,

$$F_{1n}R_{1n} + F_{2n}R_{2n} + F_{3n}R_{3n} + F_{4n}R_{4n} = 0. \tag{177}$$

2.5.3 Final form of boundary conditions

Hence, equations (135), (145), (154), (163) , (170) and (177) are obtained from the prescribed boundary conditions. These 6 equations should be further simplified by making integrations on $\rho \in (-\infty, \infty)$.

After making all simplifications by using the formulae given in appendix A, the 6 by 6 system of linear equations for the unknowns F_{in} $(i = 1,2,3,4)$, C_{1n} and C_{2n} can be written as follows;

$$F_{1n}G_{1n} + F_{2n}G_{2n} + F_{3n}G_{3n} + F_{4n}G_{4n} + 2\alpha_n e^{-\alpha_n h}C_{1n} - (-1+\kappa-2\alpha_n h)e^{-\alpha_n h}C_{2n} = \frac{4/c}{(1+\kappa)}\int_a^b g(t)(\alpha_n(t-h))(\sinh(\alpha_n|h-t|) - \cosh(\alpha_n|h-t|))dt, \quad (178)$$

$$F_{1n}H_{1n} + F_{2n}H_{2n} + F_{3n}H_{3n} + F_{4n}H_{4n} + 2\alpha_n e^{-\alpha_n h}C_{1n} - (1+\kappa-2\alpha_n h)e^{-\alpha_n h}C_{2n} = \frac{4/c}{(1+\kappa)}\int_a^b g(t)(1-\alpha_n(h-t))(\cosh(\alpha_n|h-t|) - \sinh(\alpha_n|h-t|))dt, \quad (179)$$

$$F_{1n}J_{1n} + F_{2n}J_{2n} + F_{3n}J_{3n} + F_{4n}J_{4n} - e^{-\alpha_n h}C_{1n} - he^{-\alpha_n h}C_{2n} = \frac{1/c}{(1+\kappa)}\int_a^b g(t)(2|h-t| + \frac{(\kappa-1)}{\alpha_n})(\cosh(\alpha_n|h-t|) - \sinh(\alpha_n|h-t|))dt, \quad (180)$$

$$F_{1n}L_{1n} + F_{2n}L_{2n} + F_{3n}L_{3n} + F_{4n}L_{4n} - C_{1n}e^{-\alpha_n h} + (\frac{\kappa}{\alpha_n} - h)e^{-\alpha_n h}C_{2n} = \frac{1/c}{(1+\kappa)}\int_a^b g(t)(\frac{(1+\kappa)(h-t)}{\alpha_n|h-t|} + (\cosh(\alpha_n|h-t|) - \sinh(\alpha_n|h-t|)(2(h-t) - \frac{(1+\kappa)(h-t)}{\alpha_n|h-t|}))dt, \quad (181)$$

$$F_{1n}M_{1n} + F_{2n}M_{2n} + F_{3n}M_{3n} + F_{4n}M_{4n} = 0, \quad (182)$$

$$F_{1n}R_{1n} + F_{2n}R_{2n} + F_{3n}R_{3n} + F_{4n}R_{4n} = 0. \tag{183}$$

2.6 Derivation of singular integral equation

If one writes this system of equations in matrix form, then the unknowns F_1, F_2, F_3, F_4, C_1 and C_2 can be found easily in terms of auxiliary function, $g(t)$ by inverting this matrix.

The matrix form of system of equations (178)-(183) is given as:

$$\begin{bmatrix} G_{1n} & G_{2n} & G_{3n} & G_{4n} & 2\alpha_n e^{-\alpha_n h} & -(-1+\kappa-2\alpha_n h)e^{-\alpha_n h} \\ H_{1n} & H_{2n} & H_{3n} & H_{4n} & 2\alpha_n e^{-\alpha_n h} & -(1+\kappa-2\alpha_n h)e^{-\alpha_n h} \\ J_{1n} & J_{2n} & J_{3n} & J_{4n} & -e^{-\alpha_n h} & -he^{-\alpha_n h} \\ L_{1n} & L_{2n} & L_{3n} & L_{4n} & -e^{-\alpha_n h} & (\frac{\kappa}{\alpha_n}-h)e^{-\alpha_n h} \\ M_{1n} & M_{2n} & M_{3n} & M_{4n} & 0 & 0 \\ R_{1n} & R_{2n} & R_{3n} & R_{4n} & 0 & 0 \end{bmatrix} \begin{bmatrix} F_{1n} \\ F_{2n} \\ F_{3n} \\ F_{4n} \\ C_{1n} \\ C_{2n} \end{bmatrix} = \begin{bmatrix} \int_a^b g(t)Z_1 dt \\ \int_a^b g(t)Z_2 dt \\ \int_a^b g(t)Z_3 dt \\ \int_a^b g(t)Z_4 dt \\ 0 \\ 0 \end{bmatrix}, \tag{184}$$

where

$$Z_{1n} = (\frac{4/c}{1+\kappa})(\alpha_n(t-h))(\sinh(\alpha_n|h-t|) - \cosh(\alpha_n|h-t|)), \tag{185}$$

$$Z_{2n} = (\frac{4/c}{1+\kappa})(1-\alpha_n(h-t))(\cosh(\alpha_n|h-t|) - \sinh(\alpha_n|h-t|)), \tag{186}$$

$$Z_{3n} = (\frac{1/c}{1+\kappa})(2|h-t| + \frac{(\kappa-1)}{\alpha_n})(\cosh(\alpha_n|h-t|) - \sinh(\alpha_n|h-t|)), \tag{187}$$

$$Z_{4n} = \frac{1/c}{(1+\kappa)}\left(\frac{(1+\kappa)(h-t)}{\alpha_n|h-t|}\right.$$

$$\left.+(\cosh(\alpha_n|h-t|)-\sinh(\alpha_n|h-t|)(2(h-t)-\frac{(1+\kappa)(h-t)}{\alpha_n|h-t|}))\right). \quad (188)$$

One can solve for the unknowns by inverting the matrix, i.e.,

$$\begin{bmatrix} F_{1n} \\ F_{2n} \\ F_{3n} \\ F_{4n} \\ C_{1n} \\ C_{2n} \end{bmatrix} = \begin{bmatrix} G_{1n} & G_{2n} & G_{3n} & G_{4n} & 2\alpha_n e^{-\alpha_n h} & -(-1+\kappa)e^{-\alpha_n h} \\ H_{1n} & H_{2n} & H_{3n} & H_{4n} & 2\alpha_n e^{-\alpha_n h} & -(1+\kappa)e^{-\alpha_n h} \\ J_{1n} & J_{2n} & J_{3n} & J_{4n} & -e^{-\alpha_n h} & -he^{-\alpha_n h} \\ L_{1n} & L_{2n} & L_{3n} & L_{4n} & -e^{-\alpha_n h} & (\frac{\kappa}{\alpha_n}-h)e^{-\alpha_n h} \\ M_{1n} & M_{2n} & M_{3n} & M_{4n} & 0 & 0 \\ R_{1n} & R_{2n} & R_{3n} & R_{4n} & 0 & 0 \end{bmatrix}^{-1} \begin{bmatrix} \int_a^b g(t)Z_1 dt \\ \int_a^b g(t)Z_2 dt \\ \int_a^b g(t)Z_3 dt \\ \int_a^b g(t)Z_4 dt \\ 0 \\ 0 \end{bmatrix}. \quad (189)$$

For the problem considered in this thesis, it is sufficient to solve C_{1n} and C_{2n}. Before finding them, some simplifications should be made. Therefore, the matrix equation (189) is rewritten for simplicity as shown in Appendix B. After many manipulations, C_{1n} and C_{2n} are written as follows (α_{5k} and α_{6k}, $k = 1,..,4$ are given in appendix B);

$$C_{1n} = \alpha_{51}\int_a^b Z_1 g(t)dt + \alpha_{52}\int_a^b Z_2 g(t)dt + \alpha_{53}\int_a^b Z_3 g(t)dt + \alpha_{54}\int_a^b Z_4 g(t)dt, \quad (190)$$

$$C_{2n} = \alpha_{61}\int_a^b Z_1 g(t)dt + \alpha_{62}\int_a^b Z_2 g(t)dt + \alpha_{63}\int_a^b Z_3 g(t)dt + \alpha_{64}\int_a^b Z_4 g(t)dt. \quad (191)$$

After obtaining expressions of C_{1n} and C_{2n} in terms of $g(t)$, one can substitute them into boundary condition (62) and take the limit $\lim_{y\to 0}\sigma_{yy}(x,y)$ to obtain a singular integral equation for $g(t)$.

Recalling (82) and doing the manipulations given in Appendix C;

$$\sigma_{yy}(x,y) = -\frac{4\mu_1}{\pi(1+\kappa)}\int_a^b g(t)\int_0^\infty \sin\rho(x-t)\left(\frac{\cosh(c-y)\rho}{\sinh c\rho}\right.$$
$$\left. + \rho y\frac{\sinh(c-y)\rho}{\sinh c\rho} + c\rho\frac{\cosh y\rho}{\sinh^2 c\rho}\right)d\rho dt \qquad (192)$$
$$+\mu_1\sum_{n=0}^{\infty} e^{-\alpha_n x}[2\alpha_n C_{1n} + C_{2n}(-3-\kappa+2\alpha_n x)]\cos(\alpha_n y),$$

where

$$C_{1n} = \int_a^b g(t)\hat{C}_{1n}(\alpha_n,t,c,\kappa,\beta,h), \qquad (193)$$

$$C_{2n} = \int_a^b g(t)\hat{C}_{2n}(\alpha_n,t,c,\kappa,\beta,h). \qquad (194)$$

Now, taking the limit $\lim_{y\to 0}\sigma_{yy}(x,y)$

$$\sigma_{yy} = \frac{-4\mu_1}{\pi(1+\kappa)}\int_a^b g(t)\int_0^\infty \sin(\rho(x-t))\left(\frac{\cosh(\rho(c))}{\sinh(\rho c)} + \right.$$
$$\left. \rho y\frac{\sinh(\rho c)}{\sinh(\rho c)} + \rho c\frac{1}{\sinh^2(\rho c)}\right)d\rho dt$$
$$\mu_1\sum_{n=0}^{\infty} e^{-\alpha_n x}(2\alpha_n C_{1n} + (-3-\kappa+2\alpha_n x)C_{2n}). \qquad (195)$$

Using formulae A.17-A.20 given in appendix A and switching orders of series summation and integration;

$$\sigma_{yy} = \frac{4\mu_1}{\pi(1+\kappa)} \int_a^b g(t)[-\frac{\pi}{2c}(\frac{2\sinh(\frac{\pi}{c}(x-t)) - (\frac{\pi}{c}(x-t))}{\cosh(\frac{\pi}{c}(x-t)) - 1}) + \frac{\pi(1+\kappa)}{4} \sum_{n=0}^{\infty} e^{-\alpha_n x}(2\alpha_n \hat{C}_{1n} + (-3-\kappa+2\alpha_n x)\hat{C}_{2n})]dt, \tag{196}$$

Now, by adding $\frac{1}{t-x}$ into the integral term and substracting $\frac{1}{t-x}$ from it, Cauchy and Fredholm kernels can be found respectively;

$$\sigma_{yy} = \frac{4\mu}{\pi(1+\kappa)} \int_a^b g(t)[\frac{1}{t-x} - \frac{\pi}{2c}(\frac{2\sinh(\frac{\pi}{c}(x-t)) - (\frac{\pi}{c}(x-t))}{\cosh(\frac{\pi}{c}(x-t)) - 1}) - \frac{1}{t-x} + \frac{\pi(1+\kappa)}{4} \sum_{n=0}^{\infty} e^{-\alpha_n x}(2\alpha_n \hat{C}_{1n} + (-3-\kappa+2\alpha_n x)\hat{C}_{2n})]dt, \tag{197}$$

Recognizing the fact that $\sigma_{yy}(x,0) = P(x)$ for $a < x < b$, and using (197)

$$\frac{1}{\pi} \int_a^b g(t)(\frac{1}{t-x} + K_1(x,t) + K_2(x,t))dt = \frac{(1+\kappa)}{4\mu_1} P(x), \tag{198}$$

where

$$K_1(x,t) = -\frac{\pi}{2c}(\frac{2\sinh(\frac{\pi}{c}(x-t)) - (\frac{\pi}{c}(x-t))}{\cosh(\frac{\pi}{c}(x-t)) - 1}) - \frac{1}{t-x}, \tag{199}$$

$$K_2(x,t) = \frac{\pi(1+\kappa)}{4} \sum_{n=0}^{\infty} e^{-\alpha_n x}(2\alpha_n \hat{C}_{1n} + (-3-\kappa+2\alpha_n x)\hat{C}_{2n}). \tag{200}$$

Hence, the singular integral equation is obtained. The Cauchy-kernel $\frac{1}{t-x}$ is dominant part of the equation. $K_1(x,t)$ and $K_2(x,t)$ are bounded Fredholm kernels.

A series expansion-collocation method is used to solve this singular integral equation. The solution method is outlined in the next section.

2.7 Numerical solution of singular integral equation

In order to solve integral equation (198), it should be normalized first. Then defining,

$$t = \frac{b-a}{2} s + \frac{b+a}{2} \quad \text{for } -1 < s < +1, \tag{201}$$

$$x = \frac{b-a}{2} r + \frac{b+a}{2} \quad \text{for } -1 < r < +1, \tag{202}$$

$$g(t) = g(t(s)) = G(s), \tag{203}$$

$$K_1(x(r), t(s)) = \hat{K}_1(r, s), \tag{204}$$

$$K_2(x(r), t(s), \alpha_n) = \hat{K}_2(r, s), \tag{205}$$

$$P(x(r)) = \hat{P}(r), \tag{206}$$

(198) becomes,

$$\frac{1}{\pi} \int_{-1}^{+1} G(s) \left(\frac{1}{r-s} + \frac{b-a}{2} \hat{K}_1(r, s) + \frac{b-a}{2} \hat{K}_1(r, s) \right) dr = -\frac{(1+\kappa)}{4\mu_1} \hat{P}(r). \tag{207}$$

(207) will be solved by using a series expansion method. Recognizing the singular behavior of imbedded crack at $s = \pm 1$, the unknown function $G(s)$ can be expressed as follows:

$$G(s)=\psi(s)(1-s)^{\theta}(1+s)^{\phi}, \tag{208}$$

where $\theta=\phi=-\frac{1}{2}$, (209)

$$W(s)=(1-s)^{\theta}(1+s)^{\phi}. \tag{210}$$

Now, one can express ψ in terms of a series of Jacobi Polynomials.

$$\psi(s)=\sum_{k=0}^{N} a_k P_k^{(\theta,\phi)}(s). \tag{211}$$

In (211) a_k are the unknown coefficients to be determined. Substituting (211) along with (208) into (207), the singular integral equation is expressed as follows:

$$\frac{1}{\pi}\int_{-1}^{+1}\sum_{k=0}^{N} a_k P_k^{(\theta,\phi)}(s)\left(\frac{W(s)}{r-s}+\frac{b-a}{2}W(s)\hat{K}_1(r,s)+\frac{b-a}{2}W(s)\hat{K}_2(r,s)\right)ds=\frac{(1+\kappa)}{4\mu_1}\hat{P}(r). \tag{212}$$

Switching the orders of integration and summation the singular integral equation is finally expressed as follows:

$$\sum_{k=0}^{N} a_k\left(\frac{1}{\pi}\int_{-1}^{+1}\frac{P_k^{(\theta,\phi)}(s)W(s)}{r-s}ds+\int_{-1}^{+1}\frac{b-a}{2\pi}W(s)(\hat{K}_1(r,s)+\hat{K}_2(r,s))P_k^{(\theta,\phi)}(s)ds\right) =\frac{(1+\kappa)}{4\mu_1}\hat{P}(r). \tag{213}$$

where the dominant part of the integral equation $\frac{1}{\pi}\int_{-1}^{+1}\frac{P_k^{(\theta,\phi)}(s)W(s)}{r-s}ds$ has a closed form formula for a given r so that it can be calculated easily (Kaya, 1984) where as

$\int_{-1}^{+1}\frac{b-a}{2\pi}W(s)(\hat{K}_1(r,s)+\hat{K}_2(r,s))P_k^{(\theta,\phi)}(s)ds$ can be evaluated numerically by Gauss-Jacobi quadrature. On the other hand, this integral equation has a single valuedness condition which is

$$\int_a^b g(t)dt = 0\,. \tag{214}$$

This condition ensures that the crack is closed at the tips. After normalization, this equation can be expressed as follows:

$$\int_{-1}^{+1} G(s)ds = \int_{-1}^{+1} \psi(s)(1-s)^{\theta}(1+s)^{\phi}\,ds = 0. \tag{215}$$

Substituting ψ in terms of a series of Jacobi Polynomials, one obtains

$$\int_{-1}^{+1} \sum_{k=0}^{N} a_k P_k^{(\theta,\phi)}(s)(1-s)^{\theta}(1+s)^{\phi}\,ds = 0. \tag{216}$$

Switching the orders of integration and summation again,

$$\sum_{k=0}^{N} a_k \int_{-1}^{+1} P_k^{(\theta,\phi)}(s)(1-s)^{\theta}(1+s)^{\phi}\,ds = 0. \tag{217}$$

From orthogonality relationships of Jacobi polynomials, one can observe that

$$\int_{-1}^{+1} P_k^{(\theta,\phi)}(s)(1-s)^{\theta}(1+s)^{\phi}\,ds = \begin{cases} \pi, k = 0 \\ 0, k \neq 0 \end{cases}. \tag{218}$$

Then, in the summation above, all the terms except a_0 vanishes, giving $\pi a_0 = 0$, therefore a_0=0.

Then, (213) can be written as

$$\sum_{k=1}^{N} a_k \left(\frac{1}{\pi} \int_{-1}^{+1} \frac{P_k^{(\theta,\phi)}(s)W(s)}{r-s}\,ds + \int_{-1}^{+1} \frac{b-a}{2\pi} W(s)(\hat{K}_1(r,s) + \hat{K}_2(r,s))P_k^{(\theta,\phi)}(s)ds \right)$$
$$= \frac{(1+\kappa)}{4\mu_1} \hat{P}(r). \tag{219}$$

In order to solve unknown coefficients $a_k (k = 1,..,N)$ (219) can be written for N collocation points by taking

$$r_i = \cos(\frac{\pi(2i-1)}{2N-2}) \quad , \; i = 1,..,N \tag{220}$$

and the resulting system of N*N linear equations can be solved.

Once $a_k (k = 1,..,N)$ are known, one can obtain;

$$\psi(\pm 1) = \sum_{k=0}^{N} a_k P_k^{(-1/2,-1/2)}(\pm 1). \tag{221}$$

CHAPTER 3

NUMERICAL RESULTS

Solution was obtained for mode I crack problem and hence, stress intensity factors are obtained in this section for various values of crack periodicity, crack length, crack location, layer thickness and material gradation.

The stress intensity factors can be found by using (219). After determining a_k , the stress intensity factors are defined as follows;

$$k(a) = \lim_{x \to a^-} \sqrt{2(a-x)}\sigma_{yy}(x,0) = \frac{4\mu_1}{\kappa+1}\sqrt{\frac{b-a}{2}}\psi(-1) \tag{222}$$

$$k(b) = \lim_{x \to a^-} \sqrt{2(x-b)}\sigma_{yy}(x,0) = -\frac{4\mu_1}{\kappa+1}\sqrt{\frac{b-a}{2}}\psi(+1) \tag{223}$$

3.1. Uniform loading

Remembering that the loading is applied through crack surface pressure.

$$\sigma_{yy}(x,0) = P(x) \text{ for } a < x < b, \tag{224}$$

for imbedded cracks, normalized SIFs can be expressed as;

$$k^*(a) = \frac{k(a)}{\sigma_0 \sqrt{(b-a)/2}}. \tag{225}$$

where σ_0 is the applied uniform crack surface load.

Convergence analysis is made for obtaining accuracy of results. In convergence analysis, if stress intensity factors stay stable, while NP and NS are increased, the desired accuracy is achieved. Hence, when *NP*=44 and *NS*=20, the results become stable as seen above Tables 3.1-2. On the other hand, computer program used in this study has a capacity of computing results for $0<h/a<1$, $0<h\beta<710$, $0< l/(l+2c)<1$ and $10^{-5}<l/a<10^{5}$.

Table 3.1: Comparison of *k*(a)* and *k*(b)* for a thick FGM layer under uniform loading for different *NP* and *NS* numbers and for $l/(l+2c)$=0.5 and $h\beta=10^{-3}$.

h/a=0.9	*NP*=36 *NS*=16		*NP*=40 *NS*=18		*NP*=44 *NS*=20		*NP*=48 *NS*=22	
l/a	*k*(a)*	*k*(b)*	*k*(a)*	*k*(b)*	*k*(a)*	*k*(b)*	*k*(a)*	*k*(b)*
1	0.5702	0.5702	0.5702	0.5702	0.5702	0.5702	0.5702	0.5702
10	0.5850	0.5712	0.5850	0.5712	0.5850	0.5712	0.5850	0.5712
20	0.6122	0.5706	0.6122	0.5706	0.6121	0.5706	0.6121	0.5706
30	0.6427	0.5701	0.6427	0.5701	0.6427	0.5701	0.6427	0.5701
40	0.6715	0.5698	0.6715	0.5698	0.6715	0.5698	0.6714	0.5698
50	0.6980	0.5695	0.6980	0.5695	0.6980	0.5695	0.6979	0.5695
60	0.7225	0.5692	0.7225	0.5692	0.7225	0.5692	0.7224	0.5692
70	0.7453	0.5690	0.7453	0.5690	0.7452	0.5691	0.7452	0.5691
80	0.7666	0.5689	0.7666	0.5689	0.7665	0.5689	0.7665	0.5689
90	0.7868	0.5688	0.7867	0.5688	0.7866	0.5688	0.7865	0.5688
100	0.8059	0.5686	0.8057	0.5686	0.8056	0.5686	0.8055	0.5687

Table 3.2: Comparison of *k*(a)* and *k*(b)* for a thick FGM layer under uniform loading for different *NP* and *NS* numbers and for $l/(l+2c)$=0.5 and $h\beta$=1.

h/a=0.9	*NP*=36 *NS*=16		*NP*=40 *NS*=18		*NP*=44 *NS*=20		*NP*=48 *NS*=22	
l/a	*k*(a)*	*k*(b)*	*k*(a)*	*k*(b)*	*k*(a)*	*k*(b)*	*k*(a)*	*k*(b)*
1	0.5720	0.5703	0.5720	0.5703	0.5720	0.5703	0.5720	0.5703
10	0.6059	0.5709	0.6059	0.5709	0.6059	0.5709	0.6059	0.5709
20	0.6527	0.5701	0.6527	0.5701	0.6526	0.5701	0.6526	0.5701
30	0.6961	0.5696	0.6960	0.5696	0.6959	0.5696	0.6958	0.5696
40	0.7347	0.5692	0.7344	0.5692	0.7343	0.5692	0.7342	0.5692
50	0.7693	0.5690	0.7689	0.5690	0.7687	0.5690	0.7685	0.5690
60	0.8008	0.5688	0.8004	0.5688	0.8001	0.5688	0.7998	0.5688
70	0.8299	0.5686	0.8293	0.5686	0.8289	0.5686	0.8286	0.5686
80	0.8570	0.5684	0.8563	0.5684	0.8558	0.5685	0.8554	0.5685
90	0.8825	0.5683	0.8816	0.5683	0.8810	0.5683	0.8805	0.5683
100	0.9066	0.5682	0.9054	0.5682	0.9047	0.5682	0.9042	0.5682

Moreover, finite element analysis using Ansys computer program is carried out to verify (-) results on stress intensity factors. As the results are shown in Tables 3.3-4, they are almost same with ones provided in this study. Therefore, one should notice that present study has very satisfactory accuracy with finite element method numerically.

Table 3.3: Comparison of k*(a)s provided by Ansys and current study for different nonhomogeneity parameters hβ and for a thick FGM layer under uniform loading

h/a=0.9	$h\beta=10^{-3}$ (almost homogeneous)		$h\beta=0.5$ ($\mu 1/\mu 0\approx 1.648$)		$h\beta=1$ ($\mu 1/\mu 0\approx 2.718$)	
l/a	Current Study	Obtained in Ansys	Current Study	Obtained in Ansys	Current Study	Obtained in Ansys
1	1.0067	1.0075	1.0242	1.0249	1.0415	1.0422
6	0.7609	0.7610	0.7786	0.7788	0.7960	0.7961
14	0.4892	0.4893	0.4974	0.4975	0.5054	0.5056
31	0.3280	0.3281	0.3335	0.3336	0.3389	0.3390
50	0.2582	0.2587	0.2626	0.2630	0.2669	0.2673

Table 3.4: Comparison of $k^*(a)$s provided by Ansys and current study for different nonhomogeneity parameters $h\beta$ and for a thick FGM layer under parabolic loading

h/a=0.9	$h\beta=10^{-3}$ (almost homogeneous)		$h\beta$=0.5 ($\mu 1/\mu 0 \approx 1.648$)		$h\beta$=1 ($\mu 1/\mu 0 \approx 2.718$)	
l/a	Current Study	Obtained in Ansys	Current Study	Obtained in Ansys	Current Study	Obtained in Ansys
1	0.1263	0.1261	0.1305	0.1303	0.1346	0.1343
6	0.0473	0.0474	0.0471	0.0472	0.0468	0.0469
14	0.0012	0.0012	0.0002	0.0002	-0.0009	-0.0009
31	0.0000	0.0000	-0.0001	-0.0001	-0.0003	-0.0003
50	0.0000	0.0000	-0.0000	-0.0000	-0.0001	-0.0001

In order to validate the formulation and numerical results, comparisons should be made with previously published results which are obtained for special cases of the problem considered here. For this purpose, two sets of benchmark results have been identified. First set of benchmark results (only $k^*(a)$) are given in (Murakami, 1987), for an array of imbedded periodic cracks in a homogeneous half-plane. The second set of benchmark results come from (Rizk, 2003) but in an indirect manner. In (Rizk, 2003), a thermal stress problem has been solved for a homogeneous half plane containing periodic imbedded cracks so SIFs for uniform crack traction are not available. But, the kernels for homogeneous half plane problem were given. Therefore, those kernels are programmed as well to produce homogeneous half-plane results (both $k^*(a)$ and $k^*(b)$) for a wide range of geometric parameters. In other words, Rizk's kernel is placed into our computer

program and results are tabulated in Tables 3.5-6 (Hypersingular integral equation D.1-D.3 for Rizk(2003) is given in Appendix D). These results obtained through Rizk's kernels are shortly referred to as Rizk's results for brevity. Uniform crack surface traction results are also available in (Nied, 1987) albeit in graphical form, thus lacking the desired accuracy for numerical comparisons. On the other hand, less accurate graphical comparisons can be made.

For very small βh (β being the non-homogeneity parameter) values, the results are almost the same as benchmark results for different crack periodicities as seen in Tables 3.5 and 3.6.

Table 3.5: Comparison of $k^*(a)$ for imbedded periodic cracks with Rizk (2003) and Murakami (1987), $\beta h = 10^{-3}$ and $\frac{h}{a} = 0.5$

(b-a)/(b+a)	(b-a)/(4c)	Rizk (2003)	Current Study	Murakami (1987)
0.333	0.05	1.0067	1.0067	Not available
	0.10	0.9609	0.9609	0.9608
	0.20	0.8528	0.8528	0.8528
	0.33	0.7012	0.7012	0.7015
	0.50	0.5702	0.5702	0.5729
0.5	0.05	1.0573	1.0573	Not available
	0.10	0.9888	0.9888	0.9888
	0.20	0.8594	0.8594	0.8594
	0.33	0.7087	0.7087	0.7089
	0.50	0.5729	0.5729	0.5735

Table 3.6: Comparison of $k^*(b)$ for imbedded periodic cracks with Rizk (2003), $\beta h = 10^{-3}$ and $\frac{h}{a} = 0.5$

(b-a)/(b+a)	(b-a)/(4c)	Rizk (2003)	Current Study
0.333	0.05	0.9987	0.9987
	0.10	0.9585	0.9585
	0.20	0.8501	0.8501
	0.33	0.7006	0.7006
	0.50	0.5702	0.5702
0.5	0.05	1.0226	1.0226
	0.10	0.9668	0.9668
	0.20	0.8545	0.8545
	0.33	0.7021	0.7021
	0.50	0.5703	0.5703

From Tables 3.5-6, it can be observed that results are very satisfactory when functionally graded material is almost homogeneous for $\beta h = 10^{-3}$ and $\frac{h}{a} = 0.5$.

On the one hand, variation of normalized SIFs are shown in Figures 3.1-2 with respect to $l/(l+2c)$ for $l/a = 1,\ 10,\ 100$ where $l = b - a$. Results are also printed in Table 3.7. The parameter $l/(l+2c)$ is a measure of crack period with respect to crack length. For very closely spaced cracks $l/(l+2c) \to 1$ where as for widely spaced cracks (the limiting case being single crack) $l/(l+2c) \to 0$.

Table 3.7: Comparison of $k^*(a)$ and $k^*(b)$ for $\frac{h}{a}=0.5$

$h\beta=10^{-3}$	$l/a=1$		$l/a=10$		$l/a=100$	
$l/(l+2c)$	$k^*(a)$	$k^*(b)$	$k^*(a)$	$k^*(b)$	$k^*(a)$	$k^*(b)$
1	0	0	0	0	0	0
0.9434	0.1382	0.1382	0.1382	0.1382	0.1408	0.1382
0.8333	0.2523	0.2523	0.2535	0.2523	0.2690	0.2523
0.7143	0.3568	0.3568	0.3632	0.3568	0.4155	0.3568
0.6250	0.4372	0.4372	0.4453	0.4372	0.5466	0.4372
0.5000	0.5702	0.5702	0.5850	0.5712	0.8057	0.5686
0.4386	0.6487	0.6485	0.6770	0.6511	0.9979	0.6453
0.3333	0.7924	0.7904	0.8827	0.7958	1.4622	0.7929
0.2000	0.9370	0.9354	1.1990	0.9782	2.2214	1.0331
0.1111	0.9953	0.9889	1.3779	1.0973	2.6659	1.2068
0	1.0345	1.0246	1.4637	1.1626	2.9129	1.2997

The results obtained using this study are compared with those in Nied (1987)'s study which is a very similar crack problem. In our study, only difference is that an FGM layer is coated on top of the homogeneous surface. There is no FGM coating on the homogeneous half plane in Nied's study. To compare the results FGM layer is again taken to be almost homogeneous $(\frac{\mu_1}{\mu_0}\cong 1)$.

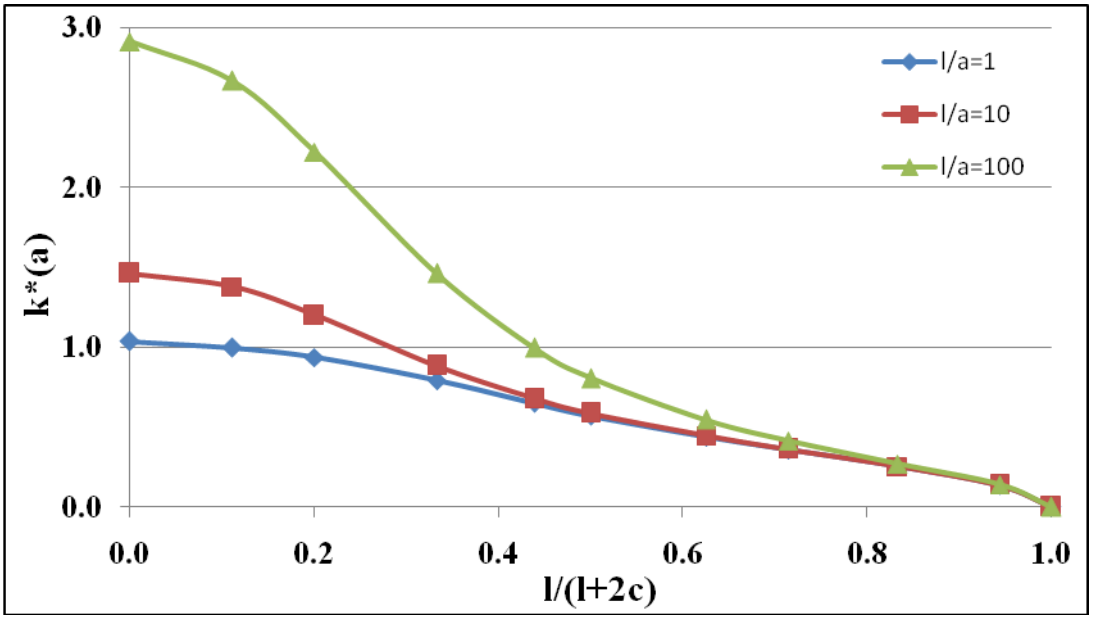

Figure 3.1: $k^*(a)$ under uniform applied stress for $\frac{h}{a}=0.5$ and $\beta h=10^{-3}$

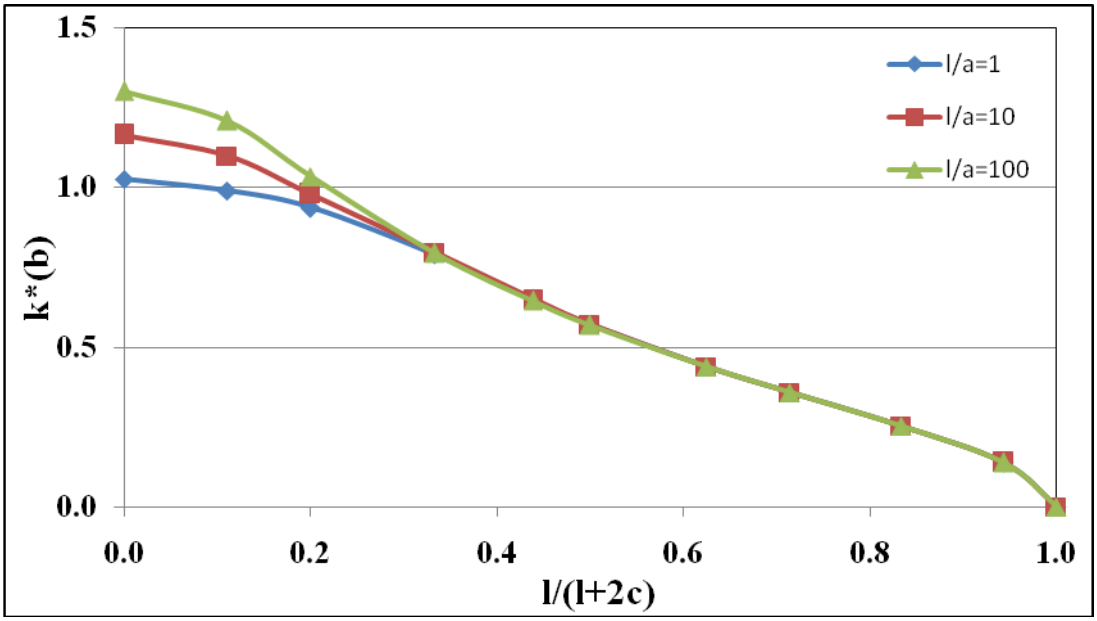

Figure 3.2: $k^*(b)$ under uniform applied stress for $\frac{h}{a}=0.5$ and $\beta h=10^{-3}$

Figures 3.1-2 agree very well with their counterparts found in Nied (1987). It is observed from figures and tables above that when the crack is near the free surface ($\frac{l}{a}$ increasing), normalized stress intensity factors become larger as crack period becomes larger. When $a \to \infty$, results are very similar and the effect of crack length is minimized (periodic cracks in an infinite plane solution). For very large values of c compared to l, the numerical solutions based on periodic crack formulations lose their accuracy. Because of that, the results at $\frac{l}{l+2c} \to 0$ are generated for single crack case for homogeneous material [1]. For such spacing, periodic cracks behave practically like a single crack (integral equation D.4 for a single crack case is given in Appendix D). From this point of view, it is inferred that the numerical solution to periodic crack problem has some limitations when c approaches ∞.

Furthermore, variation of normalized SIFs are shown in Figures 3.3-6 with respect to $l/(l+2c)$ for $l/a = 1,\ 10,\ 100$, $h\beta = 0.5$ and $h\beta = -0.5$. Results are also printed in Tables 3.8-9. As it seen from those figures and tables, results are very similar to ones provided in Table 3.7 and Figures 3.1-2. Therefore, when nonhomogeneity of FGM varies, there is only slight variation in normalized SIFs.

[1] By solving the integral equation,

$$\int_a^b g(t)\left\{\frac{1}{t-x}-\frac{1}{t+x}+\frac{6x}{(t+x)^2}-\frac{4x^2}{(t+x)^3}\right\}dt = -\pi\left(\frac{1+\kappa}{4\mu}\right)P(x), \quad a < x < b$$

Table 3.8: Comparison of $k^*(a)$ and $k^*(b)$ for $\frac{h}{a}=0.5$

$h\beta=0.5$	$l/a=1$		$l/a=10$		$l/a=100$	
$l/(l+2c)$	$k^*(a)$	$k^*(b)$	$k^*(a)$	$k^*(b)$	$k^*(a)$	$k^*(b)$
1	0	0	0	0	0	0
0.9434	0.1382	0.1382	0.1382	0.1382	0.1409	0.1382
0.8333	0.2523	0.2523	0.2539	0.2523	0.2722	0.2523
0.7143	0.3568	0.3568	0.3632	0.3568	0.4236	0.3568
0.6250	0.4372	0.4372	0.4455	0.4372	0.5592	0.4372
0.5000	0.5703	0.5702	0.5878	0.5711	0.8277	0.5685
0.4386	0.6490	0.6485	0.6829	0.6509	1.0272	0.6451
0.3333	0.7932	0.7907	0.8975	0.7956	1.5099	0.7928
0.2000	0.9381	0.9357	1.2289	0.9815	2.3017	1.0349
0.1111	1.0000	0.9910	1.4160	1.1038	2.7664	1.2106
0.0610	1.0274	1.0152	1.4794	1.1505	2.9233	1.2774

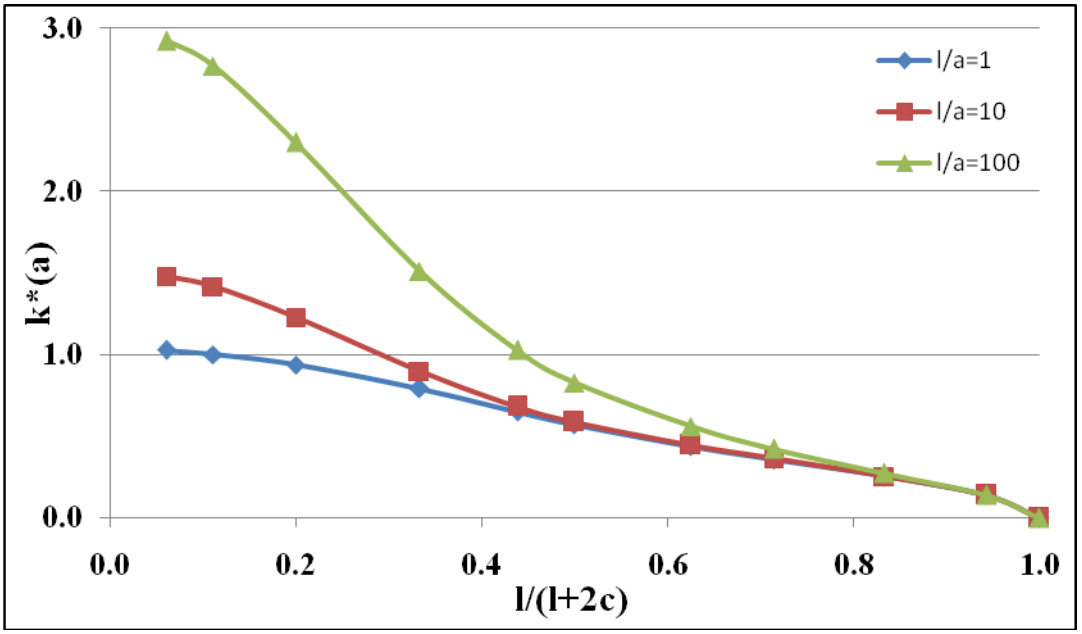

Figure 3.3: $k^*(a)$ under uniform applied stress for $\frac{h}{a} = 0.5$ and $\beta h = 0.5$

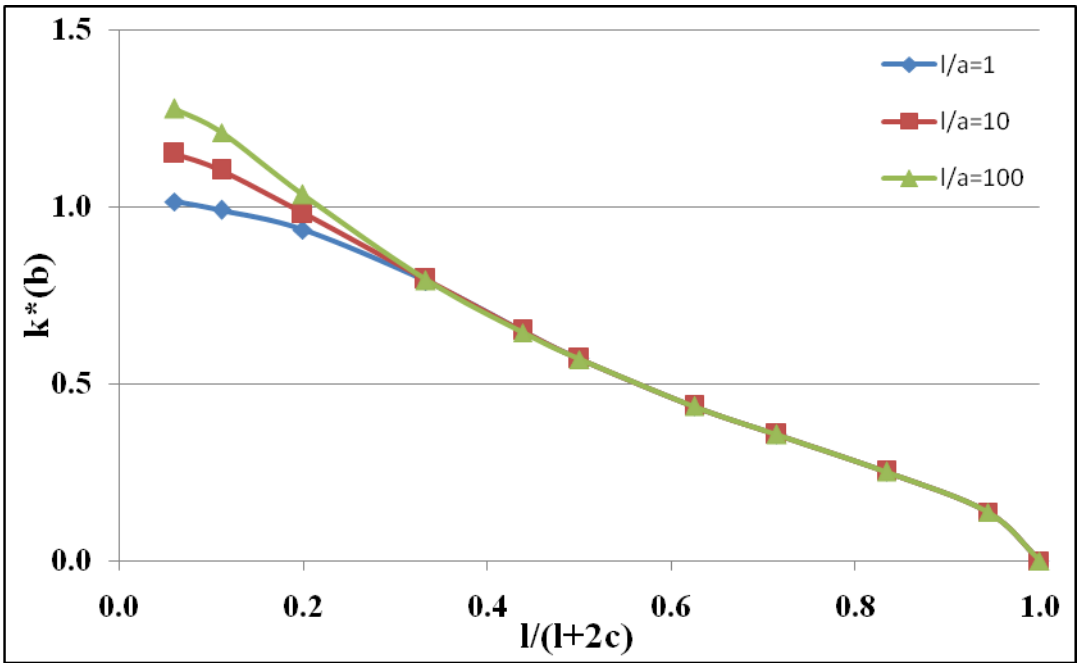

Figure 3.4: $k^*(b)$ under uniform applied stress for $\frac{h}{a} = 0.5$ and $\beta h = 0.5$

Table 3.9: Comparison of $k^*(a)$ and $k^*(b)$ for $\frac{h}{a} = 0.5$

$h\beta = -0.5$	$l/a = 1$		$l/a = 10$		$l/a = 100$	
$l/(l+2c)$	$k^*(a)$	$k^*(b)$	$k^*(a)$	$k^*(b)$	$k^*(a)$	$k^*(b)$
1	0	0	0	0	0	0
0.9434	0.1382	0.1382	0.1382	0.1382	0.1407	0.1382
0.8333	0.2523	0.2523	0.2531	0.2523	0.2653	0.2523
0.7143	0.3568	0.3568	0.3631	0.3568	0.4060	0.3568
0.6250	0.4372	0.4372	0.4452	0.4372	0.5316	0.4372
0.5000	0.5701	0.5702	0.5821	0.5713	0.7792	0.5688
0.4386	0.6484	0.6485	0.6704	0.6514	0.9626	0.6456
0.3333	0.7916	0.7901	0.8654	0.7961	1.4045	0.7930
0.2000	0.9358	0.9350	1.1637	0.9741	2.1248	1.0307
0.1111	0.9903	0.9866	1.3328	1.0893	2.5449	1.2018
0.0610	1.0145	1.0080	1.3904	1.1336	2.6889	1.2667

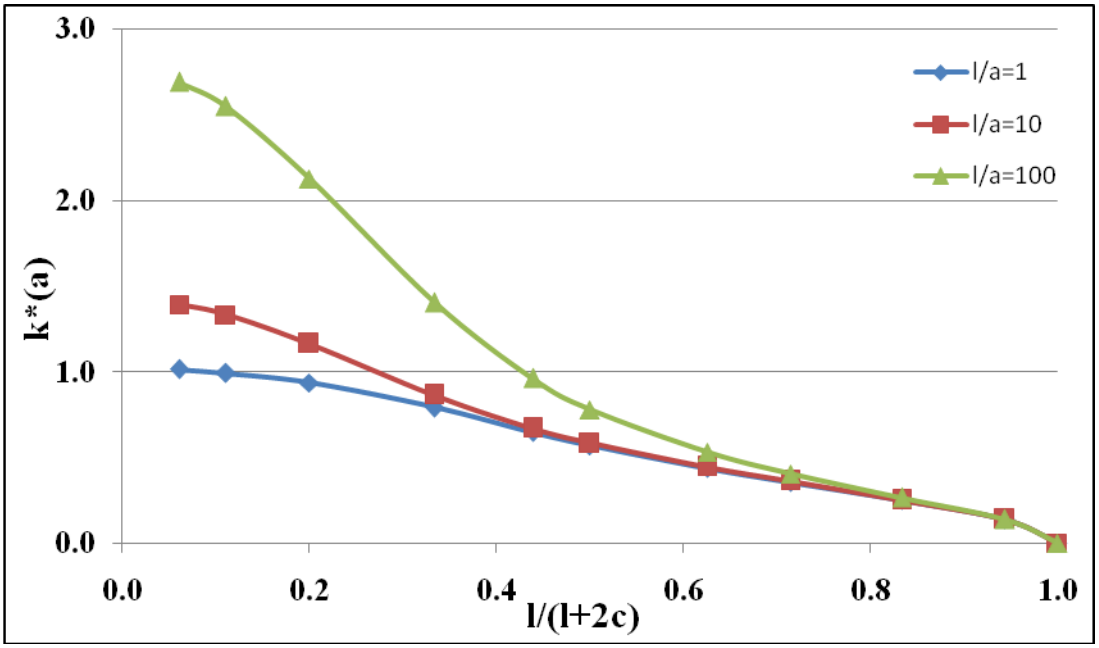

Figure 3.5: $k^*(a)$ under uniform applied stress for $\frac{h}{a} = 0.5$ and $\beta h = -0.5$

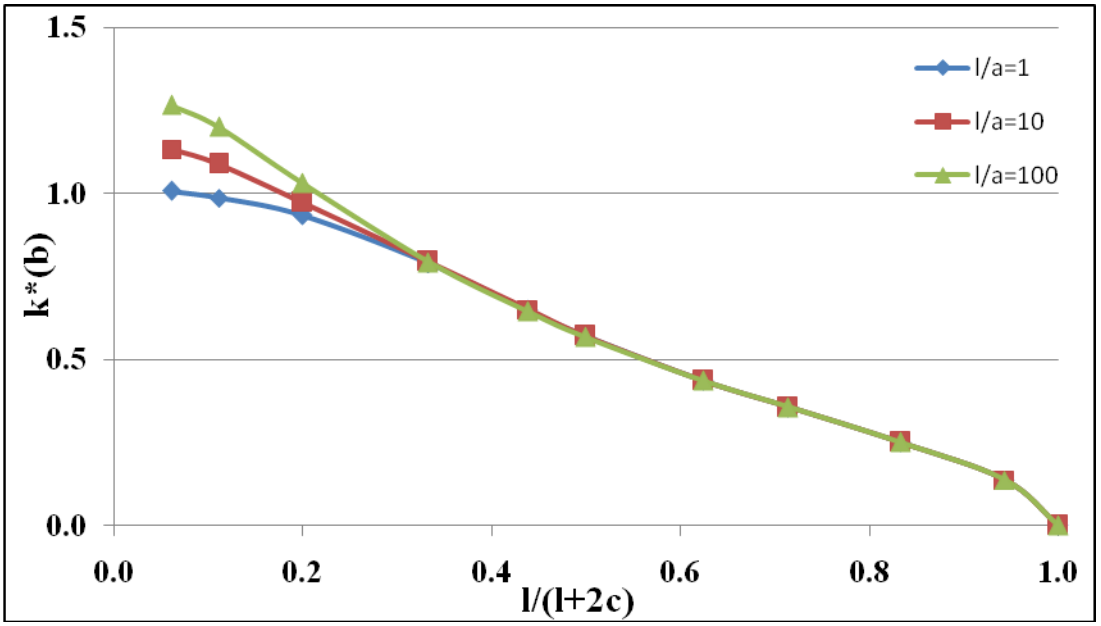

Figure 3.6: $k^*(b)$ under uniform applied stress for $\frac{h}{a} = 0.5$ and $\beta h = -0.5$

The influence of $h\beta$ on normalized stress intensity factors is shown in Tables 3.10-13 and Figures 3.7-14. It is seen that for constant *l/(l+2c)* and *h/a*, as crack length, *l/a* is

increased, normalized stress intensity factor, *k*(a)* becomes larger. Moreover, if stiffness in FGM is decreased, normalized stress intensity factor, *k*(a)* increases for constant *l/(l+2c)* and *h/a*. On the other hand, one can see from Figures 3.8, 3.10, 3.12 and 3.14, there is almost no change on normalized stress intensity factor, *k*(b)* while crack length is increased.

Table 3.10: Comparison of *k*(a)* and *k*(b)* for a thick FGM layer under uniform loading for different nonhomogeneity parameters, $h\beta$ and for *l/(l+2c)*=0.5.

h/a=0.9	$h\beta$=-0.5 ($\mu 1/\mu 0 \approx 0.606$)		$h\beta=10^{-3}$ (almost homogeneous)		$h\beta$=0.5 ($\mu 1/\mu 0 \approx 1.648$)	
l/a	*k*(a)*	*k*(b)*	*k*(a)*	*k*(b)*	*k*(a)*	*k*(b)*
1	0.5693	0.5702	0.5703	0.5702	0.5711	0.5702
10	0.5745	0.5713	0.5850	0.5712	0.5955	0.5710
20	0.5907	0.5709	0.6121	0.5706	0.6329	0.5704
30	0.6140	0.5705	0.6427	0.5701	0.6702	0.5699
40	0.6372	0.5701	0.6715	0.5698	0.7040	0.5695
50	0.6592	0.5698	0.6980	0.5695	0.7347	0.5692
60	0.6798	0.5695	0.7225	0.5692	0.7627	0.5690
70	0.6991	0.5693	0.7452	0.5691	0.7887	0.5688
80	0.7174	0.5692	0.7665	0.5689	0.8129	0.5687
90	0.7346	0.5690	0.7866	0.5688	0.8356	0.5685
100	0.7510	0.5689	0.8056	0.5686	0.8571	0.5684

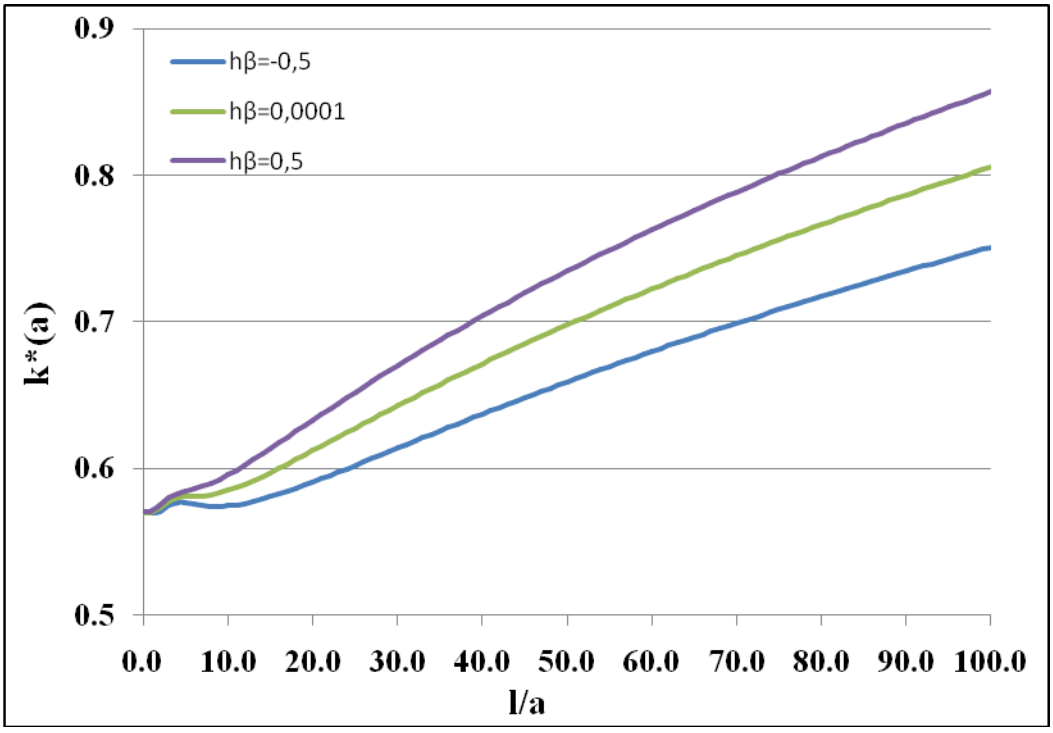

Figure 3.7: $k^*(a)$ under uniform applied stress for $\frac{h}{a}=0.9$ and $l/(l+2c)=0.5$

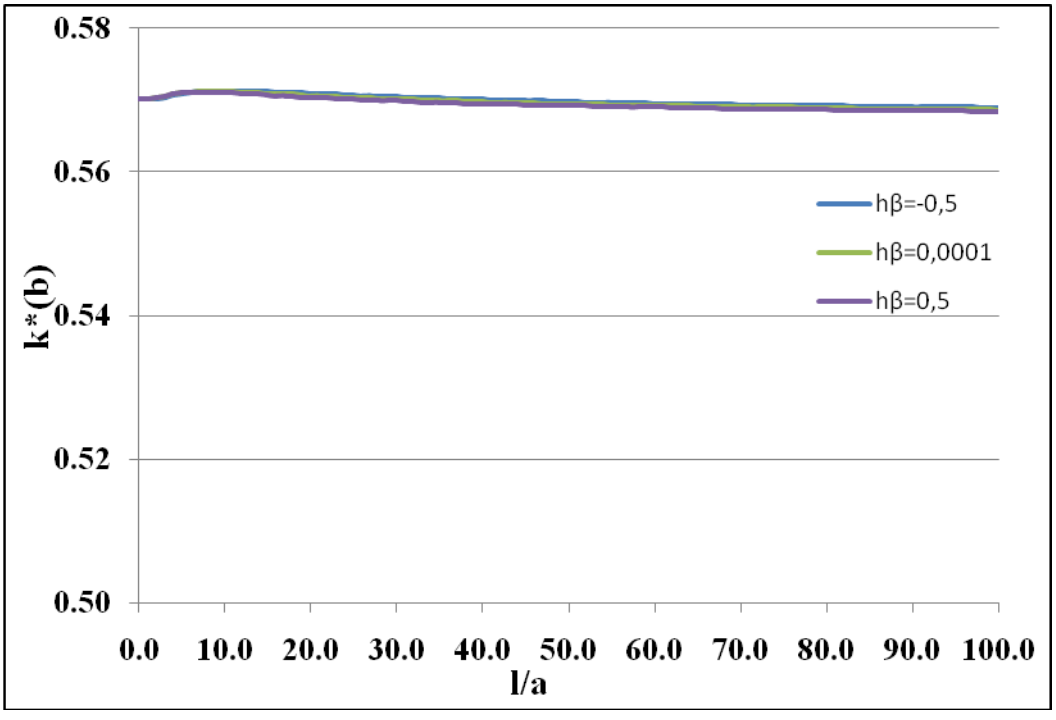

Figure 3.8: $k^*(b)$ under uniform applied stress for $\frac{h}{a}=0.9$ and $l/(l+2c)=0.5$

Table 3.11: Comparison of *k*(a)* and *k*(b)* for a thick FGM layer under uniform loading for different nonhomogeneity parameters, $h\beta$ and for *l/(l+2c)=0.8*.

h/a=0.9	$h\beta$=-0.5 ($\mu 1/\mu 0 \approx 0.606$)		$h\beta=10^{-3}$ (almost homogeneous)		$h\beta$=0.5 ($\mu 1/\mu 0 \approx 1.648$)	
l/a	*k*(a)*	*k*(b)*	*k*(a)*	*k*(b)*	*k*(a)*	*k*(b)*
1	0.2821	0.2821	0.2821	0.2821	0.2821	0.2821
10	0.2834	0.2821	0.2848	0.2821	0.2859	0.2821
20	0.2855	0.2821	0.2874	0.2821	0.2890	0.2821
30	0.2842	0.2821	0.2875	0.2821	0.2907	0.2821
40	0.2839	0.2821	0.2887	0.2821	0.2936	0.2821
50	0.2846	0.2821	0.2910	0.2821	0.2974	0.2821
60	0.2861	0.2821	0.2940	0.2821	0.3017	0.2821
70	0.2881	0.2821	0.2973	0.2821	0.3062	0.2821
80	0.2905	0.2821	0.3007	0.2821	0.3107	0.2821
90	0.2930	0.2821	0.3043	0.2821	0.3152	0.2821
100	0.2956	0.2821	0.3079	0.2821	0.3197	0.2821

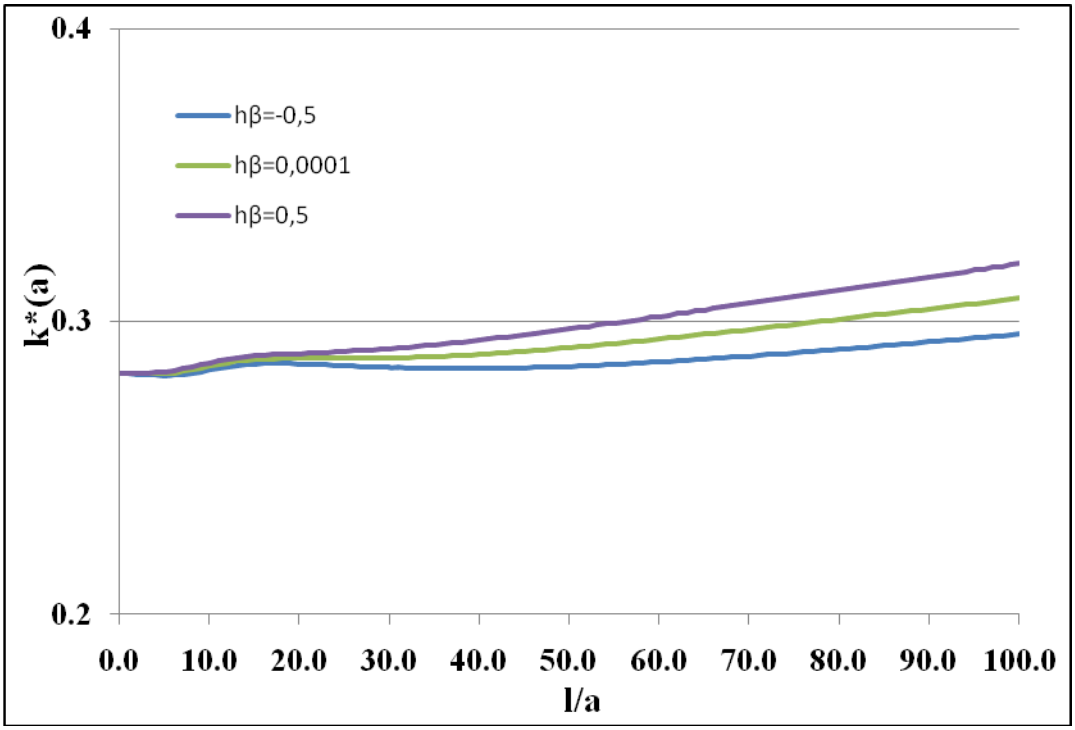

Figure 3.9: $k^*(a)$ under uniform applied stress for $\frac{h}{a}=0.9$ and $l/(l+2c)$=0.8

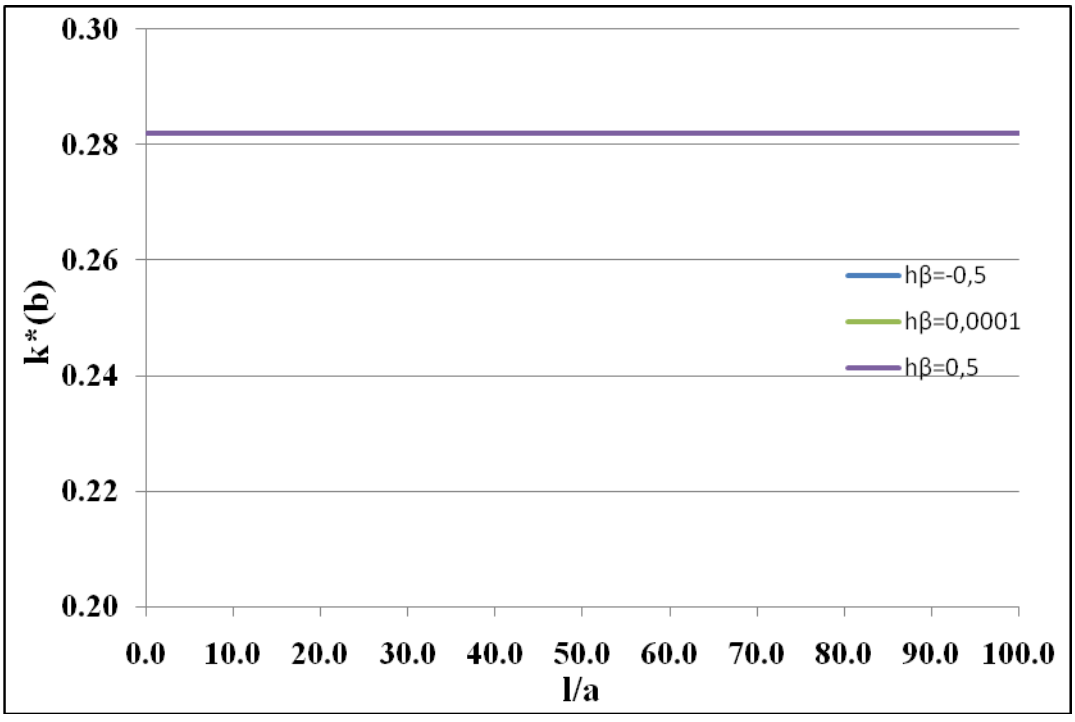

Figure 3.10: $k^*(b)$ under uniform applied stress for $\frac{h}{a}=0.9$ and $l/(l+2c)$=0.8

Table 3.12: Comparison of *k*(a)* and *k*(b)* for a thin FGM layer under uniform loading for different nonhomogeneity parameters, $h\beta$ and for *l/(l+2c)=0.5*.

h/a=0.5	$h\beta$=-0.5 ($\mu 1/\mu 0 \approx 0.606$)		$h\beta=10^{-3}$ (almost homogeneous)		$h\beta$=0.5 ($\mu 1/\mu 0 \approx 1.648$)	
l/a	*k*(a)*	*k*(b)*	*k*(a)*	*k*(b)*	*k*(a)*	*k*(b)*
1	0.5702	0.5702	0.5702	0.5702	0.5703	0.5702
10	0.5834	0.5712	0.5850	0.5712	0.5866	0.5712
20	0.6073	0.5707	0.6122	0.5706	0.6166	0.5706
30	0.6358	0.5702	0.6428	0.5701	0.6491	0.5701
40	0.6630	0.5699	0.6715	0.5698	0.6792	0.5697
50	0.6882	0.5696	0.6980	0.5695	0.7069	0.5694
60	0.7117	0.5693	0.7225	0.5692	0.7323	0.5692
70	0.7335	0.5691	0.7453	0.5691	0.7559	0.5690
80	0.7540	0.5690	0.7666	0.5689	0.7780	0.5688
90	0.7733	0.5688	0.7867	0.5688	0.7988	0.5687
100	0.7915	0.5687	0.8057	0.5686	0.8184	0.5686

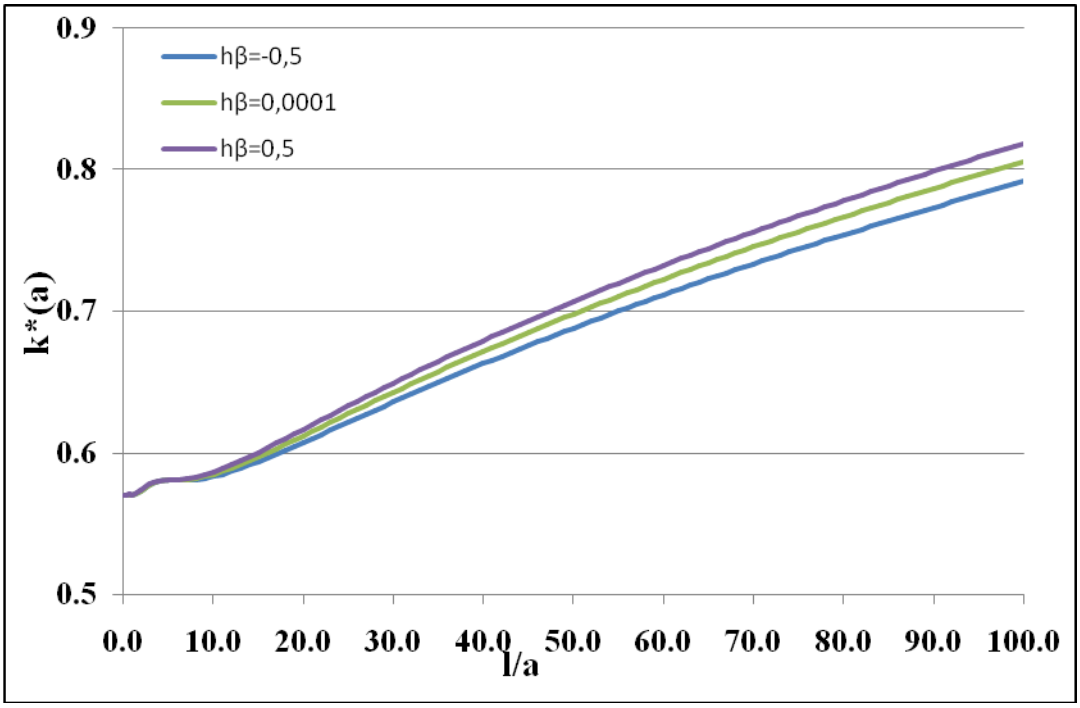

Figure 3.11: $k^*(a)$ under uniform applied stress for $\frac{h}{a} = 0.5$ and *l/(l+2c)*=0.5

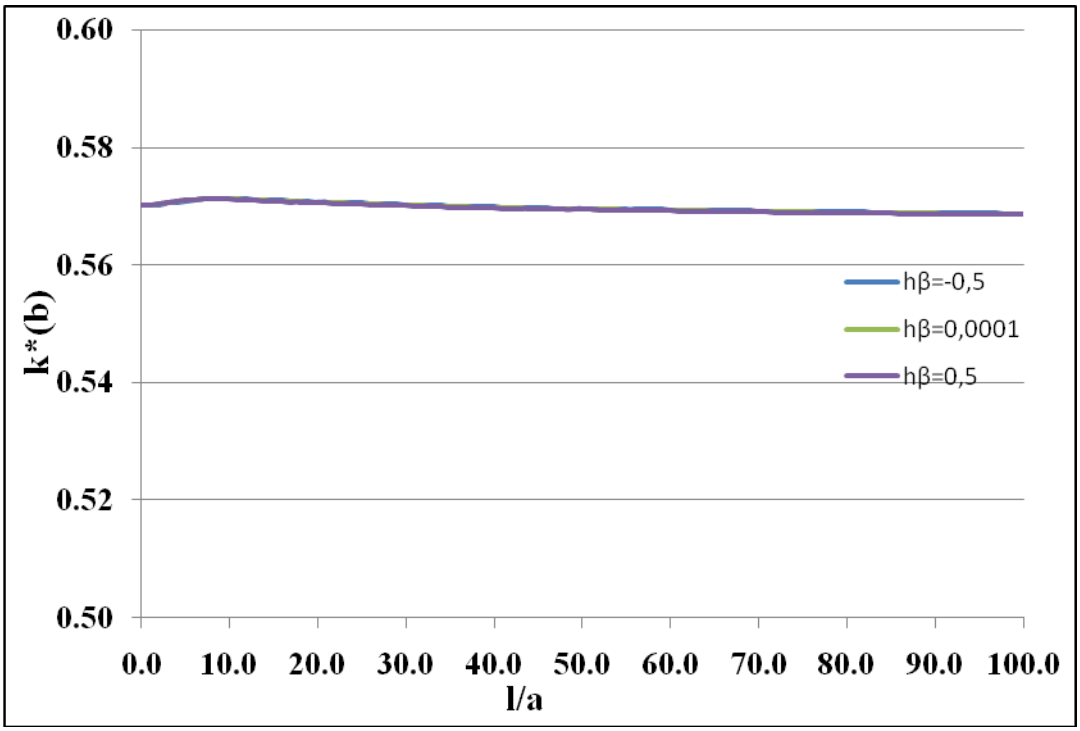

Figure 3.12: $k^*(b)$ under uniform applied stress for $\frac{h}{a} = 0.5$ and *l/(l+2c)*=0.5

Table 3.13: Comparison of *k*(a)* and *k*(b)* for a thin FGM layer under uniform loading for different nonhomogeneity parameters, $h\beta$ and for $l/(l+2c)$=0.8.

h/a=0.5	$h\beta$=-0.5 ($\mu 1/\mu 0\approx$0.606)		$h\beta=10^{-3}$ (almost homogeneous)		$h\beta$=0.5 ($\mu 1/\mu 0\approx$1.648)	
l/a	*k*(a)*	*k*(b)*	*k*(a)*	*k*(b)*	*k*(a)*	*k*(b)*
1	0.2821	0.2821	0.2821	0.2821	0.2821	0.2821
10	0.2845	0.2821	0.2848	0.2821	0.2850	0.2821
20	0.2874	0.2821	0.2874	0.2821	0.2874	0.2821
30	0.2872	0.2821	0.2875	0.2821	0.2877	0.2821
40	0.2880	0.2821	0.2887	0.2821	0.2894	0.2821
50	0.2899	0.2821	0.2911	0.2821	0.2921	0.2821
60	0.2924	0.2821	0.2940	0.2821	0.2954	0.2821
70	0.2954	0.2821	0.2973	0.2821	0.2991	0.2821
80	0.2985	0.2821	0.3008	0.2821	0.3028	0.2821
90	0.3018	0.2821	0.3043	0.2821	0.3066	0.2821
100	0.3051	0.2821	0.3079	0.2821	0.3105	0.2821

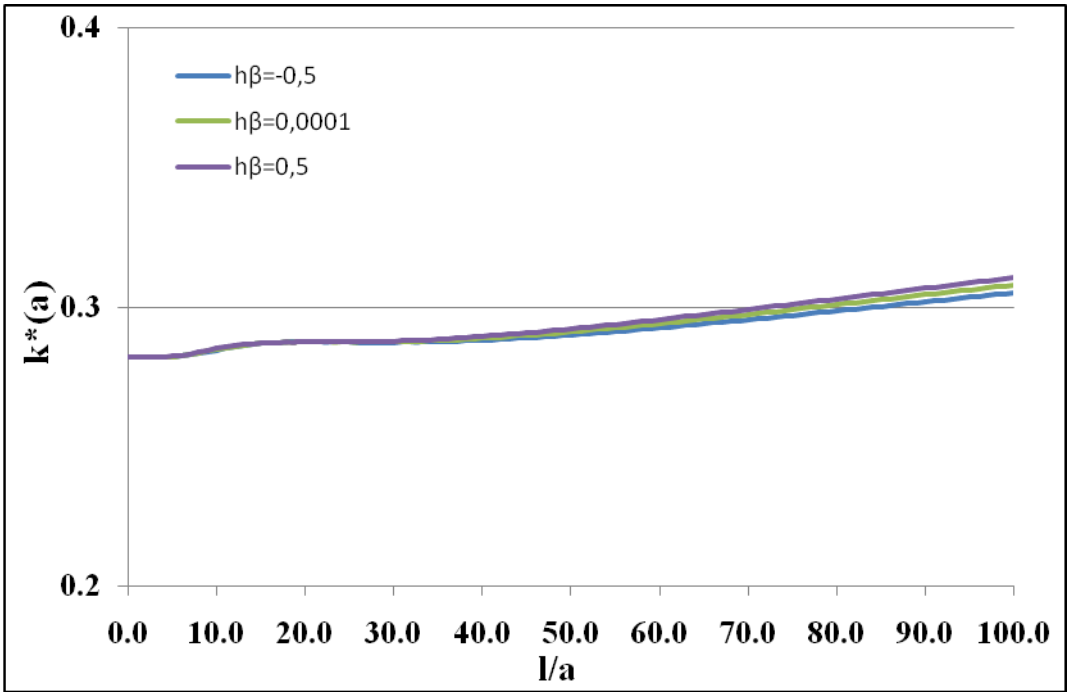

Figure 3.13: $k^*(a)$ under uniform applied stress for $\frac{h}{a} = 0.5$ and $l/(l+2c)$=0.8

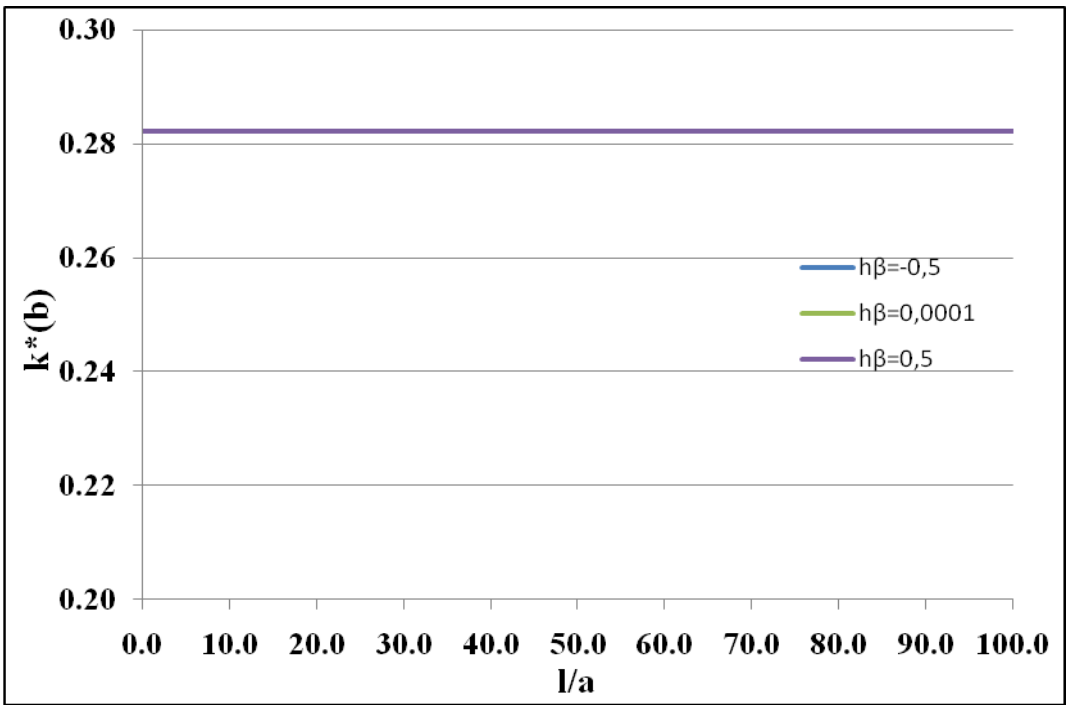

Figure 3.14: $k^*(b)$ under uniform applied stress for $\frac{h}{a} = 0.5$ and $l/(l+2c)$=0.8

Normalized stress intensity factors are presented in Table 3.14. It is seen that while crack length, l is getting larger, normalized stress intensity factors become smaller for constant crack period, $2c$ and normalized stress intensity factors are decreasing as stiffness in FGM increased. The values presented in Table 3.14 are graphically represented in Figures 3.15-16.

Table 3.14: Comparison of $k^*(a)$ and $k^*(b)$ for different nonhomogeneity parameters $h\beta$ and for a thick FGM layer under uniform loading.

h/a=0.9	$h\beta$=-1 ($\mu 1/\mu 0 \approx 0.368$)		$h\beta=10^{-3}$ (almost homogeneous)		$h\beta$=1 ($\mu 1/\mu 0 \approx 2.718$)	
l/a	$k^*(a)$	$k^*(b)$	$k^*(a)$	$k^*(b)$	$k^*(a)$	$k^*(b)$
1	0.9726	0.9843	1.0067	0.9987	1.0415	1.0131
2	0.9381	0.9548	0.9888	0.9668	1.0405	0.9787
3	0.8912	0.9096	0.9435	0.9153	0.9966	0.9210
4	0.8365	0.8550	0.8840	0.8565	0.9320	0.8579
5	0.7800	0.7971	0.8210	0.7967	0.8623	0.7963
6	0.7260	0.7408	0.7609	0.7400	0.7960	0.7391
7	0.6770	0.6894	0.7068	0.6886	0.7368	0.6877
8	0.6339	0.6441	0.6598	0.6435	0.6858	0.6428
9	0.5965	0.6050	0.6194	0.6045	0.6425	0.6040
10	0.5643	0.5715	0.5850	0.5712	0.6059	0.5709
11	0.5365	0.5428	0.5556	0.5426	0.5749	0.5424

12	0.5124	0.5182	0.5304	0.518	0.5483	0.5179
13	0.4914	0.4967	0.5084	0.4967	0.5255	0.4966
14	0.4729	0.4779	0.4892	0.4779	0.5054	0.4778
15	0.4565	0.4613	0.4721	0.4612	0.4878	0.4612
16	0.4417	0.4463	0.4568	0.4463	0.4719	0.4463
17	0.4284	0.4328	0.4430	0.4328	0.4577	0.4328
18	0.4162	0.4206	0.4305	0.4206	0.4447	0.4206
19	0.4051	0.4093	0.4189	0.4093	0.4328	0.4093
20	0.3948	0.3989	0.4083	0.3989	0.4218	0.3989
21	0.3853	0.3893	0.3985	0.3893	0.4117	0.3893
22	0.3764	0.3804	0.3893	0.3804	0.4022	0.3804
23	0.3681	0.3720	0.3807	0.3720	0.3934	0.3720
24	0.3604	0.3642	0.3727	0.3642	0.3851	0.3642
25	0.3531	0.3568	0.3652	0.3568	0.3773	0.3568
26	0.3463	0.3499	0.3581	0.3499	0.3700	0.3499
27	0.3398	0.3434	0.3514	0.3434	0.3631	0.3434
28	0.3337	0.3372	0.3451	0.3372	0.3566	0.3372
29	0.3278	0.3313	0.3391	0.3313	0.3504	0.3313
30	0.3223	0.3257	0.3334	0.3257	0.3445	0.3258
31	0.3171	0.3205	0.3280	0.3205	0.3389	0.3205
32	0.3121	0.3154	0.3228	0.3154	0.3335	0.3154
33	0.3073	0.3106	0.3179	0.3106	0.3285	0.3106
34	0.3028	0.3060	0.3132	0.3060	0.3236	0.3060

35	0.2984	0.3016	0.3087	0.3016	0.3189	0.3016
36	0.2942	0.2974	0.3043	0.2974	0.3145	0.2974
37	0.2902	0.2933	0.3002	0.2933	0.3102	0.2933
38	0.2864	0.2894	0.2962	0.2894	0.3061	0.2894
39	0.2827	0.2857	0.2924	0.2857	0.3022	0.2857
40	0.2791	0.2821	0.2887	0.2821	0.2984	0.2821
41	0.2757	0.2786	0.2852	0.2786	0.2947	0.2786
42	0.2724	0.2753	0.2818	0.2753	0.2912	0.2753
43	0.2692	0.2721	0.2785	0.2721	0.2878	0.2721
44	0.2661	0.2690	0.2753	0.2690	0.2845	0.2690
45	0.2631	0.2660	0.2722	0.2660	0.2813	0.2660
46	0.2602	0.2631	0.2692	0.2631	0.2783	0.2631
47	0.2574	0.2603	0.2664	0.2603	0.2753	0.2603
48	0.2547	0.2575	0.2636	0.2575	0.2724	0.2575
49	0.2521	0.2549	0.2609	0.2549	0.2696	0.2549
50	0.2496	0.2523	0.2582	0.2523	0.2669	0.2523
51	0.2471	0.2498	0.2557	0.2498	0.2643	0.2498
52	0.2447	0.2474	0.2532	0.2474	0.2618	0.2474
53	0.2424	0.2451	0.2508	0.2451	0.2593	0.2451
54	0.2401	0.2428	0.2485	0.2428	0.2569	0.2428
55	0.2379	0.2406	0.2462	0.2406	0.2545	0.2406
56	0.2358	0.2384	0.2440	0.2384	0.2523	0.2384
57	0.2337	0.2363	0.2419	0.2363	0.2500	0.2363

58	0.2317	0.2343	0.2398	0.2343	0.2479	0.2343
59	0.2297	0.2323	0.2377	0.2323	0.2458	0.2323
60	0.2278	0.2303	0.2357	0.2303	0.2437	0.2303
61	0.2259	0.2284	0.2338	0.2284	0.2417	0.2284
62	0.2241	0.2266	0.2319	0.2266	0.2398	0.2266
63	0.2223	0.2248	0.2301	0.2248	0.2379	0.2248
64	0.2205	0.2230	0.2283	0.2230	0.2360	0.2230
65	0.2188	0.2213	0.2265	0.2213	0.2342	0.2213
66	0.2172	0.2196	0.2248	0.2196	0.2324	0.2196
67	0.2155	0.2180	0.2231	0.2180	0.2307	0.2180
68	0.2139	0.2164	0.2214	0.2164	0.2290	0.2164
69	0.2124	0.2148	0.2198	0.2148	0.2273	0.2148
70	0.2108	0.2133	0.2183	0.2133	0.2257	0.2133
71	0.2093	0.2118	0.2167	0.2118	0.2241	0.2118
72	0.2079	0.2103	0.2152	0.2103	0.2226	0.2103
73	0.2065	0.2088	0.2137	0.2088	0.2210	0.2088
74	0.2050	0.2074	0.2123	0.2074	0.2195	0.2074
75	0.2037	0.2060	0.2109	0.2060	0.2181	0.2060
76	0.2023	0.2047	0.2095	0.2047	0.2167	0.2047
77	0.2010	0.2033	0.2081	0.2033	0.2152	0.2033
78	0.1997	0.2020	0.2068	0.2020	0.2139	0.2020
79	0.1984	0.2007	0.2055	0.2007	0.2125	0.2007
80	0.1972	0.1995	0.2042	0.1995	0.2112	0.1995

81	0.1960	0.1983	0.2029	0.1983	0.2099	0.1983
82	0.1948	0.1970	0.2017	0.1970	0.2086	0.1970
83	0.1936	0.1958	0.2004	0.1958	0.2074	0.1958
84	0.1924	0.1947	0.1992	0.1947	0.2061	0.1947
85	0.1913	0.1935	0.1981	0.1935	0.2049	0.1935
86	0.1902	0.1924	0.1969	0.1924	0.2037	0.1924
87	0.1891	0.1913	0.1958	0.1913	0.2026	0.1913
88	0.1880	0.1902	0.1947	0.1902	0.2014	0.1902
89	0.1869	0.1891	0.1936	0.1891	0.2003	0.1891
90	0.1859	0.1881	0.1925	0.1881	0.1992	0.1881
91	0.1848	0.1870	0.1914	0.1870	0.1981	0.1870
92	0.1838	0.1860	0.1904	0.1860	0.1970	0.1860
93	0.1828	0.1850	0.1894	0.1850	0.1960	0.1850
94	0.1819	0.1840	0.1884	0.1840	0.1949	0.1840
95	0.1809	0.1831	0.1874	0.1831	0.1939	0.1831
96	0.1799	0.1821	0.1864	0.1821	0.1929	0.1821
97	0.1790	0.1812	0.1854	0.1812	0.1919	0.1812
98	0.1781	0.1802	0.1845	0.1802	0.1909	0.1802
99	0.1772	0.1793	0.1836	0.1793	0.1900	0.1793
100	0.1763	0.1784	0.1826	0.1784	0.1890	0.1784

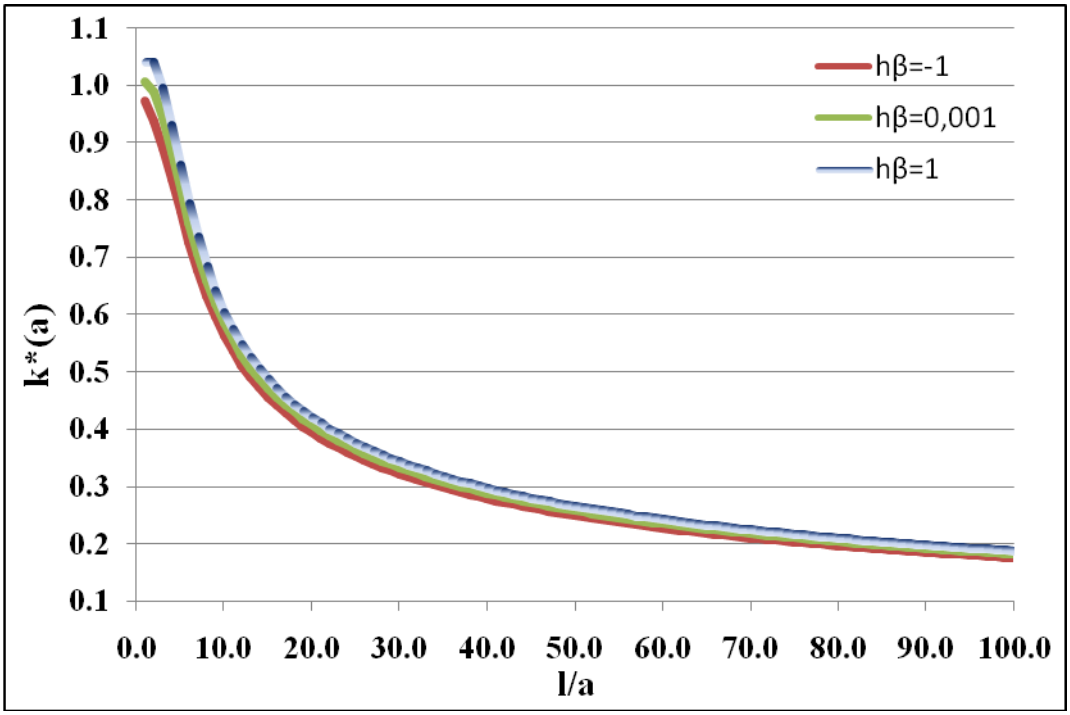

Figure 3.15: $k^*(a)$ under uniform applied stress for $\frac{h}{a} = 0.9$

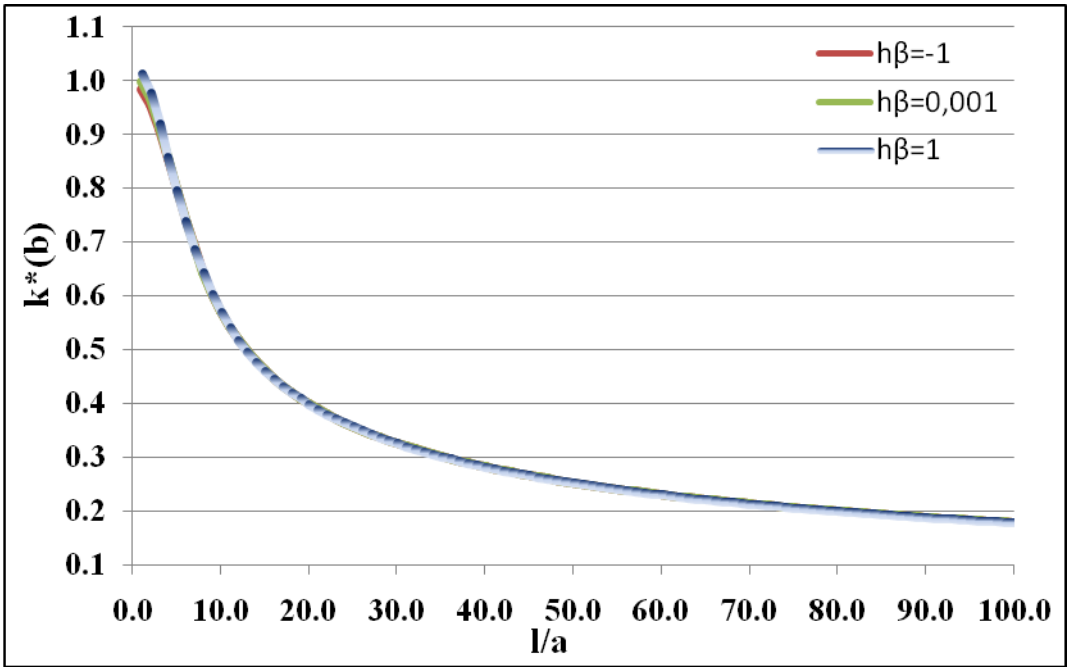

Figure 3.16: $k^*(b)$ under uniform applied stress for $\frac{h}{a} = 0.9$

Furthermore, when nonhomogeneity parameter and FGM thickness are varied, stress intensity factors may change. In Table 3.15 and 3.16, solutions for a relatively thin FGM layer coated to the homogeneous material are given. The results are tabulated for different nonhomogeneity parameters. It is observed from the results that increasing period has little effect on normalized stress intensity factors for various βh values. It should be noted that in Table 3.15 and 3.16 when $c \to \infty$ or at $\frac{l}{l+2c} = 0$, the result for $\beta h = 10^{-3}$ is obtained from single crack case since it is supposed that the cracks in that range behave like single crack and coating is almost homogeneous as it is mentioned above. Besides, another important point is that tendencies are regularly changing according material gradation. In other words, normalized stress intensity factors are increasing when βh is increased (increasing βh means homogeneous plane becomes stiffer compared to FGM). Tabulated results are graphically represented in Figures 3.17-3.20. Since the values are very close, only one data set is shown while plotting.

Table 3.15: Comparison of *k*(a)* and *k*(b)* for different nonhomogeneity parameters $h\beta$ and for a very thin FGM layer. [2]

h/a=0.1 *l/a*=1	$h\beta$=-0.5 ($\mu 1/\mu 0$≈0.606)		$h\beta=10^{-3}$ (almost homogeneous)		$h\beta$=0.5 ($\mu 1/\mu 0$≈1.648)	
l/(l+2c)	*k*(a)*	*k*(b)*	*k*(a)*	*k*(b)*	*k*(a)*	*k*(b)*
1	0	0	0	0	0	0
0.9434	0.1382	0.1382	0.1382	0.1382	0.1382	0.1382
0.8333	0.2523	0.2523	0.2523	0.2523	0.2523	0.2523
0.7143	0.3568	0.3568	0.3568	0.3568	0.3568	0.3568
0.6250	0.4372	0.4372	0.4372	0.4372	0.4372	0.4372
0.5000	0.5702	0.5702	0.5702	0.5702	0.5702	0.5702
0.4386	0.6487	0.6485	0.6487	0.6485	0.6487	0.6485
0.3333	0.7922	0.7903	0.7924	0.7904	0.7926	0.7905
0.2000	0.9368	0.9353	0.9370	0.9354	0.9371	0.9355
0.1111	0.9944	0.9884	0.9953	0.9889	0.9961	0.9892
0	1.0330(*)	1.0236(*)	1.0344	1.0244	1.0355(*)	1.0251(*)

[2] (*) In the last row of Tables 3.15, 3.17 and 3.19, $k^*(a)$ and $k^*(b)$ are calculated for $l/(l+2c)=0.0065$. Since it is not possible to find SIFs for the case of nonhomogeneous material combination at exactly $l/(l+2c)=0$.

Table 3.16: Comparison of *k*(a)* and *k*(b)* for different nonhomogeneity parameters $h\beta$ and for a very thin FGM layer.

h/a=0.1 l/a=1	$h\beta$=-2 ($\frac{\mu_1}{\mu_0} \cong 0.135$)		$h\beta$=-1 ($\frac{\mu_1}{\mu_0} \cong 0.368$)		$h\beta$=1 ($\frac{\mu_1}{\mu_0} \cong 2.718$)		$h\beta$=2 ($\frac{\mu_1}{\mu_0} \cong 7.389$)	
$l/(l+2c)$	*k*(a)*	*k*(b)*	*k*(a)*	*k*(b)*	*k*(a)*	*k*(b)*	*k*(a)*	*k*(b)*
1	0	0	0	0	0	0	0	0
0.9434	0.1382	0.1382	0.1382	0.1382	0.1382	0.1382	0.1382	0.1382
0.8333	0.2523	0.2523	0.2523	0.2523	0.2523	0.2523	0.2523	0.2523
0.7143	0.3568	0.3568	0.3568	0.3568	0.3568	0.3568	0.3568	0.3568
0.6250	0.4372	0.4372	0.4372	0.4372	0.4372	0.4372	0.4372	0.4372
0.5000	0.5702	0.5702	0.5702	0.5702	0.5702	0.5702	0.5702	0.5702
0.4386	0.6486	0.6485	0.6486	0.6485	0.6488	0.6485	0.6488	0.6485
0.3333	0.7915	0.7901	0.7920	0.7903	0.7928	0.7905	0.7930	0.7906
0.2000	0.9364	0.9350	0.9367	0.9352	0.9372	0.9355	0.9374	0.9356
0.1111	0.9901	0.9864	0.9932	0.9879	0.9967	0.9895	0.9975	0.9899
0.0065	1.0259	1.0192	1.0311	1.0224	1.0363	1.0256	1.0375	1.0263

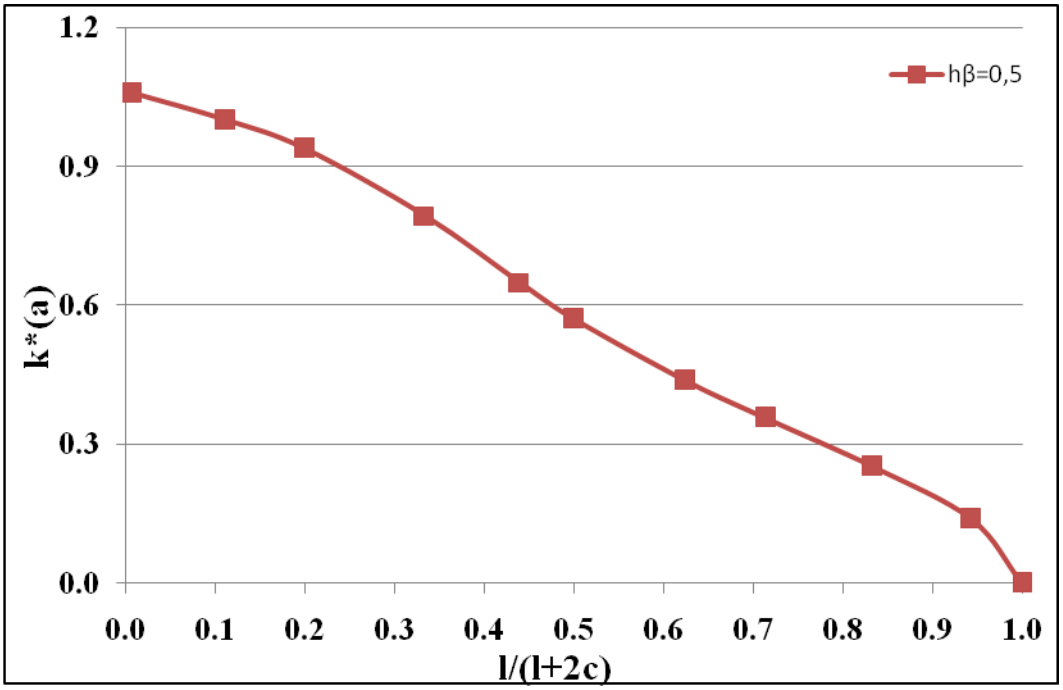

Figure 3.17: $k^*(a)$ for $h/a = 0.1$ and $l/a = 1$

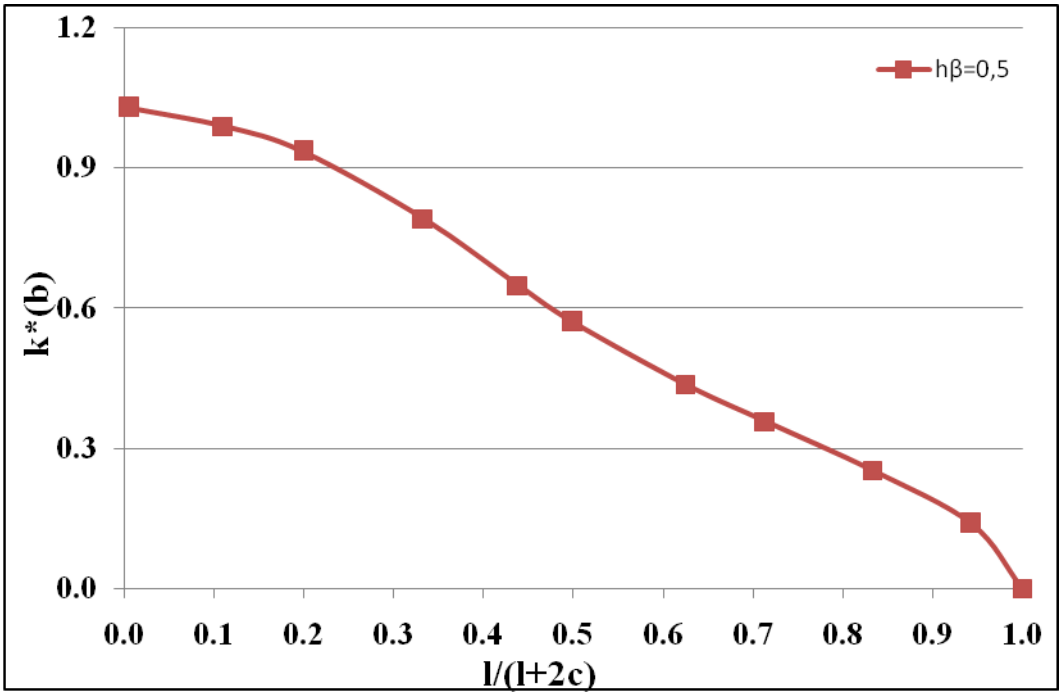

Figure 3.18: $k^*(b)$ for $h/a = 0.1$ and $l/a = 1$

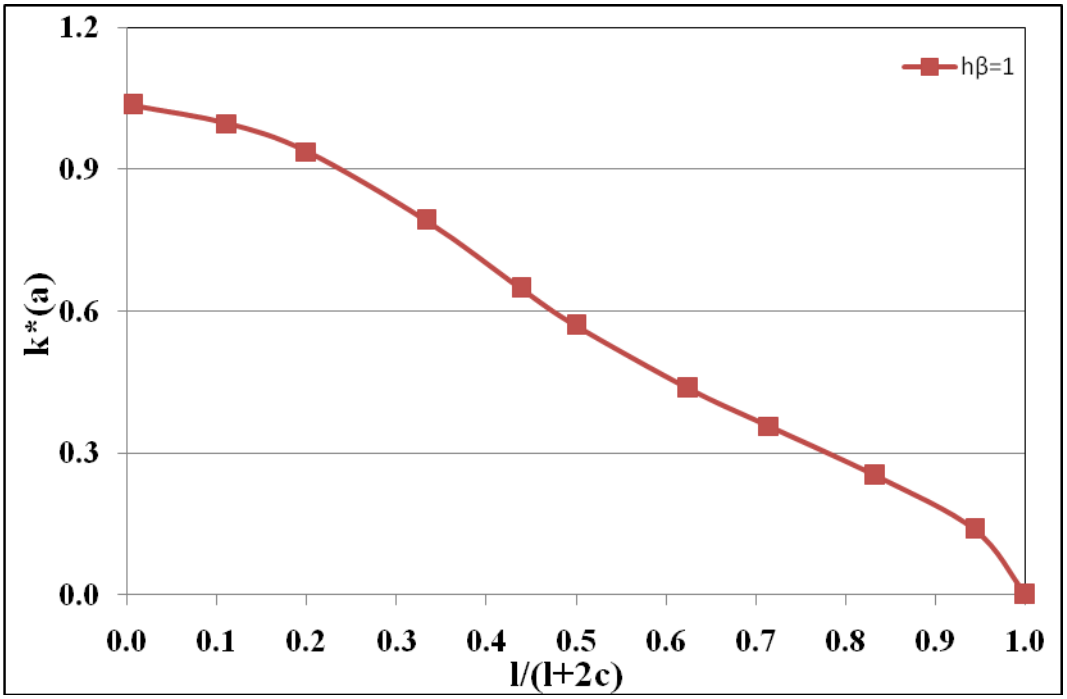

Figure 3.19: $k^*(a)$ for $h/a = 0.1$ and $l/a = 1$

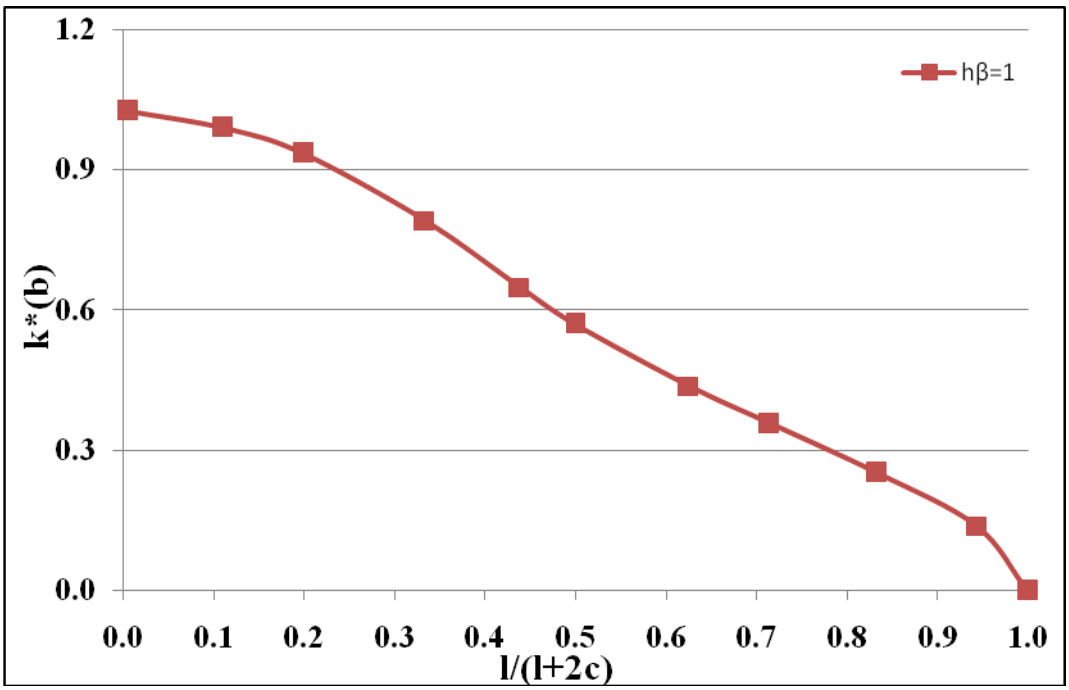

Figure 3.20: $k^*(b)$ for $h/a = 0.1$ and $l/a = 1$

In Tables 3.17-18, a thin FGM coating on a homogeneous material is considered for different nonhomogeneity parameters. As discussed in Tables 3.15-16, the results are very close for various βh values. For this reason, one data set is also shown in Figures 3.21-24.

Table 3.17: Comparison of $k^*(a)$ and $k^*(b)$ for different nonhomogeneity parameters $h\beta$ and for a thin FGM layer.

$h/a=0.5$ $l/a=1$	$h\beta=-0.5$ ($\frac{\mu_1}{\mu_0}\cong 0.606$)		$h\beta=10^{-3}$ (almost homogeneous)		$h\beta=0.5$ ($\frac{\mu_1}{\mu_0}\cong 1.648$)	
$l/(l+2c)$	$k^*(a)$	$k^*(b)$	$k^*(a)$	$k^*(b)$	$k^*(a)$	$k^*(b)$
1	0	0	0	0	0	0
0.9434	0.1382	0.1382	0.1382	0.1382	0.1382	0.1382
0.8333	0.2523	0.2523	0.2523	0.2523	0.2523	0.2523
0.7143	0.3568	0.3568	0.3568	0.3568	0.3568	0.3568
0.6250	0.4372	0.4372	0.4372	0.4372	0.4372	0.4372
0.5000	0.5701	0.5702	0.5702	0.5702	0.5703	0.5702
0.4386	0.6484	0.6485	0.6487	0.6485	0.6490	0.6485
0.3333	0.7916	0.7901	0.7924	0.7904	0.7932	0.7907
0.2000	0.9358	0.9350	0.9370	0.9354	0.9381	0.9357
0.1111	0.9903	0.9866	0.9953	0.9889	1.0000	0.9910
0	1.0272(*)	1.0203(*)	1.0344	1.0244	1.0408(*)	1.0281(*)

Table 3.18: Comparison of *k*(a)* and *k*(b)* for different nonhomogeneity parameters $h\beta$ and for a thin FGM layer.

h/a=0.5 l/a=1	$h\beta$=-2 $(\frac{\mu_1}{\mu_0} \cong 0{,}135)$		$h\beta$=-1 $(\frac{\mu_1}{\mu_0} \cong 0{,}368)$		$h\beta$=1 $(\frac{\mu_1}{\mu_0} \cong 2{,}718)$		$h\beta$=2 $(\frac{\mu_1}{\mu_0} \cong 7{,}389)$	
l/(l+2c)	*k*(a)*	*k*(b)*	*k*(a)*	*k*(b)*	*k*(a)*	*k*(b)*	*k*(a)*	*k*(b)*
1	0	0	0	0	0	0	0	0
0.9434	0.1382	0.1382	0.1382	0.1382	0.1382	0.1382	0.1382	0.1382
0.8333	0.2523	0.2523	0.2523	0.2523	0.2523	0.2523	0.2523	0.2523
0.7143	0.3568	0.3568	0.3568	0.3568	0.3568	0.3568	0.3568	0.3568
0.6250	0.4372	0.4372	0.4372	0.4372	0.4372	0.4372	0.4372	0.4372
0.5000	0.5698	0.5702	0.5700	0.5702	0.5704	0.5702	0.5707	0.5702
0.4386	0.6475	0.6484	0.6481	0.6484	0.6494	0.6485	0.6500	0.6486
0.3333	0.7889	0.7891	0.7907	0.7897	0.7940	0.7911	0.7953	0.7917
0.2000	0.9323	0.9337	0.9347	0.9346	0.9392	0.9361	0.9413	0.9366
0.1111	0.9754	0.9798	0.9852	0.9843	1.0043	0.9929	1.0114	0.9961
0.0065	1.0028	1.0054	1.0194	1.0156	1.0465	1.0313	1.0557	1.0362

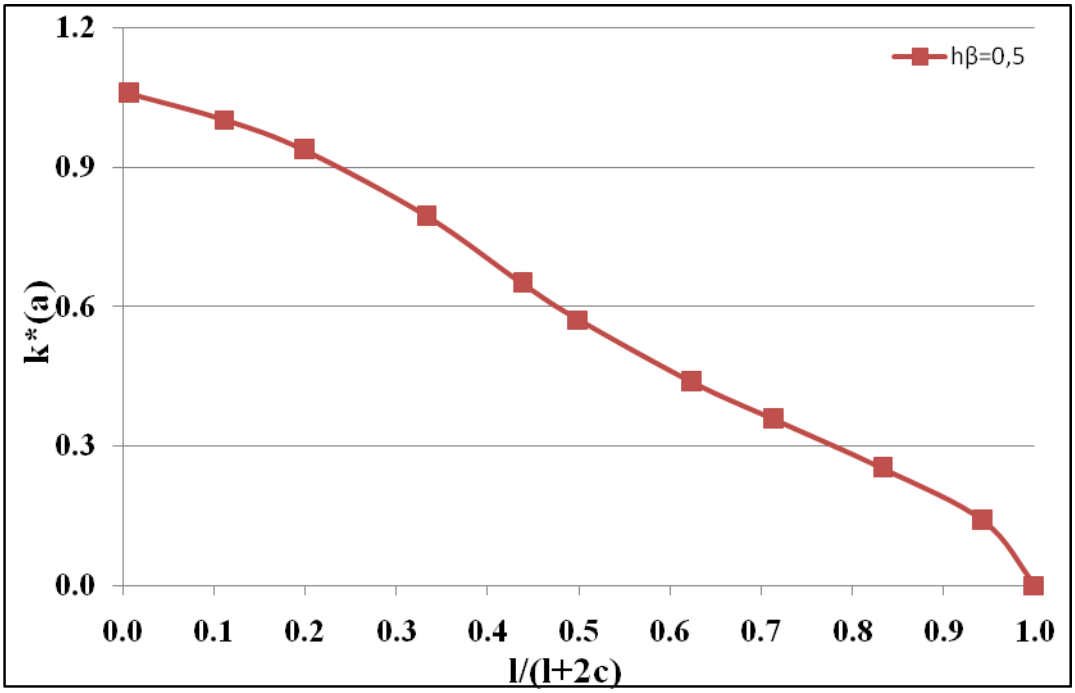

Figure 3.21: $k^*(a)$ for $h/a = 0.5$ and $l/a = 1$

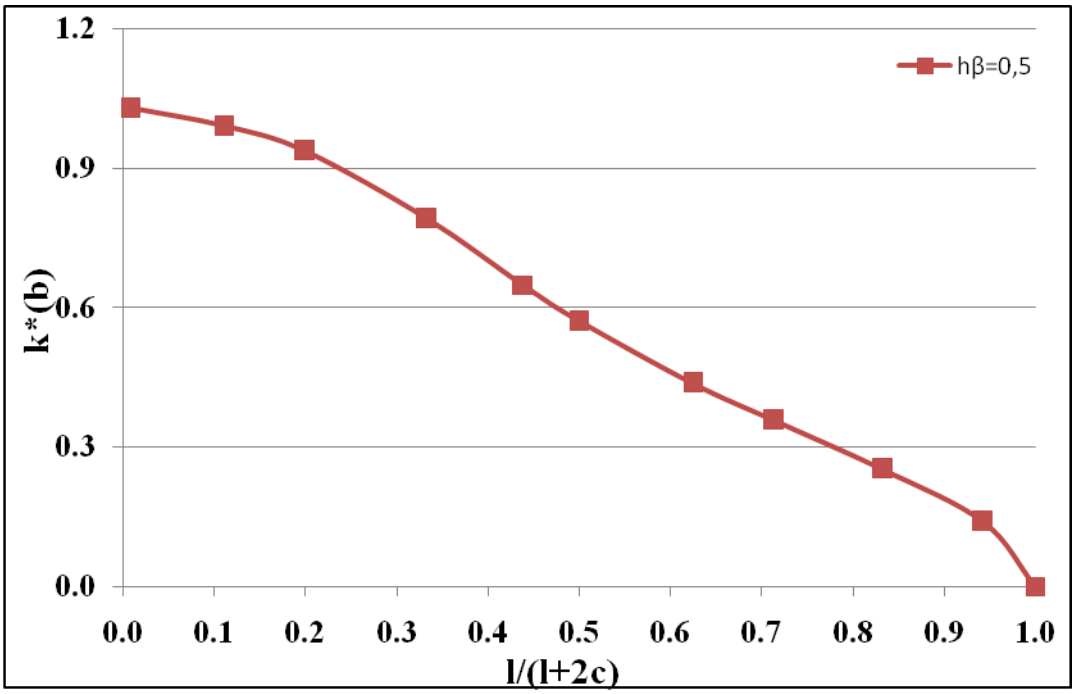

Figure 3.22: $k^*(b)$ for $h/a = 0.5$ and $l/a = 1$

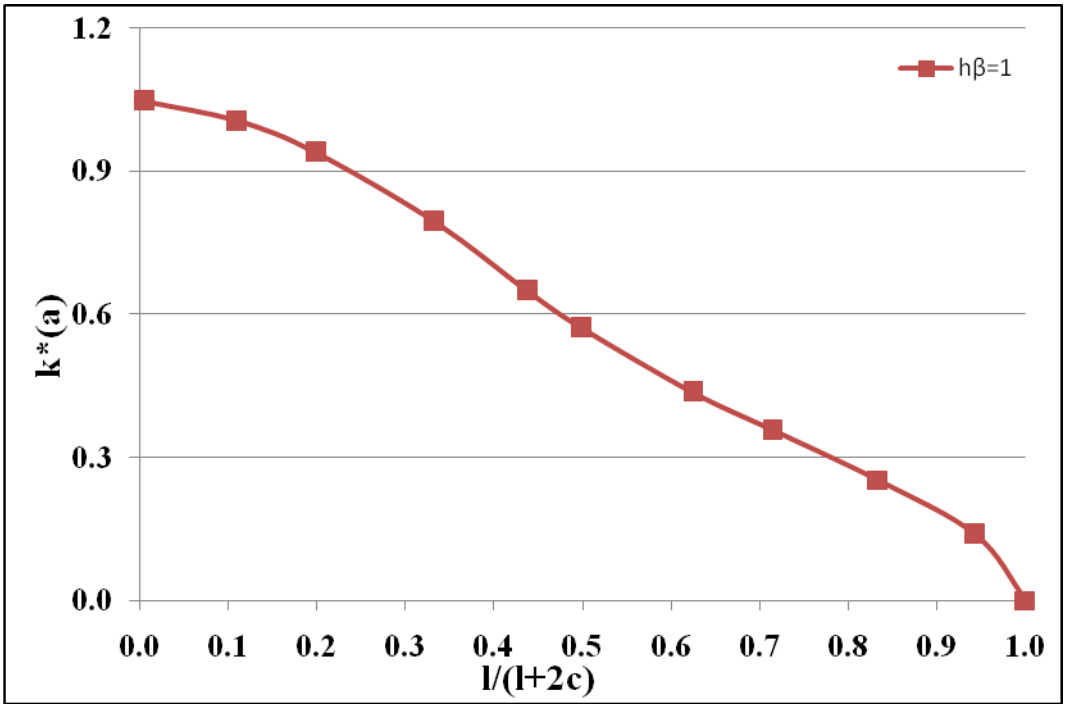

Figure 3.23: $k^*(a)$ for $h/a = 0.5$ and $l/a = 1$

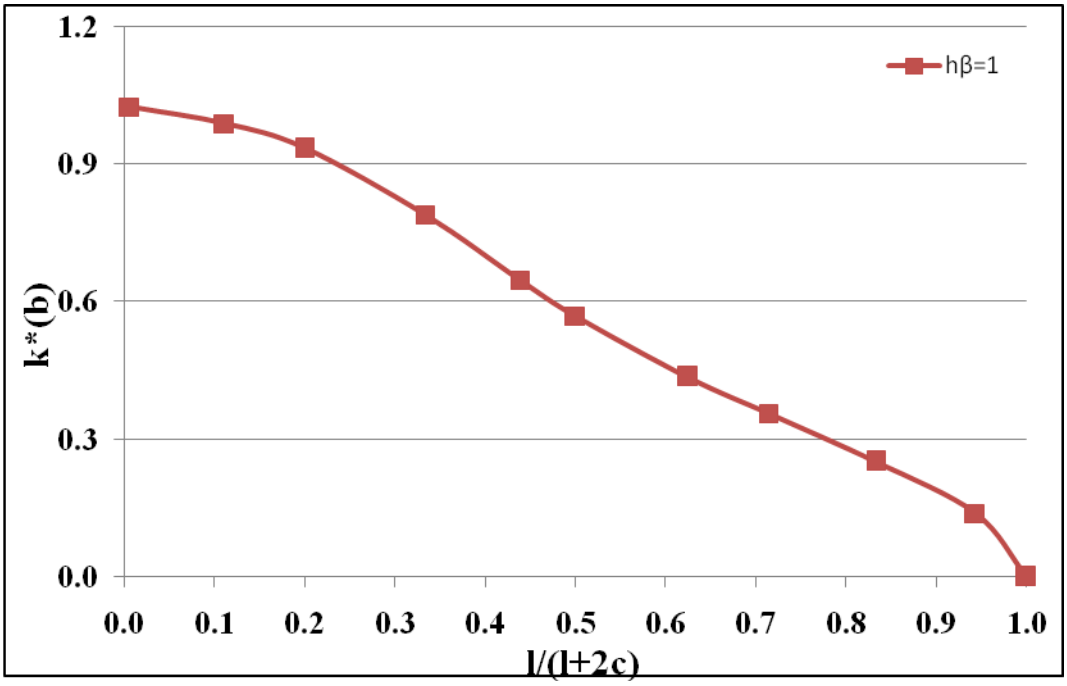

Figure 3.24: $k^*(b)$ for $h/a = 0.5$ and $l/a = 1$

Finally, the case of a thick FGM layer bonded to a homogeneous material is examined in Tables 3.19-20. The results are graphically shown in Figures 3.25-28. While FGM is getting thicker if it is stiffer than the homogeneous material $(\frac{\mu_1}{\mu_0} \cong 0.606), (\frac{\mu_1}{\mu_0} \cong 0.368)$ and $(\frac{\mu_1}{\mu_0} \cong 0.135)$, the decrease in the normalized stress intensity factors compared to $\frac{\mu_1}{\mu_0} \cong 7.389, \frac{\mu_1}{\mu_0} \cong 2.718, \frac{\mu_1}{\mu_0} \cong 1.648$ and $\frac{\mu_1}{\mu_0} = 1$ cases becomes more significant as it is seen in Tables 3.15-20.

Table 3.19: Comparison of $k^*(a)$ and $k^*(b)$ for different nonhomogeneity parameters $h\beta$ and for a thick FGM layer.

$h/a=0.9$ $l/a=1$	$h\beta=-0.5$ $(\frac{\mu_1}{\mu_0}\cong 0.606)$		$h\beta=10^{-3}$ (almost homogeneous)		$h\beta=0.5$ $(\frac{\mu_1}{\mu_0}\cong 1.648)$	
$l/(l+2c)$	$k^*(a)$	$k^*(b)$	$k^*(a)$	$k^*(b)$	$k^*(a)$	$k^*(b)$
1	0	0	0	0	0	0
0.9434	0.1382	0.1382	0.1382	0.1382	0.1382	0.1382
0.8333	0.2523	0.2523	0.2523	0.2523	0.2523	0.2523
0.7143	0.3567	0.3568	0.3567	0.3568	0.3569	0.3568
0.6250	0.4369	0.4372	0.4372	0.4372	0.4375	0.4372
0.5000	0.5693	0.5702	0.5701	0.5702	0.5711	0.5702
0.4386	0.6471	0.6483	0.6489	0.6485	0.6502	0.6487
0.3333	0.7890	0.7896	0.7924	0.7904	0.7956	0.7912
0.2000	0.9288	0.9336	0.9371	0.9354	0.9452	0.9372
0.1111	0.9796	0.9828	0.9954	0.9889	1.0113	0.9950
0	1.0146 (*)	1.0150(*)	1.0353	1.0244	1.0550(*)	1.0336(*)

Table 3.20: Comparison of *k*(a)* and *k*(b)* for different nonhomogeneity parameters $h\beta$ and for a thick FGM layer

h/a=0.9 l/a=1	$h\beta$=-2 ($\frac{\mu_1}{\mu_0} \cong 0.135$)		$h\beta$=-1 ($\frac{\mu_1}{\mu_0} \cong 0.368$)		$h\beta$=1 ($\frac{\mu_1}{\mu_0} \cong 2.718$)		$h\beta$=2 ($\frac{\mu_1}{\mu_0} \cong 7.389$)	
l/(l+2c)	*k*(a)*	*k*(b)*	*k*(a)*	*k*(b)*	*k*(a)*	*k*(b)*	*k*(a)*	*k*(b)*
1	0	0	0	0	0	0	0	0
0.9434	0.1382	0.1382	0.1382	0.1382	0.1382	0.1382	0.1382	0.1382
0.8333	0.2523	0.2523	0.2523	0.2523	0.2523	0.2523	0.2523	0.2523
0.7143	0.3564	0.3568	0.3566	0.3568	0.3570	0.3568	0.3572	0.3568
0.6250	0.4361	0.4372	0.4366	0.4372	0.4378	0.4372	0.4383	0.4372
0.5000	0.5665	0.5701	0.5684	0.5701	0.5720	0.5703	0.5736	0.5704
0.4386	0.6423	0.6478	0.6455	0.6481	0.6516	0.6488	0.6542	0.6492
0.3333	0.7776	0.7872	0.7854	0.7888	0.7985	0.7919	0.8036	0.7931
0.2000	0.9048	0.9274	0.9208	0.9316	0.9535	0.9389	0.9699	0.9421
0.1111	0.9366	0.9665	0.9644	0.9770	1.0273	1.0010	1.0580	1.0124
0.0065	0.9582	0.9871	0.9955	1.0055	1.0731	1.0422	1.1093	1.0577

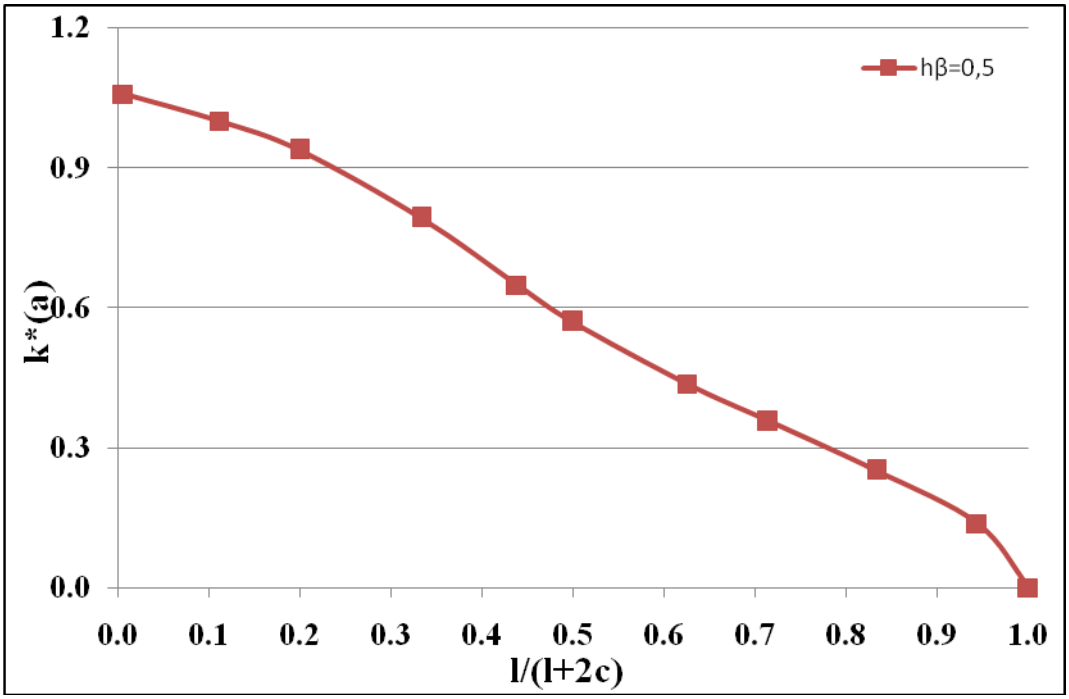

Figure 3.25: $k^*(a)$ for $h/a = 0.9$ and $l/a = 1$

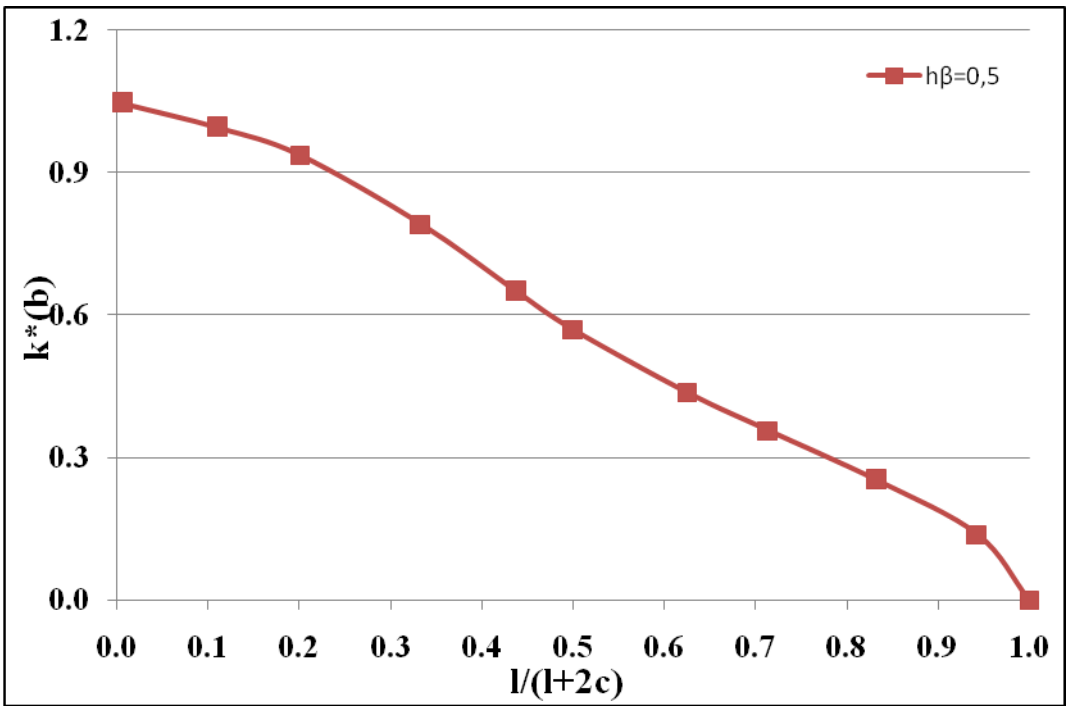

Figure 3.26: $k^*(b)$ for $h/a = 0.9$ and $l/a = 1$

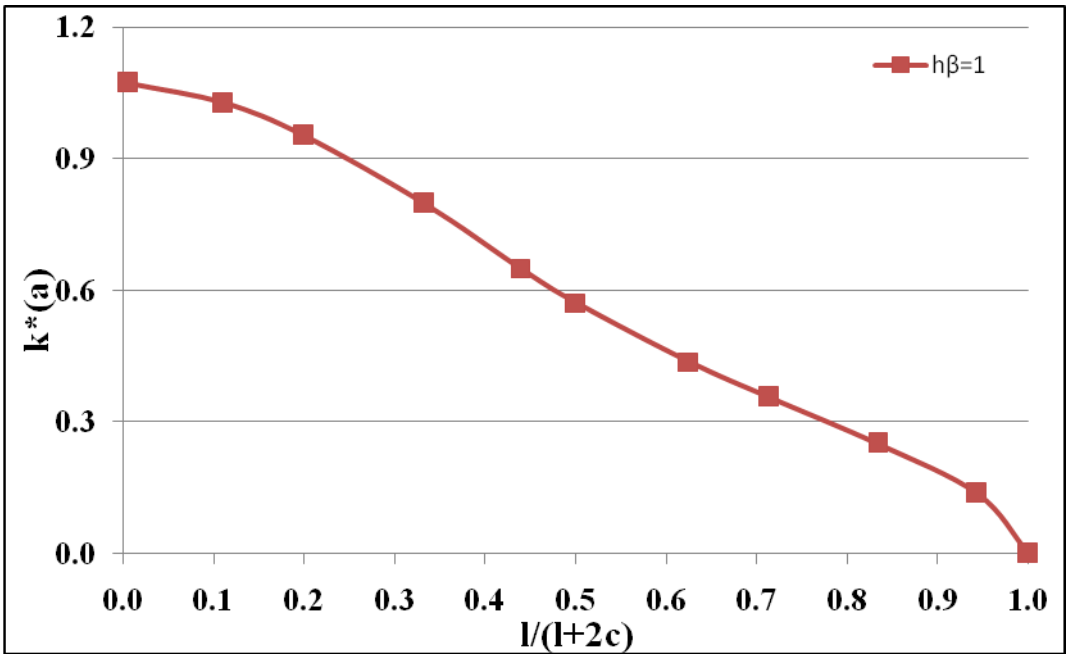

Figure 3.27: $k^*(a)$ for $h/a = 0.9$ and $l/a = 1$

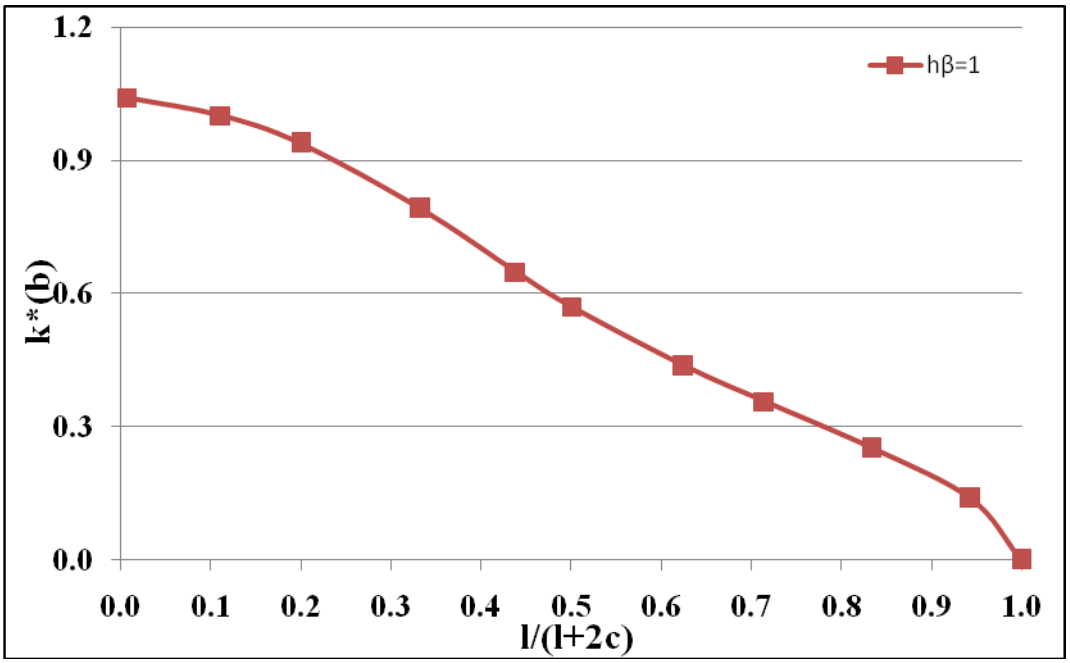

Figure 3.28: $k^*(b)$ for $h/a = 0.9$ and $l/a = 1$

For this crack problem, loadings are also taken as proportional to powers of x;

$$P(x) = \sigma_0 (\frac{x-a}{l})^k, \text{ k=0, 1, 2, 3..} \qquad (226)$$

Using the expression in (226), normalized SIFs are found and they are given in Tables 3.21-28. Such results can be used to construct solutions to more practical problems by using superposition. A sample geometry of problem for the linear crack surface traction is shown in Figure 3.29. In general, normalized SIFs at crack tip, b are greater than the ones at crack tip, a. (By appropriately combining these results, SIFs for more realistic loading cases, such as thermal loading can be obtained.) Moreover, as seen from Tables 3.23-24, 3.27-28, normalized SIFs have negative signs for some combinations of parameters. This means that at that specific location a compressive loading is applied and crack is closed. Such results are meaningful only if they are used as part of a superposition where overall SIF is positive. It is understood from Tables 3.21-28 that the effect of loading condition is much more significant when crack spacing is larger.

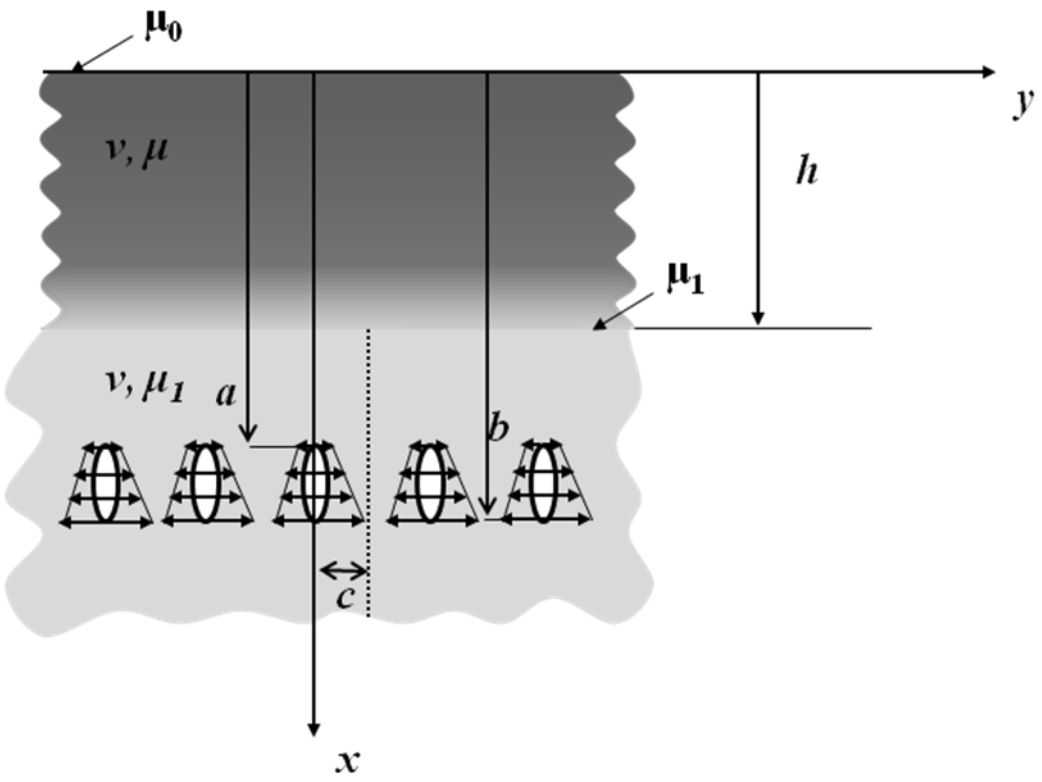

Figure 3.29: The geometry of plane when linear crack surface traction applied

Table 3.21: Comparison of $k^*(a)$ and $k^*(b)$ under uniform crack surface traction σ_0 for $h\beta = 0.5$

$h/a = 0.9$	$l/a = 1$		$l/a = 10$		$l/a = 100$	
$l/(l+2c)$	$k^*(a)$	$k^*(b)$	$k^*(a)$	$k^*(b)$	$k^*(a)$	$k^*(b)$
1	0	0	0	0	0	0
0.9434	0.1382	0.1382	0.1382	0.1382	0.1420	0.1382
0.8333	0.2523	0.2523	0.2545	0.2523	0.2780	0.2523
0.7143	0.3569	0.3568	0.3648	0.3568	0.4355	0.3568
0.6250	0.4375	0.4372	0.4488	0.4372	0.5769	0.4371
0.5000	0.5711	0.5702	0.5955	0.5710	0.8571	0.5684
0.4386	0.6502	0.6487	0.6945	0.6507	1.0656	0.6449
0.3333	0.7956	0.7912	0.9194	0.7955	1.5708	0.7928
0.2000	0.9452	0.9372	1.2677	0.9847	2.4016	1.0366
0.1111	1.0113	0.9950	1.4643	1.1099	2.8879	1.2142
0.0610	1.0401	1.0203	1.5377	1.1577	3.0463	1.2816

Table 3.22: Comparison of $k^*(a)$ and $k^*(b)$ under linear crack surface traction $\sigma_0(\frac{x-a}{l})$ for $h\beta = 0.5$

$h/a = 0.9$	$l/a = 1$		$l/a = 10$		$l/a = 100$	
$l/(l+2c)$	$k^*(a)$	$k^*(b)$	$k^*(a)$	$k^*(b)$	$k^*(a)$	$k^*(b)$
1	0	0	0	0	0	0
0.9434	0.0007	0.1375	0.0007	0.1375	0.0007	0.1375
0.8333	0.0045	0.2478	0.0046	0.2478	0.0031	0.2478
0.7143	0.0126	0.3442	0.0132	0.3442	0.0065	0.3442
0.6250	0.0235	0.4138	0.0234	0.4138	0.0099	0.4138
0.5000	0.0571	0.5133	0.0534	0.5139	0.0406	0.5140
0.4386	0.0863	0.5627	0.0839	0.5644	0.0936	0.5640
0.3333	0.1498	0.6426	0.1711	0.6461	0.2752	0.6458
0.2000	0.2215	0.7182	0.3270	0.7382	0.6288	0.7568
0.1111	0.2536	0.7470	0.4198	0.7975	0.8470	0.8363
0.0610	0.2678	0.7595	0.4542	0.8204	0.9204	0.8669

Table 3.23: Comparison of $k^*(a)$ and $k^*(b)$ under parabolic crack surface traction $\sigma_0(\frac{x-a}{l})^2$ for $h\beta = 0.5$

$h/a = 0.9$	$l/a = 1$		$l/a = 10$		$l/a = 100$	
$l/(l+2c)$	$k^*(a)$	$k^*(b)$	$k^*(a)$	$k^*(b)$	$k^*(a)$	$k^*(b)$
1	0	0	0	0	0	0
0.9434	0.0000	0.1357	0.0000	0.1367	0.0000	0.1367
0.8333	0.0001	0.2435	0.0001	0.2435	-0.0002	0.2435
0.7143	0.0004	0.3320	0.0005	0.3320	-0.0025	0.3320
0.6250	0.0014	0.3918	0.0010	0.3918	-0.0089	0.3918
0.5000	0.0127	0.4691	0.0083	0.4694	-0.0146	0.4696
0.4386	0.0272	0.5039	0.0214	0.5050	0.0037	0.5053
0.3333	0.0634	0.5569	0.0673	0.5593	0.0953	0.5593
0.2000	0.1069	0.6050	0.1583	0.6162	0.2975	0.6259
0.1111	0.1266	0.6229	0.2145	0.6521	0.4268	0.6729
0.0610	0.1354	0.6307	0.2352	0.6660	0.4709	0.6912

Table 3.24: Comparison of $k^*(a)$ and $k^*(b)$ under cubic crack surface traction $\sigma_0(\frac{x-a}{l})^3$ for $h\beta = 0.5$

$h/a = 0.9$	$l/a = 1$		$l/a = 10$		$l/a = 100$	
$l/(l+2c)$	$k^*(a)$	$k^*(b)$	$k^*(a)$	$k^*(b)$	$k^*(a)$	$k^*(b)$
1	0	0	0	0	0	0
0.9434	0.0000	0.1360	0.0000	0.1360	0.0000	0.1360
0.8333	0.0000	0.2392	0.0000	0.2392	-0.0001	0.2392
0.7143	-0.0003	0.3205	-0.0003	0.3205	-0.0013	0.3205
0.6250	-0.0010	0.3722	-0.0013	0.3722	-0.0066	0.3722
0.5000	0.0033	0.4341	0.0000	0.4343	-0.0181	0.4345
0.4386	0.0119	0.4604	0.0068	0.4611	-0.0110	0.4614
0.3333	0.0355	0.4988	0.0352	0.5005	0.0441	0.5006
0.2000	0.0653	0.5328	0.0960	0.5401	0.1778	0.5461
0.1111	0.0790	0.5453	0.1345	0.5647	0.2655	0.5780
0.0610	0.0851	0.5507	0.1488	0.5743	0.2956	0.5905

Table 3.25: Comparison of $k^*(a)$ and $k^*(b)$ under uniform crack surface traction σ_0 for $h\beta = -0.5$.

$h/a = 0.9$	$l/a = 1$		$l/a = 10$		$l/a = 100$	
$l/(l+2c)$	$k^*(a)$	$k^*(b)$	$k^*(a)$	$k^*(b)$	$k^*(a)$	$k^*(b)$
1	0	0	0	0	0	0
0.9434	0.1382	0.1382	0.1381	0.1382	0.1395	0.1382
0.8333	0.2523	0.2523	0.2525	0.2523	0.2597	0.2523
0.7143	0.3567	0.3568	0.3613	0.3568	0.3945	0.3568
0.6250	0.4369	0.4372	0.4418	0.4372	0.5146	0.4372
0.5000	0.5693	0.5702	0.5745	0.5713	0.7510	0.5689
0.4386	0.6471	0.6483	0.6593	0.6516	0.9258	0.6459
0.3333	0.7890	0.7896	0.8447	0.7961	1.3464	0.7931
0.2000	0.9288	0.9336	1.1269	0.9708	2.0300	1.0288
0.1111	0.9796	0.9828	1.2872	1.0828	2.4300	1.1979
0.0610	1.0023	1.0031	1.3419	1.1261	2.5715	1.2620

Table 3.26: Comparison of $k^*(a)$ and $k^*(b)$ under linear crack surface traction $\sigma_0(\frac{x-a}{l})$ for $h\beta = -0.5$.

$h/a=0.9$	$l/a=1$		$l/a=10$		$l/a=100$	
$l/(l+2c)$	$k^*(a)$	$k^*(b)$	$k^*(a)$	$k^*(b)$	$k^*(a)$	$k^*(b)$
1	0	0	0	0	0	0
0.9434	0.0007	0.1375	0.0007	0.1375	0.0008	0.1375
0.8333	0.0045	0.2478	0.0045	0.2478	0.0035	0.2478
0.7143	0.0126	0.3442	0.0136	0.3442	0.0073	0.3442
0.6250	0.0234	0.4138	0.0249	0.4138	0.0113	0.4138
0.5000	0.0567	0.5133	0.0559	0.5138	0.0392	0.5140
0.4386	0.0855	0.5626	0.0838	0.5644	0.0846	0.5641
0.3333	0.1478	0.6419	0.1574	0.6461	0.2377	0.6458
0.2000	0.2155	0.7166	0.2848	0.7327	0.5315	0.7544
0.1111	0.2404	0.7415	0.3612	0.7863	0.7121	0.8308
0.0610	0.2516	0.7515	0.3877	0.8073	0.7761	0.8601

Table 3.27: Comparison of $k^*(a)$ and $k^*(b)$ under parabolic crack surface traction $\sigma_0(\frac{x-a}{l})^2$ for $h\beta = -0.5$

$h/a=0.9$	$l/a=1$		$l/a=10$		$l/a=100$	
$l/(l+2c)$	$k^*(a)$	$k^*(b)$	$k^*(a)$	$k^*(b)$	$k^*(a)$	$k^*(b)$
1	0	0	0	0	0	0
0.9434	0.0000	0.1367	0.0000	0.1367	0.0000	0.1367
0.8333	0.0001	0.2435	0.0001	0.2435	-0.0001	0.2435
0.7143	0.0004	0.3320	0.0007	0.3320	-0.0018	0.3320
0.6250	0.0014	0.3918	0.0019	0.3918	-0.0067	0.3918
0.5000	0.0125	0.4691	0.0115	0.4693	-0.0102	0.4696
0.4386	0.0269	0.5038	0.0242	0.5049	0.0058	0.5052
0.3333	0.0625	0.5565	0.0636	0.5593	0.0835	0.5593
0.2000	0.1038	0.6041	0.1383	0.6132	0.2521	0.6246
0.1111	0.1192	0.6197	0.1847	0.6458	0.3593	0.6700
0.0610	0.1261	0.6259	0.2010	0.6587	0.3976	0.6876

Table 3.28: Comparison of $k^*(a)$ and $k^*(b)$ under cubic crack surface traction $\sigma_0(\frac{x-a}{l})^3$ for $h\beta = -0.5$

$h/a=0.9$	$l/a=1$		$l/a=10$		$l/a=100$	
$l/(l+2c)$	$k^*(a)$	$k^*(b)$	$k^*(a)$	$k^*(b)$	$k^*(a)$	$k^*(b)$
1	0	0	0	0	0	0
0.9434	0.0000	0.1360	0.0000	0.1360	0.0000	0.1360
0.8333	0.0000	0.2392	0.0000	0.2392	0.0000	0.2392
0.7143	-0.0003	0.3205	-0.0002	0.3205	-0.0010	0.3205
0.6250	-0.0010	0.3722	-0.0007	0.3722	-0.0053	0.3722
0.5000	0.0033	0.4341	0.0024	0.4343	-0.0142	0.4345
0.4386	0.0117	0.4603	0.0094	0.4611	-0.0077	0.4614
0.3333	0.0350	0.4985	0.0341	0.5005	0.0391	0.5006
0.2000	0.0634	0.5322	0.0841	0.5382	0.1509	0.5453
0.1111	0.0741	0.5432	0.1160	0.5606	0.2237	0.5762
0.0610	0.0790	0.5475	0.1273	0.5695	0.2498	0.5882

CHAPTER 4

DISCUSSION

In Chapter 3, calculations are made under uniform loading and different surface tractions by using the singular integral equation obtained in Chapter 2 and results are shown graphically and in tabular form. First of all, numerical results in literature for normalized SIFs are compared with studies similar to the current study. For this reason, results and figures are compared to those in Murakami (1987) and Nied (1987a). FGM coating is the only difference between these studies and, it is seen in Figures 3.1-2 and Tables 3.5-7 that there is a close agreement between these studies. It is understood that when the nonhomogeneity parameter is taken small enough, problem is reduced to that of a homogeneous layer containing periodic cracks. Because of this, comparison with literature is made easily. Furthermore, a numerical comparison using Ansys computer program is also made (Yıldırım, 2012) and it is seen that the results found in Ansys are very close to the ones provided in this study. It is also noted that crack period has a very significant effect on SIFs. When crack period approaches to 0, normalized stress intensity factors tend to 0. While crack period is increasing, normalized SIFs are increasing significantly. When c goes to ∞, the crack problem should be treated as a coated homogeneous half plane containing single crack. For an uncoated homogeneous half plane, solution can be easily obtained and those results are shown in all tables by setting $h\beta = 10^{-3}$. The influence of $h\beta$ on normalized stress intensity factors in Tables 3.10-13 and Figures 3.7-14 shows that as crack length, l/a is increased and stiffness in FGM is decreased, normalized stress intensity factor, $k^*(a)$ becomes larger for constant $l/(l+2c)$ and h/a.

In Figures 3.8, 3.10, 3.12 and 3.14, there is almost no change on normalized stress intensity factor, *k*(b)* while crack length is increased. It can be observed that crack tip, *a* is more critical than crack tip, *b* since it is closer to free surface. It is also seen in Table 3.14 and Figures 3.15-16 that while crack length, *l* is getting larger, normalized stress intensity factors become smaller for constant crack period, *2c* and normalized stress intensity factors are decreasing as stiffness in FGM increased. Therefore, one can point out that the effect of crack period is decreased while crack length is getting larger. Another important point is that when the crack location is closer to FGM boundary, normalized SIFs are decreasing for a constant crack period, *2c* as seen in Figures 3.15-16 and Table 3.14. Then, calculations are carried out for different FGM thicknesses and nonhomogenities. These are tabulated in Tables 3.15-20 and graphically shown in Figures 3.17-28. In the results, one observes that there is little difference on normalized SIFs while FGM thicknesses and nonhomogenities are varying. Yet, it is observed that while normalized SIFs are changing, they exhibit very clear trends according to the material gradation. To remember, periodic cracks are in homogeneous material and therefore it is the more critical part. That is to say, while homogeneous part is more rigid compared to the FGM coating, normalized SIFs are higher. When these two materials have the same properties, there is almost no difference from the above mentioned studies in literature. The calculations are also carried out for crack surface pressures changing along x- direction. It is seen from Tables 3.22-24 and 3.26-28 that normalized SIFs are much more significant at the crack tip, b since the crack surface pressure increases as x gets larger. This can also be understood from Figure 3.29 that the pressure applied at crack tip, b is considerably greater. On the other hand, for some cases there are negative SIF results at crack tip a as one can see in Tables 3.23-24 and 3.27-28. This means that the tips of periodic array of cracks near the FGM layer and the free surface are under compressive loading although the applied loading seems to be opening the crack. This can be explained by considering the constraint on displacements in *y* direction. The symmetry line between two adjacent cracks behaves like a boundary fixed in y direction. As a result the layer of material lying between the crack and the symmetry

line is predominantly in a state of compressive stress. In other words material is being squeezed. Then, the interaction of this compressive stress with the constraining FGM coating, combined with the very weak opening action near crack tip *a*, (which is actually exactly zero at *a*) gives rise to some very small negative SIFs at *a*. Such negative stress intensity factors are not meaningful by themselves, but they can be used as a part of a superposition procedure.

CHAPTER 5

CONCLUSION

In this thesis, an FGM coated homogeneous half plane containing periodic cracks was considered. The problem's importance, its place in literature and similar studies made up to now are mentioned in Introduction. In Formulation, the physical crack problem was modelled mathematically. By using Fourier transforms and Fourier series, first homogeneous part and then FGM coating were considered. The equations for stresses and displacements were derived and boundary conditions are applied in this section. The two sets of elasticity solutions were combined and singular integral equation was derived to solve the periodic crack problem. After the integral equation was obtained, a computer program was created in fortran language. Then, numerical calculations were made for various values of crack period *(2c)*, crack length *(l)*, crack location *(a)*, FGM layer thickness *(h)* and material gradation *(β)*. Under uniform loading, some discussions were made and the highlights of the results can be listed as follows;

- Under uniform loading, if nonhomogeneity is taken as sufficiently small (close to 0), crack problem reduces to homogeneous half plane containing periodic cracks,
- While crack period increases, normalized SIFs increase under uniform loading for all βh values,

- As crack location is getting closer to FGM layer ($\frac{l}{a}$ increasing), normalized SIFs decrease significantly under uniform loading,

- When FGM layer thickness and nonhomogeneity of FGM vary ($\frac{h}{a}$ and βh varying, $\frac{l}{a}$ constant), there is only a slight variation in normalized SIFs under uniform loading,

- Under uniform loading, normalized SIFs are increasing as FGM becomes more compliant compared to homogeneous half plane,

- Under linear, parabolic and cubic surface tractions, while crack spacing is getting larger ($2c$ increasing), normalized SIFs are increasing.

To sum up, this study is similar in many respects to earlier studies in literature for instance, Nied (1987a). Even the numerical results do not differ much from those obtained for an uncoated half plane. In fact, the problem under consideration can be regarded as a transition between the two limiting cases, namely periodic crack problem in a homogeneous half plane with free surface and periodic crack problem in a homogeneous half plane with fixed surface as shown in Figure 5.1. As $\beta h \to 0$, the results for free surface problem are recovered. As $\beta h \to -\infty$, FGM layer becomes stiffer compared to homogeneous half plane and SIFs decrease as one would expect in fixed surface problem (Solution to this problem is not found in literature). This thesis provides quantitative results for SIFs in this transition. Nevertheless, the work in this thesis lays foundation for future studies. For example, an FGM coated homogenoues half plane with imbedded periodic cracks under thermal loading can be studied by solving the conduction and thermal stress problems for the crack-free medium.

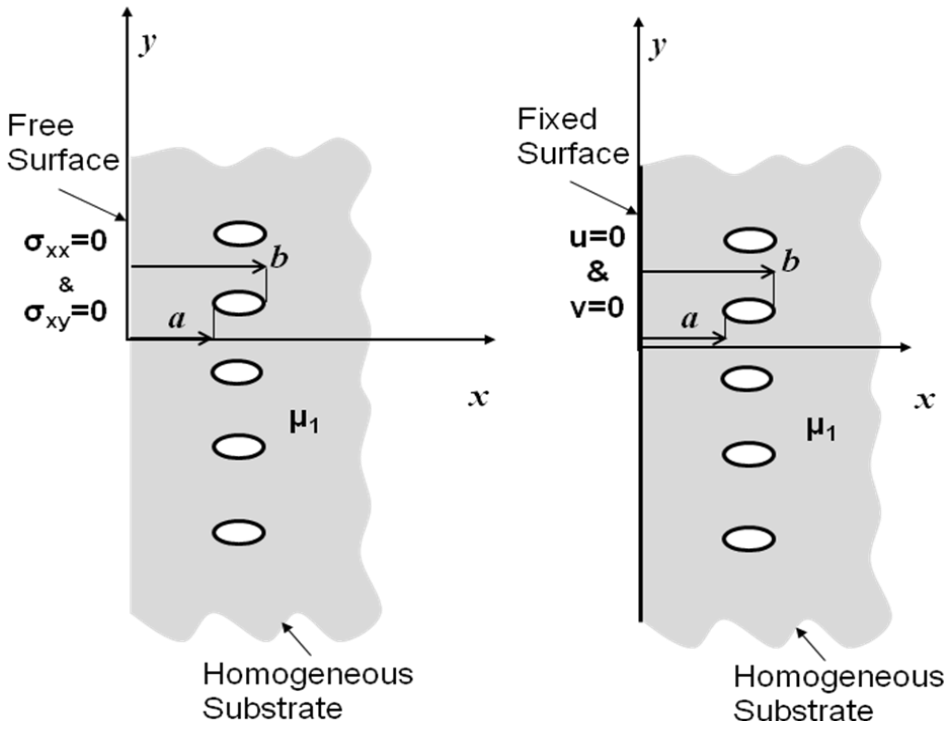

Figure 5.1: Geometry of periodic crack problem when homogeneous half plane with free surface (left) and with fixed surface (right)

REFERENCES

[1] Aboudi J., Pindera M.J., Arnold S. M., Higher-Order Theory for Functionally Graded Materials, http://www.grc.nasa.gov/WWW/RT/RT2000/5000/5920arnold3.html, June 2001, Last accessed date 15/05/2012.

[2] Afsar A. M., Sekine H., 2000. Crack spacing effect on the brittle fracture characteristics of semi-infinite functionally graded materials with periodic edge cracks. Int. J. Fract., 102, L61-L66.

[3] Bao G. and Wang L. , 1995. Multiple cracking in functionally graded ceramic/metal coatings. Int. J. Solids Struct., 32, 2853- 2871.

[4] Chen J. , 2006. Anti-plane problem of periodic cracks in a functionally graded coating-substrate structure. Arch. Appl. Mech., 75,138-152.

[5] Choi H. J. , 1997. A periodic array of cracks in a functionally graded nonhomogeneous medium loaded under in-plane normal and shear. Int. J. Fract., 88,107-128.

[6] Dag S., Yildirim B., Erdogan F., 2008. Three dimensional analysis of periodic cracking in fgm coatings under thermal stresses. AIP Conf. Proc. Multiscale And Functionally Graded Materials 2006, 973,676-681.

[7] Ding S. H., Li X. , 2008. Anti-plane problem of periodic interface cracks in a functionally graded coating-substrate structure. Int. J. Fract., 153,53-62.

[8] Erdogan F. And Ozturk M., 1995. Periodic cracking of functionally graded coatings. Int. J. Eng. Sci., 33,2179-2195.

[9] Feng Y. Z., Jin Z. H. , 2009. Thermal fracture of functionally graded plate with parallel surface cracks. Acta Mech. Solida Sinica, 22,453-464.

[10] Jin Z. H., Feng Y. Z. , 2008. Effects of multiple cracking on the residual strength behavior of thermally shocked functionally graded ceramics. Int. J. Solids Struct., 45,5973-5986.

[11] Jin Z. H., Feng Y. Z. , 2009. An array of parallel edge cracks with alternating lengths in a strip subjected to a thermal shock. J. Therm. Stress., 32,431-447.

[12] Kaya, A.C., Applications of Integral Equations with Strong Singularities in Fracture Mechanics, Ph.D. Dissertation, Lehigh University, USA, 1984

[13] Murakami, Y., Stress Intensity Factors Handbook, Pergamon Press, Oxford, New York Tokyo, 1987

[14] Nied H.F. , 1984. Thermal shock in a circumferentially cracked hollow cylinder with cladding, Engng. Fract. Mech., vol. 20, pp. 113-137.

[15] Nied H.F. , 1987a. Periodic array of cracks in a half-plane subjected to arbitrary loading. ASME J. Appl. Mech., 45,642-648.

[16] Nied H. F. ,1987b. Thermal shock in an edge cracked plate subjected to uniform surface heating, Engng. Fract. Mech., vol. 26, pp. 239-246.

[17] Private communication with Yildirim, B., 2012.

[18] Rizk A. A. , 2003. Transient stress intensity factors for periodic array of cracks in a half-plane due to convective cooling. J. Therm. Stress., 26,443-456.

[19] Rizk A. A. , 2005. Convective thermal shock of an infinite plate with periodic edge cracks. J. Therm. Stress., 28,103-119.

[20] Ruys, A., Sun, D., Functionally Graded Materials (FGM) and Their Production Methods, http://www.azom.com/details.asp?ArticleID=1592, September 2006.

[21] Schulze G.W. and Erdogan F. , 1998. Periodic cracking of elastic coatings. Int. J. Solids Struct., 35,3615-3634.

[22] Ueda S., 2002. Transient thermal singular stresses of multiple cracking in a w-cu functionally graded divertor plate. J. Therm. Stress., 25,83-95.

[23] Wang B. L., Mai Y. W., 2005. A periodic array of cracks in a functional graded materials subjected to thermo-mechanical loading. Int. J. Eng. Sci., 43,432-446.

[24] Wang B. L., Mai Y. W., 2006a. Periodic antiplane cracks in graded coatings under static or transient loading. ASME J. Appl. Mech., 73,134-142.

[25] Wang B. L., Mai Y. W., 2006b. A periodic array of cracks in functionally graded materials subjected to transient loading. Int. J. Eng. Sci., 44,351-364.

[26] El-Borgi S., Djemel M. F., Abdelmoula R., 2008. A surface crack in a graded coating bonded to a homogeneous substrate under thermal loading. J. Therm. Stress., 31,176-194.

[27] Noda N., Guo L. C., 2008. Thermal shock analysis for a functionally graded plate with a surface crack. Acta Mechanica, 195, 157-166.

[28] Yildirim B., Erdogan F., 2004. Edge crack problems in homogeneous and functionally graded material thermal barrier coatings under uniform thermal loading. J. Therm. Stress., 27,311-329.

[29] Yildirim B., Dag S., Erdogan F., 2005. Thress dimensional fracture analysis of FGM coatings under thermomechanical loading. Int. J. Fract., 132,369-395.

APPENDIX A

REQUIRED INTEGRALS

By using Mathematica tool, following integrals can be taken:

$$I_1 = \int_0^c e^{-y|\rho|}\cos(\alpha_n y)dy = \frac{|\rho|(1-(-1)^n e^{-|\rho|c})}{\rho^2+\alpha_n{}^2},$$

(A.1)

$$I_2 = \int_0^c y e^{-y|\rho|}\cos(\alpha_n y)dy = \frac{\rho^2-\alpha_n{}^2}{(\rho^2+\alpha_n{}^2)^2} + \frac{(\alpha_n{}^2-\rho^2-|\rho|c(\rho^2+\alpha_n{}^2))(-1)^n e^{-|\rho|c}}{(\rho^2+\alpha_n{}^2)^2}, \quad \text{(A.2)}$$

$$I_3 = \int_0^c e^{y|\rho|}\cos(\alpha_n y)dy = \frac{-|\rho|(1-(-1)^n e^{|\rho|c})}{\rho^2+\alpha_n{}^2},$$

(A.3)

$$I_4 = \int_0^c y e^{y|\rho|}\cos(\alpha_n y)dy = \frac{\rho^2-\alpha_n{}^2}{(\rho^2+\alpha_n{}^2)^2} + \frac{(\alpha_n{}^2-\rho^2+|\rho|c(\rho^2+\alpha_n{}^2))(-1)^n e^{|\rho|c}}{(\rho^2+\alpha_n{}^2)^2}, \quad \text{(A.4)}$$

$$II_1 = \int_0^c e^{-y|\rho|}\sin(\alpha_n y)dy = \frac{\alpha_n(1-(-1)^n e^{-|\rho|c})}{\rho^2+\alpha_n{}^2}, \quad \text{(A.5)}$$

$$II_2 = \int_0^c y e^{-y|\rho|}\sin(\alpha_n y)dy = \frac{2|\rho|\alpha_n}{(\rho^2+\alpha_n{}^2)^2}(1-(-1)^n e^{-|\rho|c}) - \frac{\alpha_n c(\rho^2+\alpha_n{}^2)(-1)^n e^{-|\rho|c}}{(\rho^2+\alpha_n{}^2)^2}, \quad \text{(A.6)}$$

$$II_3 = \int_0^c e^{y|\rho|} \sin(\alpha_n y) dy = \frac{\alpha_n (1-(-1)^n e^{|\rho|c})}{\rho^2 + {\alpha_n}^2}, \tag{A.7}$$

$$II_4 = \int_0^c y e^{y|\rho|} \sin(\alpha_n y) dy = -\frac{2|\rho|\alpha_n}{(\rho^2 + {\alpha_n}^2)^2}(1-(-1)^n e^{|\rho|c}) - \frac{\alpha_n c(\rho^2 + {\alpha_n}^2)(-1)^n e^{|\rho|c}}{(\rho^2 + {\alpha_n}^2)^2}, \tag{A.8}$$

$$CI_0 = \int_{-\infty}^{\infty} e^{-i\rho t} \frac{1}{\rho^2 + {\alpha_n}^2} d\rho = \frac{\pi}{\alpha_n}(\cosh(\alpha_n |h-t|) - \sinh(\alpha_n |h-t|)), \tag{A.9}$$

$$CI_1 = \int_{-\infty}^{\infty} e^{-i\rho(t-h)} \frac{\rho}{\rho^2 + {\alpha_n}^2} d\rho = i\pi \operatorname{sgn}(h-t)(\cosh(\alpha_n |h-t|) - \sinh(\alpha_n |h-t|)), \tag{A.10}$$

$$CI_2 = \int_{-\infty}^{\infty} e^{-i\rho(t-h)} \frac{\rho}{(\rho^2 + {\alpha_n}^2)^2} d\rho = \frac{i|h-t|\pi}{2\alpha_n}(\cosh(\alpha_n |h-t|) - \sinh(\alpha_n |h-t|)), \tag{A.11}$$

$$CI_3 = \int_{-\infty}^{\infty} e^{-i\rho(t-h)} \frac{\rho^2}{(\rho^2 + {\alpha_n}^2)^2} d\rho = \frac{\pi}{2\alpha_n}(1+|h-t|\alpha_n)(\cosh(\alpha_n |h-t|) - \sinh(\alpha_n |h-t|)), \tag{A.12}$$

$$CI_4 = \int_{-\infty}^{\infty} e^{-i\rho(t-h)} \frac{\rho^3}{(\rho^2 + {\alpha_n}^2)^2} d\rho = \\ -\frac{i\pi}{2}(-2+|h-t|\alpha_n)\operatorname{sgn}(h-t)(\sinh(\alpha_n |h-t|) - \cosh(\alpha_n |h-t|)), \tag{A.13}$$

$$CI_5 = \int_{-\infty}^{\infty} e^{-i\rho(t-h)} \frac{1}{\rho(\rho^2 + {\alpha_n}^2)} d\rho = \frac{i\pi(h-t)}{{\alpha_n}^2 |h-t|}(1-\cosh(\alpha_n |h-t|) + \sinh(\alpha_n |h-t|)), \tag{A.14}$$

$$CI_6 = \int_{-\infty}^{\infty} e^{-i\rho(t-h)} \frac{1}{(\rho^2 + {\alpha_n}^2)^2} d\rho = \\ \frac{\pi}{2{\alpha_n}^2}(|h-t| + \frac{1}{\alpha_n})(\cosh(\alpha_n |h-t|) - \sinh(\alpha_n |h-t|)), \tag{A.15}$$

where $e^{-i\rho t} = \cos(\rho t) - i\sin(\rho t),$ (A.16)

$$III_1 = \int_0^{\infty} \frac{\sin[\rho(x-t)]\cosh[\rho(c-y)]}{\sinh(\rho c)} d\rho = \\ -\frac{\pi(\coth[\frac{\pi}{2c}(t-x-iy)] + \coth[\frac{\pi}{2c}(t-x+iy)]}{4c}, \tag{A.17}$$

$$III_2 = \int_0^{\infty} \rho y \frac{\sin[\rho(x-t)]\cosh[\rho(c-y)]}{\sinh(\rho c)} d\rho = \\ \frac{i\pi^2 y(\mathrm{cs}c\,\mathrm{h}[\frac{\pi}{2c}(t-x-iy)]^2 - \mathrm{csch}[\frac{\pi}{2c}(t-x+iy)]^2}{8c^2}, \tag{A.18}$$

$$III_3 = \int_0^{\infty} c\rho \frac{\sin[\rho(x-t)]\cosh(\rho y)}{\sinh^2(\rho c)} d\rho, \tag{A.19}$$

$$III_4 = \frac{\pi(-2\coth[\frac{\pi}{2c}(t-x-iy)] - 2c\coth[\frac{\pi}{2c}(t-x+iy)]}{8c^2} \\ + \frac{\pi[(t-x-iy)(\mathrm{cs}c\,\mathrm{h}[\frac{\pi}{2c}(t-x-iy)]^2 + (t-x+iy)\,\mathrm{csch}[\frac{\pi}{2c}(t-x+iy)]^2]}{8c^2}, \tag{A.20}$$

APPENDIX B

SOLUTION OF THE RESULTING MATRIX

$$\begin{bmatrix} z_1 \\ z_2 \\ z_3 \\ z_4 \\ 0 \\ 0 \end{bmatrix} = \begin{bmatrix} a_{11} & a_{12} & a_{13} & a_{14} & a_{15} & a_{16} \\ a_{21} & a_{22} & a_{23} & a_{24} & a_{25} & a_{26} \\ a_{31} & a_{32} & a_{33} & a_{34} & a_{35} & a_{36} \\ a_{41} & a_{42} & a_{43} & a_{44} & a_{45} & a_{46} \\ a_{51} & a_{52} & a_{53} & a_{54} & 0 & 0 \\ a_{61} & a_{62} & a_{63} & a_{64} & 0 & 0 \end{bmatrix} \begin{bmatrix} b_1 \\ b_2 \\ b_3 \\ b_4 \\ c_1 \\ c_2 \end{bmatrix}. \tag{B.1}$$

Firstly, solution for b_3 and b_4 is made in terms of b_1 and b_2.

$$a_{51}b_1 + a_{52}b_2 + a_{53}b_3 + a_{54}b_4 = 0, \tag{B.2}$$

$$a_{61}b_1 + a_{62}b_2 + a_{63}b_3 + a_{64}b_4 = 0, \tag{B.3}$$

$$b_3 = -\frac{(a_{54}a_{61} - a_{51}a_{64})b_1}{a_{54}a_{63} - a_{53}a_{64}} - \frac{(a_{54}a_{62} - a_{52}a_{64})b_2}{a_{54}a_{63} - a_{53}a_{64}}, \tag{B.4}$$

or,

$$b_3 = a_{331}b_1 + a_{332}b_2, \tag{B.5}$$

where

$$a_{331} = -\frac{a_{54}a_{61} - a_{51}a_{64}}{a_{54}a_{63} - a_{53}a_{64}}, \tag{B.6}$$

$$a_{332} = -\frac{a_{54}a_{62} - a_{52}a_{64}}{a_{54}a_{63} - a_{53}a_{64}}, \tag{B.7}$$

and,

$$b_4 = -\frac{(a_{53}a_{61} - a_{51}a_{63})b_1}{-a_{54}a_{63} + a_{53}a_{64}} - \frac{(-a_{53}a_{62} + a_{52}a_{63})b_2}{a_{54}a_{63} - a_{53}a_{64}}, \tag{B.8}$$

or,

$$b_4 = a_{441}b_1 + a_{442}b_2, \tag{B.9}$$

where

$$a_{441} = -\frac{a_{53}a_{61} - a_{51}a_{63}}{-a_{54}a_{63} + a_{53}a_{64}}, \tag{B.10}$$

$$a_{442} = -\frac{-a_{53}a_{62} + a_{52}a_{63}}{a_{54}a_{63} - a_{53}a_{64}}. \tag{B.11}$$

Now, one can find c_1 and c_2 in terms of b_1 and b_2.

$$a_{11}b_1 + a_{12}b_2 + a_{13}b_3 + a_{14}b_4 + a_{15}c_1 + a_{16}c_2 = z_1, \tag{B.12}$$

$$a_{21}b_1 + a_{22}b_2 + a_{23}b_3 + a_{24}b_4 + a_{25}c_1 + a_{26}c_2 = z_2. \tag{B.13}$$

Substituting b_3 and b_4 into above equations,

$$a_{11}b_1 + a_{12}b_2 + a_{13}(a_{331}b_1 + a_{332}b_2) + a_{14}(a_{441}b_1 + a_{442}b_2) + a_{15}c_1 + a_{16}c_2 = z_1, \tag{B.14}$$

$$a_{21}b_1 + a_{22}b_2 + a_{23}(a_{331}b_1 + a_{332}b_2) + a_{24}(a_{441}b_1 + a_{442}b_2) + a_{25}c_1 + a_{26}c_2 = z_2. \tag{B.15}$$

Now, solving for b_5 and b_6,

$$c_1 = a_{551}b_1 + a_{552}b_2 + a_{553}z_1 + a_{554}z_2, \tag{B.16}$$

$$c_2 = a_{661}b_1 + a_{662}b_2 + a_{663}z_1 + a_{664}z_2, \tag{B.17}$$

where

$$a_{551} = -\frac{(a_{16}a_{21} - a_{11}a_{26} + a_{16}a_{23}a_{331} - a_{13}a_{26}a_{331} + a_{16}a_{24}a_{441} - a_{14}a_{26}a_{441})}{a_{16}a_{25} - a_{15}a_{26}}, \tag{B.18}$$

$$a_{552} = -\frac{(a_{16}a_{22} - a_{12}a_{26} + a_{16}a_{23}a_{332} - a_{13}a_{26}a_{332} + a_{16}a_{24}a_{442} - a_{14}a_{26}a_{442})}{a_{16}a_{25} - a_{15}a_{26}}, \tag{B.19}$$

$$a_{553} = \frac{a_{26}}{-a_{16}a_{25} + a_{15}a_{26}}, \tag{B.20}$$

$$a_{554} = \frac{a_{16}}{a_{16}a_{25} - a_{15}a_{26}}, \tag{B.21}$$

$$a_{661} = -\frac{(-a_{15}a_{21} + a_{11}a_{25} - a_{15}a_{23}a_{331} + a_{13}a_{25}a_{331} - a_{15}a_{24}a_{441} + a_{14}a_{25}a_{441})}{a_{16}a_{25} - a_{15}a_{26}}, \tag{B.22}$$

$$a_{662} = -\frac{(-a_{15}a_{22} + a_{12}a_{25} - a_{15}a_{23}a_{332} + a_{13}a_{25}a_{332} - a_{15}a_{24}a_{442} + a_{14}a_{25}a_{442})}{a_{16}a_{25} - a_{15}a_{26}}, \tag{B.23}$$

$$a_{663} = \frac{a_{25}}{a_{16}a_{25} - a_{15}a_{26}}, \tag{B.24}$$

$$a_{664} = \frac{a_{15}}{-a_{16}a_{25} + a_{15}a_{26}}. \tag{B.25}$$

Then, solution for b_1 and b_2 is made,

$$a_{31}b_1 + a_{32}b_2 + a_{33}b_3 + a_{34}b_4 + a_{35}c_1 + a_{36}c_2 = z_3, \tag{B.26}$$

$$a_{41}b_1 + a_{42}b_2 + a_{43}b_3 + a_{44}b_4 + a_{45}c_1 + a_{46}c_2 = z_4. \tag{B.27}$$

Substituting b_3, b_4, b_5 and b_6 into above equations,

$$a_{31}b_1 + a_{32}b_2 + a_{33}(a_{331}b_1 + a_{332}b_2) + a_{34}(a_{441}b_1 + a_{442}b_2) + a_{35}(a_{551}b_1 + a_{552}b_2 + a_{553}z_1 + a_{554}z_2) + a_{36}(a_{661}b_1 + a_{662}b_2 + a_{663}z_1 + a_{664}z_2) = z_3, \quad \text{(B.28)}$$

$$a_{41}b_1 + a_{42}b_2 + a_{43}(a_{331}b_1 + a_{332}b_2) + a_{44}(a_{441}b_1 + a_{442}b_2) + a_{45}(a_{551}b_1 + a_{552}b_2 + a_{553}z_1 + a_{554}z_2) + a_{46}(a_{661}b_1 + a_{662}b_2 + a_{663}z_1 + a_{664}z_2) = z_4. \quad \text{(B.29)}$$

Now, solving for b_1 and b_2,

$$b_1 = \alpha_{11}z_1 + \alpha_{12}z_2 + \alpha_{13}z_3 + \alpha_{14}z_4, \quad \text{(B.30)}$$

$$b_2 = \alpha_{21}z_1 + \alpha_{22}z_2 + \alpha_{23}z_3 + \alpha_{24}z_4, \quad \text{(B.31)}$$

where

$$\alpha_{11} = \frac{(-(-a_{42} - a_{43}a_{332} - a_{44}a_{442} - a_{45}a_{552} - a_{46}a_{662})(a_{35}a_{553} + a_{36}a_{663}) - (a_{32} + a_{33}a_{332} + a_{34}a_{442} + a_{35}a_{552} + a_{36}a_{662})(a_{45}a_{553} + a_{46}a_{663}))}{((a_{41} + a_{43}a_{331} + a_{44}a_{441} + a_{45}a_{551} + a_{46}a_{661})(a_{32} + a_{33}a_{332} + a_{34}a_{442} + a_{35}a_{552} + a_{36}a_{662}) - (a_{31} + a_{33}a_{331} + a_{34}a_{441} + a_{35}a_{551} + a_{36}a_{661})(a_{42} + a_{43}a_{332} + a_{44}a_{442} + a_{45}a_{552} + a_{46}a_{662}))}, \quad \text{(B.32)}$$

$$\alpha_{12} = \frac{(-(-a_{42} - a_{43}a_{332} - a_{44}a_{442} - a_{45}a_{552} - a_{46}a_{662})(a_{35}a_{554} + a_{36}a_{664}) - (a_{32} + a_{33}a_{332} + a_{34}a_{442} + a_{35}a_{552} + a_{36}a_{662})(a_{45}a_{554} + a_{46}a_{664}))}{((a_{41} + a_{43}a_{331} + a_{44}a_{441} + a_{45}a_{551} + a_{46}a_{661})(a_{32} + a_{33}a_{332} + a_{34}a_{442} + a_{35}a_{552} + a_{36}a_{662}) - (a_{31} + a_{33}a_{331} + a_{34}a_{441} + a_{35}a_{551} + a_{36}a_{661})(a_{42} + a_{43}a_{332} + a_{44}a_{442} + a_{45}a_{552} + a_{46}a_{662}))}, \quad \text{(B.33)}$$

$$\alpha_{13} = \frac{(-a_{42} - a_{43}a_{332} - a_{44}a_{442} - a_{45}a_{552} - a_{46}a_{662})}{((a_{41} + a_{43}a_{331} + a_{44}a_{441} + a_{45}a_{551} + a_{46}a_{661})(a_{32} + a_{33}a_{332} + a_{34}a_{442} + a_{35}a_{552} + a_{36}a_{662}) - (a_{31} + a_{33}a_{331} + a_{34}a_{441} + a_{35}a_{551} + a_{36}a_{661})(a_{42} + a_{43}a_{332} + a_{44}a_{442} + a_{45}a_{552} + a_{46}a_{662}))}, \quad \text{(B.34)}$$

$$\alpha_{14} = \frac{(a_{32} + a_{33}a_{332} + a_{34}a_{442} + a_{35}a_{552} + a_{36}a_{662})}{((a_{41} + a_{43}a_{331} + a_{44}a_{441} + a_{45}a_{551} + a_{46}a_{661})(a_{32} + a_{33}a_{332} + a_{34}a_{442} + a_{35}a_{552} + a_{36}a_{662}) - (a_{31} + a_{33}a_{331} + a_{34}a_{441} + a_{35}a_{551} + a_{36}a_{661})(a_{42} + a_{43}a_{332} + a_{44}a_{442} + a_{45}a_{552} + a_{46}a_{662}))}, \quad \text{(B.35)}$$

$$\alpha_{21} = -\frac{a_{35}a_{553} + a_{36}a_{663}}{a_{32} + a_{33}a_{332} + a_{34}a_{442} + a_{35}a_{552} + a_{36}a_{662}} +$$
$$\frac{\begin{array}{l}((a_{31} + a_{33}a_{331} + a_{34}a_{441} + a_{35}a_{551} + a_{36}a_{661})((-a_{42} - a_{43}a_{332} - a_{44}a_{442} - a_{45}a_{552} - a_{46}a_{662})\\ (a_{35}a_{553} + a_{36}a_{663})\\ +(a_{32} + a_{33}a_{332} + a_{34}a_{442} + a_{35}a_{552} + a_{36}a_{662})(a_{45}a_{553} + a_{46}a_{663})))\end{array}}{\begin{array}{l}((a_{32} + a_{33}a_{332} + a_{34}a_{442} + a_{35}a_{552} + a_{36}a_{662})((a_{41} + a_{43}a_{331} + a_{44}a_{441} + a_{45}a_{551} + a_{46}a_{661})\\ (a_{32} + a_{33}a_{332} + a_{34}a_{442} + a_{35}a_{552} + a_{36}a_{662}) - (a_{31} + a_{33}a_{331} + a_{34}a_{441} + a_{35}a_{551} + a_{36}a_{661})\\ (a_{42} + a_{43}a_{332} + a_{44}a_{442} + a_{45}a_{552} + a_{46}a_{662})))\end{array}}, \quad \text{(B.36)}$$

$$\alpha_{22} = -\frac{a_{35}a_{554} + a_{36}a_{664}}{a_{32} + a_{33}a_{332} + a_{34}a_{442} + a_{35}a_{552} + a_{36}a_{662}} +$$
$$\frac{\begin{array}{l}((a_{31} + a_{33}a_{331} + a_{34}a_{441} + a_{35}a_{551} + a_{36}a_{661})((-a_{42} - a_{43}a_{332} - a_{44}a_{442} - a_{45}a_{552} - a_{46}a_{662})\\ (a_{35}a_{554} + a_{36}a_{664}) +\\ (a_{32} + a_{33}a_{332} + a_{34}a_{442} + a_{35}a_{552} + a_{36}a_{662})(a_{45}a_{554} + a_{46}a_{664})))\end{array}}{\begin{array}{l}((a_{32} + a_{33}a_{332} + a_{34}a_{442} + a_{35}a_{552} + a_{36}a_{662})\\ ((a_{41} + a_{43}a_{331} + a_{44}a_{441} + a_{45}a_{551} + a_{46}a_{661})(a_{32} + a_{33}a_{332} + a_{34}a_{442} + a_{35}a_{552} + a_{36}a_{662}) -\\ (a_{31} + a_{33}a_{331} + a_{34}a_{441} + a_{35}a_{551} + a_{36}a_{661})(a_{42} + a_{43}a_{332} + a_{44}a_{442} + a_{45}a_{552} + a_{46}a_{662})))\end{array}}, \quad \text{(B.37)}$$

$$\alpha_{23} = \frac{1}{a_{32} + a_{33}a_{332} + a_{34}a_{442} + a_{35}a_{552} + a_{36}a_{662}} +$$
$$\frac{\begin{array}{l}((a_{31} + a_{33}a_{331} + a_{34}a_{441} + a_{35}a_{551} + a_{36}a_{661})(a_{42} + a_{43}a_{332} + a_{44}a_{442} + a_{45}a_{552} + a_{46}a_{662}))\\ ((a_{32} + a_{33}a_{332} + a_{34}a_{442} + a_{35}a_{552} + a_{36}a_{662})\\ ((a_{41} + a_{43}a_{331} + a_{44}a_{441} + a_{45}a_{551} + a_{46}a_{661})(a_{32} + a_{33}a_{332} + a_{34}a_{442} + a_{35}a_{552} + a_{36}a_{662}) -\\ (a_{31} + a_{33}a_{331} + a_{34}a_{441} + a_{35}a_{551} + a_{36}a_{661})(a_{42} + a_{43}a_{332} + a_{44}a_{442} + a_{45}a_{552} + a_{46}a_{662})))\end{array}}, \quad \text{(B.38)}$$

$$\alpha_{24} = \frac{\begin{array}{l}((a_{31} + a_{33}a_{331} + a_{34}a_{441} + a_{35}a_{551} + a_{36}a_{661})(-a_{32} - a_{33}a_{332} - a_{34}a_{442} - a_{35}a_{552} - a_{36}a_{662}))\\ ((a_{32} + a_{33}a_{332} + a_{34}a_{442} + a_{35}a_{552} + a_{36}a_{662})\\ ((a_{41} + a_{43}a_{331} + a_{44}a_{441} + a_{45}a_{551} + a_{46}a_{661})(a_{32} + a_{33}a_{332} + a_{34}a_{442} + a_{35}a_{552} + a_{36}a_{662}) -\\ (a_{31} + a_{33}a_{331} + a_{34}a_{441} + a_{35}a_{551} + a_{36}a_{661})(a_{42} + a_{43}a_{332} + a_{44}a_{442} + a_{45}a_{552} + a_{46}a_{662})))\end{array}}{\begin{array}{l}((a_{32} + a_{33}a_{332} + a_{34}a_{442} + a_{35}a_{552} + a_{36}a_{662})\\ ((a_{41} + a_{43}a_{331} + a_{44}a_{441} + a_{45}a_{551} + a_{46}a_{661})(a_{32} + a_{33}a_{332} + a_{34}a_{442} + a_{35}a_{552} + a_{36}a_{662}) -\\ (a_{31} + a_{33}a_{331} + a_{34}a_{441} + a_{35}a_{551} + a_{36}a_{661})(a_{42} + a_{43}a_{332} + a_{44}a_{442} + a_{45}a_{552} + a_{46}a_{662})))\end{array}}. \quad \text{(B.39)}$$

Solving for b_3 and b_4;

$$b_3 = \alpha_{31}z_1 + \alpha_{32}z_2 + \alpha_{33}z_3 + \alpha_{34}z_4, \quad \text{(B.40)}$$

$$b_4 = \alpha_{41} z_1 + \alpha_{42} z_2 + \alpha_{43} z_3 + \alpha_{44} z_4, \tag{B.41}$$

where

$$\alpha_{31} = a_{111} a_{331} + a_{221} a_{332}, \tag{B.42}$$

$$\alpha_{32} = a_{112} a_{331} + a_{222} a_{332}, \tag{B.43}$$

$$\alpha_{33} = a_{113} a_{331} + a_{223} a_{332}, \tag{B.44}$$

$$\alpha_{34} = a_{114} a_{331} + a_{224} a_{332}, \tag{B.45}$$

$$\alpha_{41} = a_{111} a_{441} + a_{221} a_{442}, \tag{B.46}$$

$$\alpha_{42} = a_{112} a_{441} + a_{222} a_{442}, \tag{B.47}$$

$$\alpha_{43} = a_{113} a_{441} + a_{223} a_{442}, \tag{B.48}$$

$$\alpha_{44} = a_{114} a_{441} + a_{224} a_{442}. \tag{B.49}$$

And, c_1 and c_2 can also be expressed as

$$c_1 = \alpha_{51} z_1 + \alpha_{52} z_2 + \alpha_{53} z_3 + \alpha_{54} z_4, \tag{B.50}$$

$$c_2 = \alpha_{61} z_1 + \alpha_{62} z_2 + \alpha_{63} z_3 + \alpha_{64} z_4, \tag{B.51}$$

where

$$\alpha_{51} = a_{111} a_{551} + a_{221} a_{552} + a_{553}, \tag{B.52}$$

$$\alpha_{52} = a_{112} a_{551} + a_{222} a_{552} + a_{554}, \tag{B.53}$$

$$\alpha_{53} = a_{113} a_{551} + a_{223} a_{552}, \tag{B.54}$$

$$\alpha_{54} = a_{114} a_{551} + a_{224} a_{552}, \tag{B.55}$$

$$\alpha_{61} = a_{111}a_{661} + a_{221}a_{662} + a_{663}, \tag{B.56}$$

$$\alpha_{62} = a_{112}a_{661} + a_{222}a_{662} + a_{664}, \tag{B.57}$$

$$\alpha_{63} = a_{113}a_{661} + a_{223}a_{662}, \tag{B.58}$$

$$\alpha_{64} = a_{114}a_{661} + a_{224}a_{662}. \tag{B.59}$$

Remembering,

$$z_1 = \int_a^b g(t)Z_1 dt, \tag{B.60}$$

$$z_2 = \int_a^b g(t)Z_2 dt, \tag{B.61}$$

$$z_3 = \int_a^b g(t)Z_3 dt, \tag{B.62}$$

$$z_4 = \int_a^b g(t)Z_1 dt. \tag{B.63}$$

APPENDIX C

DERIVATION OF SINGULAR INTEGRAL EQUATION

$$\sigma_{yy}(x,y) = -\frac{2i\mu_1}{\pi(1+\kappa)}\left\{\int_a^b g(t)\int_{-\infty}^{\infty} e^{i\rho(x-t)}\left(e^{(c-y)|\rho|}\,\frac{(\mathrm{sgn}(\rho)+\rho y)(e^{-c|\rho|}-e^{c|\rho|})-2c\rho e^{-c|\rho|})}{(e^{-c|\rho|}-e^{c|\rho|})^2}\right.\right.$$
$$\left.\left. + e^{(y-c)|\rho|}\,\frac{(\mathrm{sgn}(\rho)-\rho y)(e^{-c|\rho|}-e^{c|\rho|})-2c\rho e^{c|\rho|})}{(e^{-c|\rho|}-e^{c|\rho|})^2}\right)d\rho dt\right\} \qquad \text{(C.1)}$$
$$+\mu_1\sum_{n=0}^{\infty} e^{-\alpha_n x}[2\alpha_n C_{1n} + C_{2n}(-3-\kappa+2\alpha_n x)]\cos(\alpha_n y),$$

$$\sigma_{yy}(x,y)_1 = -\frac{2i\mu_1}{\pi(1+\kappa)}\left\{\int_a^b g(t)\int_{-\infty}^{\infty} e^{i\rho(x-t)}\left(e^{(c-y)|\rho|}\,\frac{(\mathrm{sgn}(\rho)+\rho y)(e^{-c|\rho|}-e^{c|\rho|})-2c\rho e^{-c|\rho|})}{(e^{-c|\rho|}-e^{c|\rho|})^2}\right.\right.$$
$$\left.\left. + e^{(y-c)|\rho|}\,\frac{(\mathrm{sgn}(\rho)-\rho y)(e^{-c|\rho|}-e^{c|\rho|})-2c\rho e^{c|\rho|})}{(e^{-c|\rho|}-e^{c|\rho|})^2}\right)d\rho dt\right\}, \qquad \text{(C.2)}$$

Considering the inner integral and let it be A;

$$A = \int_{-\infty}^{\infty} e^{i\rho(x-t)}\left(e^{(c-y)|\rho|}\,\frac{(\mathrm{sgn}(\rho)+\rho y)(e^{-c|\rho|}-e^{c|\rho|})-2c\rho e^{-c|\rho|})}{(e^{-c|\rho|}-e^{c|\rho|})^2} + \right.$$
$$\left. e^{(y-c)|\rho|}\,\frac{(\mathrm{sgn}(\rho)-\rho y)(e^{-c|\rho|}-e^{c|\rho|})-2c\rho e^{c|\rho|})}{(e^{-c|\rho|}-e^{c|\rho|})^2}\right)d\rho \qquad \text{(C.3)}$$

Splitting up A as $\int_{-\infty}^{0}$ and $\int_{0}^{\infty}$ and also observing $|\rho| \to -\rho$ in $\int_{-\infty}^{0}$

$$A=\int_{-\infty}^{0} e^{i\rho(x-t)}(e^{-(c-y)\rho}\frac{((2\sinh c\rho)(-1+\rho y)-2c\rho e^{c\rho})}{(+2\sinh c\rho)^2}+$$
$$e^{-(y-c)\rho}\frac{((2\sinh c\rho)(-1-\rho y)-2c\rho e^{-c\rho}))}{(+2\sinh c\rho)^2}d\rho$$
$$+\int_{0}^{\infty} e^{i\rho(x-t)}(e^{(c-y)\rho}\frac{((-2\sinh c\rho)(1+\rho y)-2c\rho e^{-c\rho})}{(-2\sinh c\rho)^2}+ \quad (C.4)$$
$$e^{(y-c)\rho}\frac{((-2\sinh c\rho)(1-\rho y)-2c\rho e^{c\rho}))}{(-2\sinh c\rho)^2}d\rho$$

Consider first integral in A as A_1 and letting $\rho \to -\rho$;

$$A_1=\int_{0}^{\infty} e^{-i\rho(x-t)}(e^{(c-y)\rho}\frac{((2\sinh c\rho)(1+\rho y)+2c\rho e^{-c\rho})}{4\sinh^2 c\rho}+$$
$$e^{(y-c)\rho}\frac{((2\sinh c\rho)(1-\rho y)+2c\rho e^{c\rho}))}{4\sinh^2 c\rho}d\rho \quad (C.5)$$

$$A_2=\int_{0}^{\infty} e^{i\rho(x-t)}(e^{(c-y)\rho}\frac{((-2\sinh c\rho)(1+\rho y)-2c\rho e^{-c\rho})}{4\sinh^2 c\rho}+$$
$$e^{(y-c)\rho}\frac{((-2\sinh c\rho)(1-\rho y)-2c\rho e^{c\rho}))}{4\sinh^2 c\rho}d\rho \quad (C.6)$$

Combining A_1 and A_2;

$$A=\int_{0}^{\infty}\frac{1}{4\sinh^2 c\rho}(e^{(c-y)\rho}((2\sinh c\rho)(1+\rho y)+2c\rho e^{-c\rho})(e^{-i\rho(x-t)}-e^{i\rho(x-t)})$$
$$+e^{(y-c)\rho}((2\sinh c\rho)(1-\rho y)+2c\rho e^{c\rho}))(e^{-i\rho(x-t)}-e^{i\rho(x-t)}))d\rho \quad (C.7)$$

note that

$$e^{-i\theta}-e^{i\theta}=-2i\sin\theta$$

$$A=-i\int_0^{\infty}\frac{\sin\rho(x-t)}{\sinh^2 c\rho}(\sinh c\rho(e^{(c-y)\rho}+e^{(y-c)\rho}) + \rho y(e^{(c-y)\rho}-e^{(y-c)\rho})\sinh c\rho + c\rho(e^{-y\rho}-e^{y\rho}))d\rho \tag{C.8}$$

where

$$e^{(c-y)\rho}+e^{(y-c)\rho}=2\cosh(c-y)\rho \tag{C.9}$$

$$e^{(c-y)\rho}-e^{(y-c)\rho}=2\sinh(c-y)\rho \tag{C.10}$$

$$e^{-y\rho}+e^{y\rho}=2\cosh y\rho \tag{C.11}$$

Then,

$$A=-2i\int_0^{\infty}\frac{\sin\rho(x-t)}{\sinh^2 c\rho}(\sinh c\rho\cosh(c-y)\rho + \rho y\sinh c\rho\sinh(c-y)\rho + c\rho\cosh y\rho)d\rho \tag{C.12}$$

Thus,

$$\sigma_{yy}(x,y)_1=-\frac{4\mu_1}{\pi(1+\kappa)}\int_a^b g(t)\int_0^{\infty}\sin\rho(x-t)(\frac{\cosh(c-y)\rho}{\sinh c\rho} + \rho y\frac{\sinh(c-y)\rho}{\sinh c\rho}+c\rho\frac{\cosh y\rho}{\sinh^2 c\rho})d\rho dt \tag{C.13}$$

Final form can expressed as;

$$\sigma_{yy}(x,y)=-\frac{4\mu_1}{\pi(1+\kappa)}\int_a^b g(t)\int_0^{\infty}\sin\rho(x-t)(\frac{\cosh(c-y)\rho}{\sinh c\rho} + \rho y\frac{\sinh(c-y)\rho}{\sinh c\rho}+c\rho\frac{\cosh y\rho}{\sinh^2 c\rho})d\rho dt + \mu_1\sum_{n=0}^{\infty}e^{-\alpha_n x}[2\alpha_n C_{1n}+C_{2n}(-3-\kappa+2\alpha_n x)]\cos(\alpha_n y), \tag{C.14}$$

APPENDIX D

MANIPULATIONS ON RIZK'S SINGULAR INTEGRAL EQUATION

Rizk's singular integral equation,

$$\frac{1}{\pi}\int_a^b g(t)\left(\frac{1}{(t-x)}+K_1(x,t)+K_2(x,t)\right)dt=\frac{(1+\kappa)}{4\mu_1}P(x), \tag{D.1}$$

where

$$K_1(x,t)=\frac{2}{t+x}-\frac{3t+x}{(t+x)^2}+\frac{4tx}{(t+x)^3}, \tag{D.2}$$

$$\begin{aligned}K_2(x,t)=&\left(\frac{1}{c}\right)*\left(\pi*\coth\left(\pi*\frac{(t+x)}{2c}\right)-\left(\frac{2c}{t+x}\right)-\left(\frac{(t+x)}{c}+\frac{(t-x)}{2c}\right)*\right.\\&\left(\left(\frac{\pi^2}{2}\right)*\operatorname{csch}^2\left(\pi*\frac{(t+x)}{2c}\right)-\frac{2c^2}{(t+x)^2}\right)+\\&\left(\left(\frac{(t+x)}{2c}\right)^2-\left(\frac{(t-x)}{2c}\right)^2\right)*\left(\left(\frac{\pi^3}{2}\right)*\operatorname{csch}^2\left(\pi*\frac{(t+x)}{2c}\right)*\coth\left(\pi*\frac{(t+x)}{2c}\right)\right.\\&-\frac{1}{2*\left(\frac{(t+x)}{2c}\right)^3}\left.\right)+\pi*\coth\left(\pi*\frac{(t-x)}{2c}\right)-\pi^2*\frac{(t-x)}{c}*\frac{\operatorname{csch}^2\left(\pi*\frac{(t-x)}{2c}\right)}{2}-\\&\left.\frac{c}{t-x}\right).\end{aligned} \tag{D.3}$$

Integral equation for homogeneous half plane containing single crack,

$$\frac{1}{\pi}\int_a^b g(t)\left(\frac{-1}{t+x}+\frac{6x}{(t+x)^2}-\frac{4x^2}{(t+x)^3}\right)dt=\frac{(1+\kappa)}{4\mu_1}P(x), \qquad \text{(D.4)}$$